

VOL.1/ ISSUE1/APRIL 2018

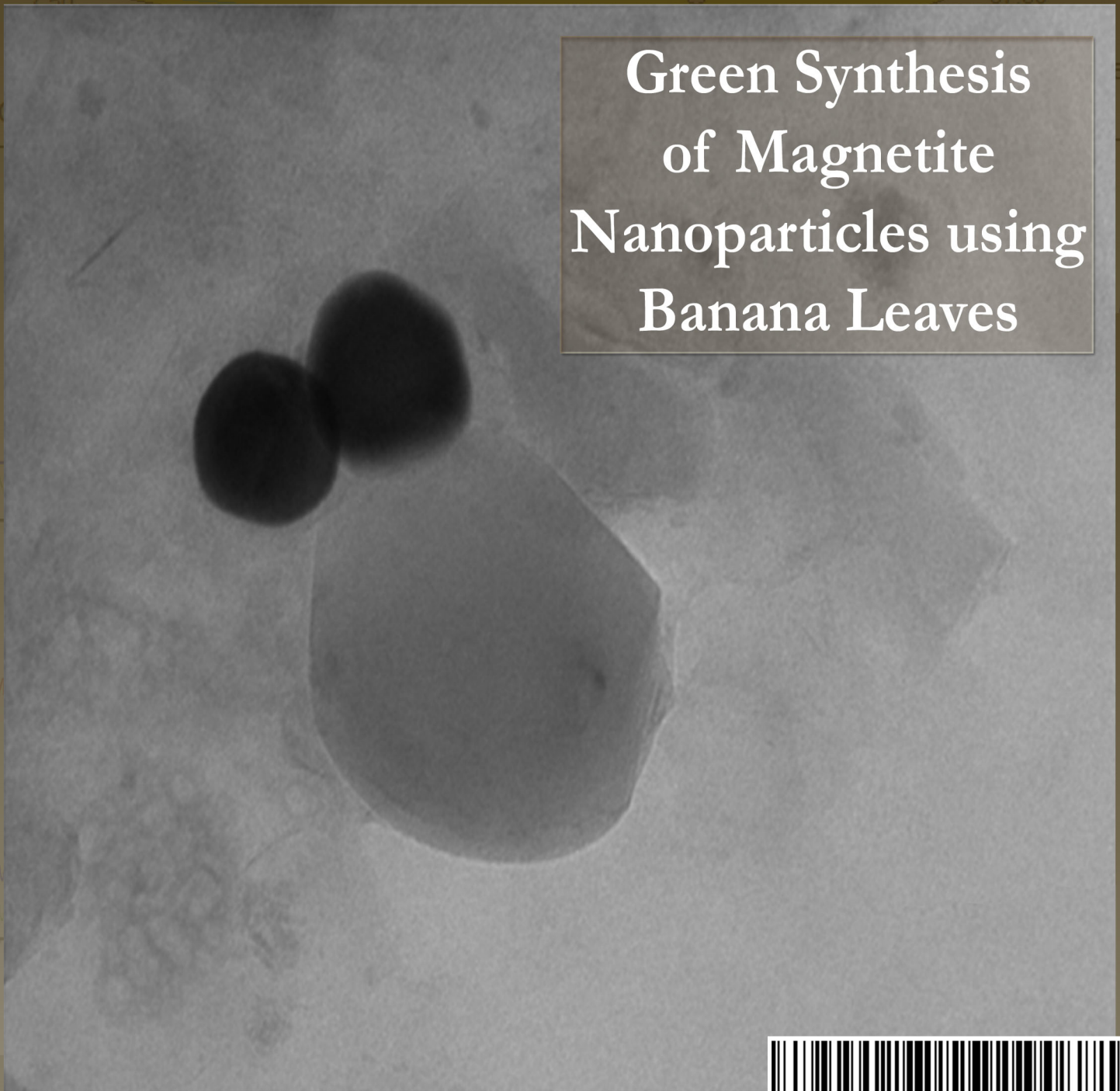
ISSN 2516-8150 (Print)

ISSN 2516-8169 (Online)

# European Journal of Sciences (EJS)<sup>®</sup>

MONTHLY SCIENTIFIC ACADEMIC JOURNAL

Green Synthesis  
of Magnetite  
Nanoparticles using  
Banana Leaves



ISSN 2516-8169

[WWW.EUROPEANJOURNALOFSCIENCES.CO.UK](http://WWW.EUROPEANJOURNALOFSCIENCES.CO.UK)

[WWW.EJSCI.COM](http://WWW.EJSCI.COM)



**WORLD  
CONFERENCE**  
*...helping to converge and collaborate*

[www.worldconference.co.uk](http://www.worldconference.co.uk)

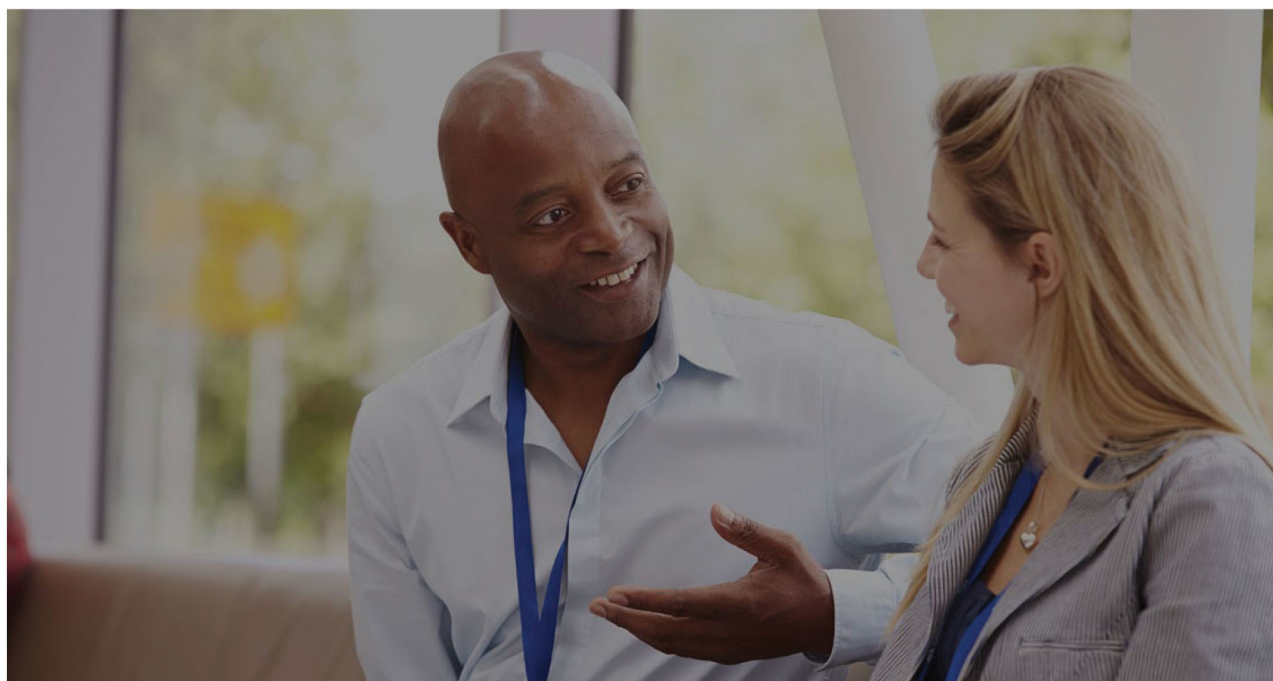
Email: [info@worldconference.co.uk](mailto:info@worldconference.co.uk)



**UK  
EDUCATION** <sup>®</sup>  
*...helping you realise your dreams*

[www.uk-education.com](http://www.uk-education.com)

Email: [info@uk-education.com](mailto:info@uk-education.com)



ISSUE 1/ APRIL 2018

## Contents

EDITOR-IN-CHIEF: *Prof (Dr) Ravi Prakash*  
ADVISOR: *Rajeev Soni, Ph.D.*  
ASSOCIATE EDITOR: *Jasmita Gill, Ph.D.*  
CREATIVE & DIGITAL: *Carl Saunders*

01. Effect of P-EPQ as a secondary antioxidant on the properties of Biaxially Oriented Polypropylene film
10. Applications of pyrolysis for carbonaceous wastes in solid waste management – A mini-review
26. Green synthesis of magnetite nanoparticles using banana leaves
35. Rapid method for determination of dehydro abietic acid in gum rosin and disproportionate rosin by proton nuclear magnetic resonance spectroscopy
43. Parabolic trough solar collectors

### NOTE FROM THE FOUNDER

We value inclusive dissemination. We wish to enhance access to system and processes of dissemination of new knowledge acquired through primary scientific research. We find that there is a genuine need for a more specific journal dedicated to the scientific community where scientists can publish up-to-date, high-quality and original research papers alongside relevant and insightful reviews about their cutting-edge work. Hence, here we are with the maiden issue of European Journal of Sciences (EJS)<sup>®</sup>!

European Journal of Sciences (EJS)<sup>®</sup> aim to report original scientific research of significance through robust evaluation by way of peer review of the findings and to disseminate novel findings to the scientific community at large. The journal shall cover all areas of sciences including but not limited to physical sciences, biological sciences, chemical sciences, mathematical sciences, computer sciences, engineering sciences, environmental sciences and earth sciences.

In addition, the journal aspires to provide a vibrant, engaging, integrative and challenging platform for scientists to present their work that is subject to rigorous peer review process.

Umesh Prasad

## Effect of P-EPQ as a secondary antioxidant on the properties of Biaxially Oriented Polypropylene film

Vishal Goel<sup>1</sup>, Suresh Mani<sup>2</sup>, Anil Yadav<sup>1</sup>, Jatinder Singh Dhaliwal<sup>1\*</sup>, Shashikant<sup>1</sup> and Gurpreet Singh Kapur<sup>1</sup>

### ABSTRACT

P-EPQ (Tetrakis(2,4-di-tert-butylphenyl)-4,4-biphenyldiphosphonite) is a well-known phosphorus based secondary antioxidant used in Polyolefins for stabilization. P-EPQ has a low melting point and promotes good solubility in Polyolefins. It also helps in reduction of undesired colour during the processing. Biaxially Oriented Polypropylene (BOPP) film is a multilayer film, prepared at very high temperature and shear, and needs to be properly stabilized with primary and secondary antioxidant. Apart from the colour, other properties like dyne retention and compatibility with impact copolymers are also prime requisites of the BOPP. In this paper, a method was developed for analysis of P-EPQ using HPLC. Further, the effect of P-EPQ on dyne retention properties in BOPP films is discussed. A hypothesis for improvement in dyne retention has been proposed. Structural comparison of two different P-EPQ samples by HPLC was carried out and their effect on properties of BOPP film was studied.

### KEYWORDS

P-EPQ, Biaxially Oriented Polypropylene (BOPP) Film, antioxidants, Polypropylene, dyne retention

<sup>1</sup>Indian Oil Corporation Ltd, R&D Division, Faridabad, Haryana, India

<sup>2</sup>Indian Oil Corporation Ltd, Product Application and Development Centre, Panipat, Haryana, India

\*Corresponding author; email [singhj4@indianoil.in](mailto:singhj4@indianoil.in)

### INTRODUCTION

Polypropylene is being considered the perfect material for various applications, especially packaging, because of its various advantages over other polyolefin materials and its low cost and good thermal stability. Biaxially oriented films, especially based on polyolefins, represent a major component of the film packaging industry. Biaxially oriented polypropylene films are mostly produced through a sequential biaxial stretching process, in which films are cold drawn in two consecutive steps at two different temperatures (Philips et al., 2001; Dias et al., 2006; Lupke et al., 2004; Rettenberger et al., 2002).

Metallized biaxially oriented polypropylene (BOPP) films offer excellent gas and water vapor barrier and now are being extensively used in food packaging applications mainly in the form of multi-layer structure and also in general packaging or lamination of other materials. The Polypropylene being non-polar in nature has a low surface energy (Decker et al., 2002) and hence pre-treatment of the BOPP film is essential to have good adhesion with metal. There are methods of pre-treatment mentioned in the literature (Blythe et al., 2978; Markgraf MP 1993) like corona atmosphere or low-pressure plasma pre-treatment which provides surface functionality and thus proper adhesion.

To measure the surface functionality, Dyne value on the metalized side of BOPP film is measured and as a rule it should not drop very fast within the stipulated time (Markgraf DA, 1998) The dyne level is measured as a way of

indicating the chemical cleanliness of the surface. There will be a dyne level that indicates that the surface is clean and a value of around 38 units is perceived acceptable by converters over a period of 6 months. Drop in dyne levels beyond this particular value can result in problem during metallization and lead to inferior optical properties.

Since the BOPP film production includes multiple steps of production and the film is prepared at a very high temperature and shear, it needs to be properly stabilized with primary and secondary antioxidant (Kenneth and Harrison, 2010). The main requirement of BOPP films is that a) it should not be yellowish, b) it should have optimum mechanical and optical properties, c) it should not break at high line speed, d) it should be able to retain the dyne value, e) it should have good compatibility with impact polypropylene in multilayer application. The trend towards using wider and faster production lines makes it necessary to develop effective stabilization that resist the stresses encountered during processing without loss of mechanical and optical properties. There are many secondary antioxidants (Krohnke and Werner 2001, Tolinski M 2009) available in the market, sold by trade names like Irgafos 168, P-EPQ, Ultrinox 626 etc. PEP-Q is not a single compound and is comprised of a mixture of various compounds including its isomers.

The objective of this paper was to showcase the difference in properties of BOPP films containing different secondary antioxidants. Also, how the secondary antioxidant, particularly P-EPQ, improves the surface properties of the BOPP film. In addition, an HPLC method was developed to separate

various components of P-EPQ. Moreover, P-EPQ from two different sources was obtained and characterized by HPLC and difference in composition was highlighted.

## RESULTS AND DISCUSSION

### Characterization of P-EPQ from different sources

P-EPQ is not single component and is mixture of many components (Bruheim et al, 20). Table 3.1 summarizes different components present along with their typical concentration in P-EPQ.

S. No	Components	Composition (%)
1	4,4'-PEPQ	36 - 46
2	4,3'-PEPQ	17 - 23
3	3,3'-PEPQ	2 - 5
4	Oxidized P-EPQ	2 - 5
5	Mono-P-EPQ	11 - 19
6	Irgafos 168	9 -18

**Table 3.1** Composition of P-EPQ

Major component present in P-EPQ is 4,4'-PEPQ, Irgafos 168 content in P-EPQ varies from 9-18%. P-EPQ1 and P-EPQ2 available from two different commercial sources were characterized by liquid chromatography. Figure 3.2 shows that number of components present in P-EPQ1 and P-EPQ2 are similar but their concentration varies. Since standards of different components of P-EPQ were not available; hence it was not possible to assign the individual component in the HPLC chromatogram. Only Irgafos 168 was available and in HPLC chromatogram it is marked as component 4. A comparison of area counts of P-EPQ1 and P-EPQ2 sample at same concentration level was done and is presented in Table 3.2

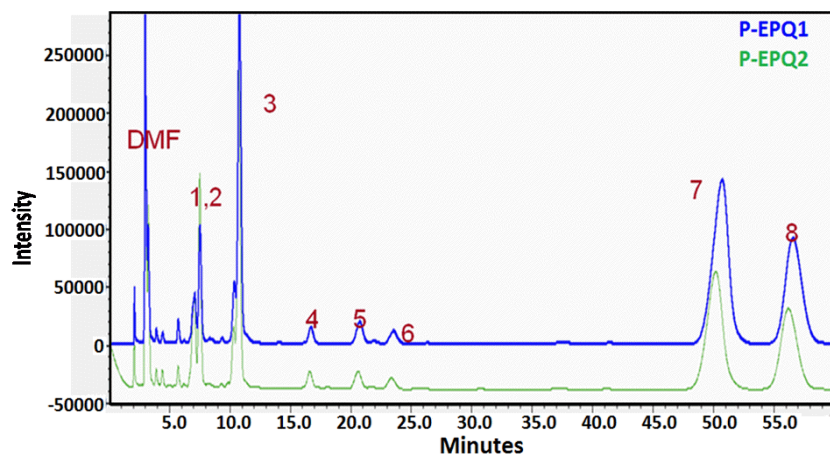


**Fig. 3.1** HPLC chromatogram of PEPQ1 and PEPQ2

	P-EPQ1	P-EPQ2
Major peak #	Area counts	Area counts
1	1801	942
2	2760	1526
3	6000	6454
4*(Irgafos 168)	459 (16.1% of Irgafos 168)	415 (14.6% of Irgafos 168)
5	619	782
6	443	517
7	9619	13418
8	6716	8988

**Table 3.2** Area count of 0.5% solution of different components of P-PEPQ samples

From Table 3.2, Irgafos 168 present in both P-EPQ was almost similar in the range of 14-16%. However, there was significant variation in area count of component 1, component 2, component 7 and component 8 in P-EPQ1 and P-EPQ2 samples. It can be concluded from the above data that both P-EPQ have same number of components but have significantly different composition.

#### Characterization of commercial BOPP samples

The MFI and Xylene soluble of the 3 different batches of commercial BOPP grades are summarized in Table 3.3.

Sample Detail	MFI @ 2.16 Kg g/10 min	Xylene Soluble (wt%)
BOPP- N	3.2	4.5
BOPP – PEPQ1	3.0	4.4
BOPP – PEPQ2	3.0	4.3

**Table 3.3** Physico-chemical properties of Polypropylene

Sample Detail	AO 1010	Irgafos 168	P-EPQ-1	P-EPQ-2	DHT-4A
	<b>Concentration in ppm</b>				
BOPP- N	463	940	nil	nil	261
BOPP – PEPQ1	593	nil	900	nil	225
BOPP – PEPQ2	488	nil	nil	864	222

**Table 3.4** Additives composition in Polypropylene

As seen from the Table 3.3, there is not much variation in MFI and xylene soluble of the samples taken for the study. The antioxidant and acid scavenger concentration in all the three samples of Polypropylene was determined using HPLC and XRF respectively. The results are summarized in Table 3.4. As mentioned earlier, that composition of both P-EPQ1 and P-EPQ2 is different, therefore, different calibration was carried in order to do the quantification of P-EPQ in Polypropylene.

Results indicate the difference in additive package in different Polypropylene samples. BOPP-N contains additive package comprising of primary antioxidant and secondary antioxidant, AO-1010 and Irgafos-168 in the ratio of 1: 2 respectively, the workhorse antioxidants of Polyolefin industry. BOPP-PEPQ1 and BOPP-PEPQ2 contain a different secondary antioxidant namely P-EPQ instead of Irgafos168 at similar concentration ranges. The concentration of AO 1010 and DHT-4A in both samples was comparable.

#### **Melt Flow Rate Studies**

Multiple extrusion studies were carried out to study the efficacy of antioxidant package in polypropylene samples keeping processing conditions constant. As a thumb rule for multiple extrusion studies, the ratio of melt flow index at 2.16 Kg load for 5<sup>th</sup> pass to 1<sup>st</sup> pass should not exceed 1.5 at the application temperature. Multiple extrusion studies at

230°C (Fig. 3.2a) indicate that there was no significant variation in MFI from 1<sup>st</sup> to 5<sup>th</sup> pass for 3 different samples (BOPP-N, BOPP-PEPQ1 and BOPP-PEPQ2). At the higher extrusion temperature of 250°C (Fig. 3.2b), variation of MFI at different passes was significant. The MFI ratio of 5<sup>th</sup> pass to 1<sup>st</sup> pass is summarized in Table 3.5. BOPP-N has MFI ratio of 1.2 at 250°C and BOPP-PEPQ1 and BOPP-PEPQ2 have MFI ratio of 1.03 and 1.02 respectively.

Results show that at extrusion temperature of 230°C, MFI of all the PP samples was comparable but real distinction could be observed at higher extrusion temperature of 250°C. However, it is well known that P-EPQ is superior secondary antioxidant than Irgafos 168 and hence gives better thermal stability. BOPP-PEPQ1 and BOPP-PEPQ2 samples behaved similarly in terms of their thermal stability in multiple extrusion studies.

#### **Variation of Yellowness Index with different passes**

Slight improvement in yellowness index (YI) was observed at different passes with the samples containing P-EPQ as compared to sample containing Irgafos 168. At 250°C (Fig. 3.3b), the difference between samples containing P-EPQ and sample containing Irgafos 168 is magnified. The yellowness index of BOPP-N sample increased abruptly from -1.9 units to 7.3 units, whereas for the samples containing P-EPQ, yellowness index increases from -1.9 units to

max -0.2 units. PEPQ2 sample showed better yellowness index retention P-EPQ1 from 1<sup>st</sup> pass to 5<sup>th</sup> pass. It can be concluded from the multiple pass study that P-EPQ is better secondary antioxidant than Irgafos 168 in terms of thermal stability and colour retention. Also, both P-EPQ samples provide good thermo-oxidative stability to Polypropylene maintaining the initial MFI and colour even though they have different concentration of components. Studies were further extended to see the effect of additive package on the surface and optical properties of BOPP film.

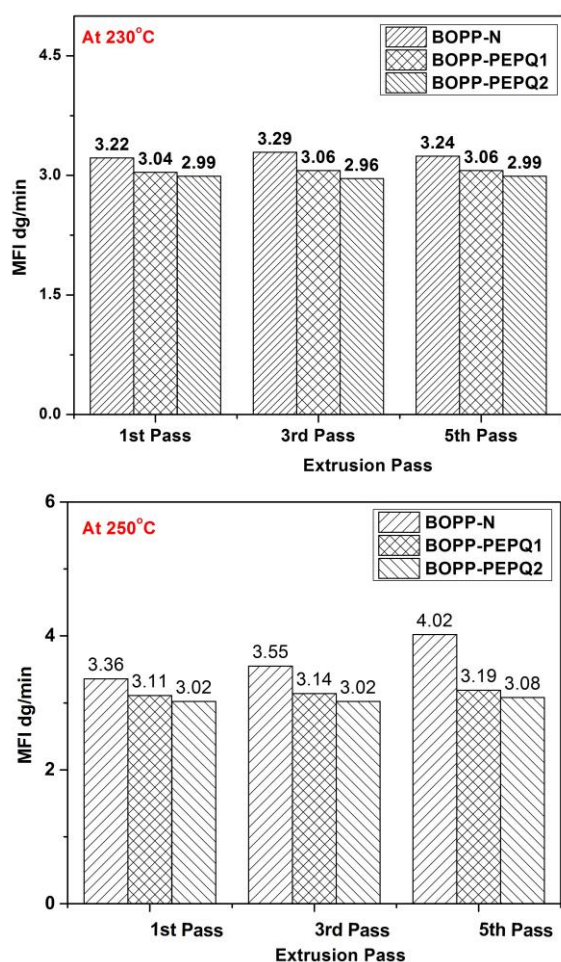


**Fig. 3.2** Melt flow rate at different passes at two different temperatures; a) 230°C; b) 250°C.

Sample Detail	MFI Ratio of 5 <sup>th</sup> / 1 <sup>st</sup> pass at 230°C	MFI Ratio of 5 <sup>th</sup> / 1 <sup>st</sup> pass at 250°C
BOPP- Normal	1.01	1.20
BOPP – PEPQ1	1.01	1.04
BOPP – PEPQ2	1.00	1.02

**Table 3.5** MFI ratio of 5<sup>th</sup> passes to 1<sup>st</sup> passes at 2.16 Kg load

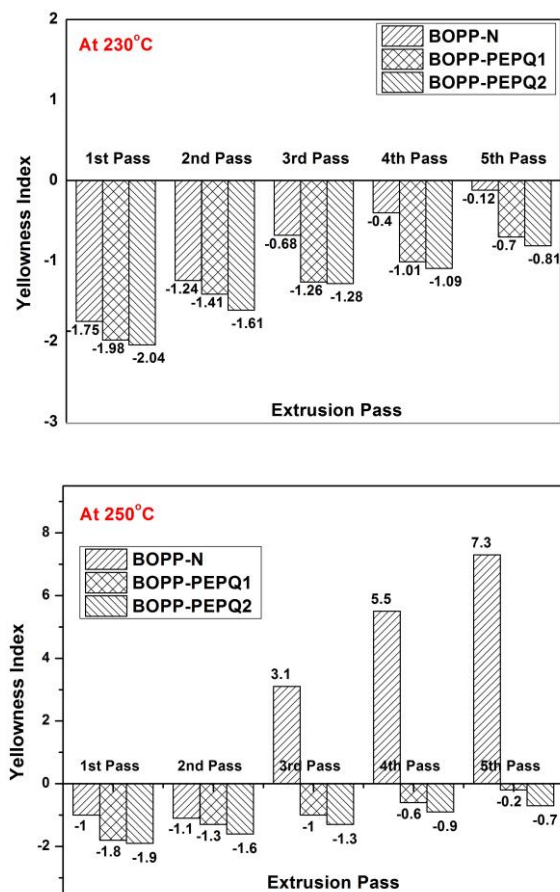


**Fig. 3.3** yellowness index at 1<sup>st</sup> to 5<sup>th</sup> pass at two different temperatures; a) 230°C; b) 250°C.

### Effect of P-EPQ on surface and optical properties of BOPP Film

Three layered BOPP films prepared were slitted after 24 hrs of maturation time and the development of colour was observed. Table 3.6 summarizes the optical properties obtained with different secondary antioxidants present in films.



Sample Detail	Color
BOPP- N	Yellowish
BOPP – PEPQ1	Light yellow
BOPP – PEPQ2	White

**Table 3.6** colour of the slitted roll of BOPP film

Sample Detail	Initial Dyne Retention	Dyne Retention after 1 month	Dyne Retention after 6 months	Compatibility with ICP
BOPP- N	46	<36	< 36	Poor
BOPP– PEPQ1	48	47	41	Good
BOPP– PEPQ2	48	46	40	Good

**Table 3.7** Dyne retention of BOPP films

The BOPP film prepared with Irgafos 168 gave yellowish colour to the film which is not acceptable in the market whereas film containing P-EPQ showed no or lower yellowish tinge indicating PEPQ as better secondary antioxidant than Irgafos 168. However, in comparison within different P-EPQ, it was surprising to see that P-EPQ2 gave whitish colour in the slitted role compared to P-EPQ1. These results obtained were contrary to multiple extrusion studies which indicate that both P-EPQ gave almost equivalent thermo-oxidative and colour stability. From the earlier results, it was analysed and observed that both P-EPQ samples have different composition although the number of components is similar. This difference in the composition of different components of P-EPQ may have led to difference of colour in the final application. BOPP films prepared with P-EPQ2 gave better colour compared to films prepared with P-EPQ1. Another major requirement for

metallizable BOPP film grade is dyne retention and compatibility with impact copolymers. In metalized BOPP grade, core layer is BOPP grade and skin layer is a combination of impact polypropylene and anti-block additive.

Metallized biaxially oriented polypropylene (BOPP) films offer excellent gas and water vapor barrier properties, making it of an exceptional value as a barrier packaging film. The metal adhesion to BOPP is normally poor due to its low surface energy, however, pre-treatment of the film surface imparts surface functionality which in turn improves metal adhesion and this surface functionality is measured by dyne retention. As a thumb rule, after 6 months dyne retention of the metalized BOPP film should not be less than 38 units. Lower dyne retention in BOPP film indicates poor compatibility with impact co-polymer polypropylene (ICP). Dyne retention values of BOPP films are in Table 3.

Dyne retention value of all the three film samples initially was at par with each other. However, a sharp dip in dyne retention value was observed in BOPP film produced with Irgafos 168. Lower value indicates poor compatibility of core layer (homopolymer) and skin layer (impact copolymer). Dyne retention value even after six months was found to be in the acceptable range for the BOPP film having P-EPQ, values were found to be higher (46) than the required (36) limit. The reason of poor dyne retention and yellowish colour of the BOPP film produced with Irgafos 168 vis-à-vis P-EPQ could be due to following:

- *Irgafos 168 has higher melting temperature and relatively poor miscibility with Polypropylene matrix while P-EPQ has lower melting temperature and has good miscibility within polymer matrix. Since the line temperature, line speed and shear in the BOPP manufacturing process is very demanding, P-EPQ gives better thermo-oxidative stability than Irgafos 168.*

BOPP film if not properly stabilized may result in degraded product (lower molecular weight species) which migrate to the surface of the film after certain time period and affect the film dyne retention property and also lowers the compatibility with impact polypropylene. P-EPQ being better secondary antioxidant, if added to polypropylene controls the degradation in a much efficient way compared to AO-168 and relatively less amount of low molecular weight species will be formed compared to Irgafos 168 and hence better properties.

## CONCLUSION

In the present paper, an HPLC based method was established to separate different components of P-EPQ. Analysis of two P-EPQ showed different composition of similar components. BOPP samples containing PEPQ1 and PEPQ2 showed lower change in MFI and

yellowness index value than BOPP-N. Apart from its primary function of protecting degradation of polypropylene, this paper also demonstrates that P-EPQ also imparts other functions like improvement in dyne retention and compatibility with impact polypropylene. Study also prove the hypothesis “degradation always leads to formation of low molecular weight species. Addition of P-EPQ in the BOPP film will curtail the amount of low molecular weight species as compared to Irgafos 168 and hence lower a migration of these species to the surface of film will lead to better dyne retention efficiency and compatibility with impact copolymer of polypropylene.

## EXPERIMENTAL

### Material

Three different lots of commercial homopolymer polypropylene resin of IndianOil Corporation Ltd. (MFI 3g/10min and xylene solubles of 4.5 wt%) was used. Two different P-EPQ samples were designated as PEPQ-1 and PEPQ-2. Polypropylene samples were designated as BOPP-N (with Irgafos 168), BOPP-PEPQ1 and BOPP-PEPQ2 corresponding to P-EPQ1 and P-EPQ2 respectively.

### Methods

*Melt Flow Index (MFI):* Melt flow index of polypropylene granules was determined at 2.16 Kg load and 230°C on Goettfert MI-4 MFI machine as per ASTM D1238.

*Xylene Soluble (XS):* Xylene Soluble of polypropylene granules was determined gravimetrically as per ASTM D5492.

*Yellowness Index (YI):* Yellowness Index of polypropylene granules was determined as per ASTM E313 on M/s HuneterLab Lab Scan XE instrument.

*Dyne Retention Studies:* Dyne retention of the BOPP films was determined as per ASTM D2578-04a.

*Extraction of Additives:* The polypropylene granules (3mm) were grounded to powder to 300-500 micron size in Retsch Cryo Mill under

liquid nitrogen. 2g of polypropylene powder was taken into a extraction vessel having 25mL of solvent (mixture of acetone: cyclohexane 70:30). Extraction was carried out in CEM International microwave extraction machine at a temperature of 125°C.

*HPLC for additive quantification:* The additive quantification was carried in ThermoFisher reverse phase HPLC, using a gradient of water, isopropanol and acetonitrile at a temperature of 50°C

*HPLC for P-EPQ analyses:* The High-performance liquid chromatography analysis was carried on Shimadzu machine (LC-2010 CHT). Machine comprises of a degasser unit (DGU-20A) for extracting any dissolved air from the solvents, quaternary pump (LC-30AD) for isocratic and gradient solvent program, an auto sampler (SIL-30AC) for sample injection, column oven (CTO-20AC) to maintain the temperature and UV-DAD (SPD-M20A) detector. Method developed for analysis of PEP-Q is

*Optimized Analytical Conditions*

- Stationary phase: C-18 Column (Eurosphere: 5u, 250X4.6mm)
- Mobile phase: HPLC grade Methanol
- Reference Standard solution was prepared in Methanol-Acetonitrile taken in 9:1 ratio.
- The two samples were first dissolved in DMF at 1% (w/v) conc. level. The solutions were then diluted with equal volume of methanol.
- Sample injection: 10 ul
- Detector: Photo Diode Array (PDA) 200-400nm; monitored at 254 nm.

*XRF:* The quantification of acid scavenger and P-EPQ was carried using XRF.

*Multiple Extrusion Studies:* Multiple extrusion studies were carried in Haake single screw extruder having L/D of 24 and screw speed of 80 rpm. Polypropylene was extruded five times. The multiple extrusion studies were carried at two different temperature 230°C and 250°C.

The melt flow rate (MFR) and yellowness index (YI) was determined of each pass. Since BOPP films are produced at higher temperature therefore extrusion study was carried out at higher temperatures.

*BOPP films:* Three layered tape textile BOPP film having average thickness of 23micron was prepared on 8.7m wide Bruckener line having output of 5.5m/hr using three different polypropylene samples (BOPP-N, BOPP-PEPQ1 and BOPP-PEPQ2). Processing was carried out at barrel zone temperatures from 230°C-255°C and die zone temperature from 255°C-260°C. Stretching Ratios in machine direction was 4.83 and transverse direction was 9.65. All three layers of BOPP films comprised 3MFI PP homopolymer.

## REFERENCES

- Aniunoh, K. and Harrison, GM. 2010, 'The processing of polypropylene cast films. I. Impact of material properties and processing conditions on film formation', *Polymer Engg. and Sc.*, vol. 50, no. 6, pp.1151-1160.
- Blythe AR, et al. 1978, 'Surface modification of polyethylene by electrical-discharge treatment and the mechanism of auto-adhesion', *Polymer*, vol. 19, no. 11, pp.1273-1278. (1978).
- Bruheim, I., Molander, P., Lundanes, E. and Greibrokk T. 2000, 'Temperature-Programmed Packed Capillary Liquid Chromatography Coupled to Fourier-Transform Infrared Spectroscopy', *J. High Resol. Chromatography*, vol. 23, no. 9, pp.525-530.
- Decker, W., Pirzada, S., Michael, M., Yializis, A. 2000, 43rd Annual Technical Conference Proceedings.
- Dias, P., Hiltner, A., Baer, E., Van Dun, J., Chen, H.Y., Chum, S.P. 2006, *Annual Tech Conference, Society of Plastic Engineers*, vol. 64, pp.2660.
- Krohnke, C. and Werner, F. 2001, 'Stabilizers for Polyolefins', *Rapra Review Reports*, vol. 11, no. 21.
- Lupke, T., Dunger, S., Sanze, J., Radosch, H. 2004, 'Sequential biaxial drawing of polypropylene films', *Polymer*, vol. 45, no. 20, pp.6861-6872.
- Markgraf, M.P. 1993, 'Corona Treatment: An Adhesion Promoter for UV/EB Converting', *Rad Tech Report*, vol. 7, no. 5.

Markgraf, D.M. 1998, 'Corona Treatment – An overview', Enercon Industries Corp.

Phillips, R.A., Nguyen, T. 2001, 'Structure, processing, morphology, and property relationships of biaxially drawn Ziegler–Natta/metallocene isotactic polypropylene film'. *J. Appl Poly Sc.*, vol. 80, no. 13, pp.2400-2415.

Rettenberger, S., Capt, L., Munstedt, H., Stopperka, K., Sanze, J. 2002, 'Uniaxial deformation behavior of

different polypropylene cast films at temperatures near the melting point', *J. Rheol Acta.*, vol. 41, no. 4, pp.332-336.

Tolinski, M. 2009, *Additives for Polyolefin's*, first edition, Elsevier Inc.

## Applications of pyrolysis for carbonaceous wastes in solid waste management – A mini-review

Rushikesh Joshi, Ganesh R. Kale\*, Atul N. Vaidya

### ABSTRACT

Due to the aggravating problem of solid waste disposal and rising demand of fuels for energy generation, pyrolysis can serve as a promising solution to both these challenges. The majority of the municipal solid wastes are constituted of carbonaceous wastes including biomass. Pyrolysis can be universally applied to all these types of wastes to obtain non-condensable fuel gases, pyrolysis oils and solid coke achieving complete waste disposal. In the present study, a review of pyrolysis with respect to various types of waste feedstock is presented. The interactions of the various types of waste feeds during co-pyrolysis were also reviewed. The applications of the products obtained as well as their further upgrading is also discussed. The presence of catalyst, reaction conditions, heating rate as well as the type of reactor, influence the yield as well as the composition of the products to a great extent. Pyrolysis of single feed as well as co-pyrolysis is also reviewed. Some co-pyrolysis studies reported better results than single feed pyrolysis owing to the synergistic interactions between waste feeds. This paper provides an overall outlook of the current scenario of the pyrolysis techniques for solid waste management.

### KEYWORDS

Pyrolysis, Co-Pyrolysis, Solid Waste Management, Pyrolysis oil, Non-Volatile gases, Char.

### INTRODUCTION

The challenges in ever-increasing amount of solid wastes has brought about noteworthy research in solid waste management.

-----  
Solid and Hazardous Waste Management Division,  
CSIR-National Environmental Engineering Research  
Institute, Nehru Marg, Nagpur 440020,  
Maharashtra, India.

\*Corresponding author; email: gr\_kale@neeri.res.in

Depending on nature and source of wastes, they can be classified as medical, industrial, agricultural, municipal, vehicular waste, etc. Currently, the major disposal techniques for waste management are: a) landfilling b) composting c) sewage treatment d) incineration and e) recycling (Rushton 2003). Out of these, recycling of wastes is restricted to only reusable wastes, while composting is restricted to biodegradable solid wastes and sewage treatment to sewage sludge. These methods require proper segregation of waste feedstock before disposal implementation. Majority of wastes are preferably landfilled due to its cheap and simple nature (Arsova et al. 2008). However, landfilling requires a huge land which leads to strain on land resources (Omar and Rohani 2015). The leaching out of heavily polluted leachates and emission of landfill gases from landfills has led to many harmful consequences on environment and people residing nearby (Bernard et al. 1996; Crowley et al. 2003; El-Fadel et al. 1997; Vrijheid 2000). The leachates are a mixture of high concentration organic and inorganic contaminants including heavy metals and are highly toxic due to their synergistic or antagonistic effects and different physical-chemical properties of contaminants (Cameron and Koch 1980; Kjeldsen et al. 2002; Marttinen et al. 2002; Wiszniowski et al. 2006). Incineration allows better mass and volume reduction of wastes and good energy recovery and seems to be a better option than landfilling (Roy et al. 2011). However, the fly ash emissions released during incineration are hazardous due to high content of chlorides and fluorides, sulfur and nitrogen compounds, heavy metals like mercury and organic compounds. Some deadly side-effects on human beings reported are congenital abnormalities, birth weight, twinning, still births, sex ratios, infant death, facial clefts, urinary tract defects, neural tube and heart defects (Ashworth et al. 2014; Margallo et al. 2015; van Velzen et al. 2002; Williams 1990). Sometimes greater amount of fuel is required to be supplied to ensure adequate combustion temperatures,

making the incineration process less energy efficient (Ji et al. 2016; Yang et al. 2006).

Pyrolysis is a thermal degradation process of heating in absence of oxygen or air to produce gaseous components, tar and pyrolysis char residues (Ahmed and Gupta 2009). The pyrolysis process can be divided into three subclasses: conventional pyrolysis, fast pyrolysis, and flash pyrolysis (Demirbas and Arin 2002). Due to 'carbon negative' energy approach, pyrolysis deserves serious research and development worldwide for energy and controlling global warming (Lee et al. 2010). The liquid and gaseous fractions obtained are a valuable fuel source; while the solid fraction (char) has the potential of low grade carbon black or as carbon adsorbent (Lee et al. 2015; Martínez et al. 2013; Mohan et al. 2006b; Phan et al. 2008). Pyrolysis of waste also produces products that can be used as chemicals and high performance materials (carbon fibers and ceramics) other than fuels (Blazsó 1997). During recent years, pyrolysis has undergone an important evolution from a promising scientific idea to an alternative that is very close to reality with commercial opportunities (Aguado et al. 2008). Although the pyrolysis oils cannot be directly used as engine ready fuel but the fuel quality and contamination issues can be resolved by fuel additives and fuel finishing operations in terms of physical, catalytic and chemical upgrading (Butler et al. 2011a; Isahak et al. 2012).

Presently, fast pyrolysis of biomass is deemed as robust alternate technology for the paradigm shift from current crude oil fuel platform to a sustainable, more flexible fuel platform (Butler et al. 2011b). Based on ways of energy transfer, microwave assisted pyrolysis has an advantage of providing rapid and energy-efficient heating compared to conventional technologies, and thus facilitating increased production rates (Jones et al. 2002; Lam and Chase 2012). Hence pyrolysis can be a promising technique for waste management.

Literature has reported several significant reviews on the development of the pyrolysis process. Blazsó (1997) has reviewed the studies on the thermal decomposition mechanisms of polyolefines, polystyrenes, acrylic polymers,

polyesters, polyethers, formaldehyde resins, polyamides, sulfur and silicon containing polymers. Aguado et al. (2008) have reviewed in detail the thermal and catalytic processes for recycling of plastics and several commercial processes for the preparation of diesel fuel. Butler et al. (2011a) has studied the state of art of commercial pyrolysis processes for the production of liquid transport fuels from waste polyolefins (polyethylenes and polypropylenes). Bulushev and Ross (2011) have reviewed chemistry of various catalytic processes for production and upgrading of the pyrolysis oils obtained from biomass pyrolysis. White et al. (2011) have reviewed the kinetic models and mathematical approximations currently employed in solid state thermal analysis and isoconversional model-fitting methods for estimating the related kinetic parameters. Isahak et al. (2012) have presented an updated review of biomass pyrolysis focusing on the characterization of feedstock, reactor design, product formation and physical, catalytic and chemical upgrading of the products. Jahirul et al. (2012) have discussed the status of biomass pyrolysis technology and its potential for commercial applications to produce bio-fuel in light of pyrolysis principles, biomass sources and characteristics, types of pyrolysis, reactor design, products and the economics of bio-fuel production. Mohan et al. (2006a) have reviewed in detail the pyrolysis of wood biomass and the characteristics of bio-oil produced. Butler et al. (2011b) have reviewed the laboratory work and developments on fast pyrolysis and upgrading techniques for its commercialization. Fonts et al. (2012) have reviewed the state of art of the sewage sludge pyrolysis for liquid production, focusing on the various factors influencing the process and chemical and physical properties of the pyrolysis oil obtained. Yang et al. (2013) have reviewed the pyrolysis of the waste electronic and electric plastic wastes and the dehalogenation of the pyrolysis oils.

A review based on the study of feedstock of pyrolysis and their interaction during co-pyrolysis has not been reported yet. The aim of this review is to study pyrolysis and co-pyrolysis focusing on the properties, composition and nature of waste feeds and their effect on the interactions during co-pyrolysis for solid waste

management. The effect of the reaction conditions such as temperature, heating rate, presence of carrier gas, nature of catalyst on the yield and physicochemical properties of products are also discussed. The potential of pyrolysis products to serve as a source of high quality fuels and chemicals is also discussed. The review provides an outlook of waste pyrolysis from the aspect of feedstock, particularly required for an insight for waste-to-energy processes. The nature of interaction of the different feeds with each other and their effect on the yield and composition of the products during co-pyrolysis studied in this review provides a novel aspect in environmental engineering. Similar work has been reported previously by Sannita et al. (2012), but their study is restricted to triglyceride-based materials, wood and compounds derived from wood and few hydrocarbon and oxygenated polymers. This review includes pyrolysis of carbonaceous wastes including paper wastes.

## **1 Single Feed Pyrolysis**

### **1.1 Biomass**

Pyrolysis is a promising and environment friendly way of energy recovery from biomass as biomass is the only renewable source of fixed carbon (Bridgwater and Bridge 1991; Serrano-Ruiz and Dumesic 2011; Zhong et al. 2010). Considerable work has been reported to study the potential of agricultural wastes as a source of biofuels. Pyrolysis of rice husks (Meesuk et al. 2012; Williams and Nugranad 2000; Worasuwanarak et al. 2007), pine biomass (Aho et al. 2007), chlorella algae (Babich et al. 2011), wheat straw and husks (Krishna et al. 2015), beech wood (Stephanidis et al. 2011), combed cotton wastes (Barışçı and Öncel 2014), guayule (Boateng et al. 2016), douglas fir, para rubber seed (Chaiya and Reubroycharoen 2013), white ash, switchgrass, corn stover (Chen et al. 2016c), olive cake (Gerçel and Gerçel 2007), miscanthus, douglas fir and oak (Le Brech et al. 2015), cassava plant residues (Pattiya 2011), mangaba seed (Santos et al. 2015), rapeseed cake (Smets et al. 2011), posidonia oceanica, lacustrine alga and white-pine (Chiodo et al. 2016), corn cob (Yu et al. 2010), tobacco wastes (Wu et al. 2015b) has been reported.

The yield and chemical composition of the products is influenced by a variety of factors

such as temperature, presence of catalyst, size of the feed particles, etc. (Chaiya and Reubroycharoen 2013; Chen et al. 2016a; Demirbas 2010; Krishna et al. 2015). Various ways for upgrading the quality of the products, especially for use of pyrolysis oil as fuel have been reported.

One of the important products obtained during pyrolysis of the materials is bio-char. It possesses high calorific value and relatively low ash content making it suitable as a good solid fuel (Gil et al. 2012). Some other value-added products are also obtained. A high percentage of silica (88%) was recovered from overall valorization of the bio-char of rice husk flash pyrolysis (Alvarez et al. 2014). Potassium silicate of electronic grade can be obtained from bio-char more easily than from fusion of sand along with a good quality activated carbon as a by-product (Jain et al. 1994). The char could be used as an additive material or good solid fuel with binders and additives due to its high energy content (Barışçı and Öncel 2014; Maiti et al. 2006). Due to good absorbing properties, bio-char also finds its uses as adsorbent. The char obtained at high temperatures is highly porous with effective tar removal capacity (Paethanom and Yoshikawa 2012). Increase in the pyrolysis temperature increases the carbon content in biochar and gases (Chen et al. 2016c). The char is mainly aromatic polymer of carbon atoms (Hu et al. 2008). Li et al. (2015a) have reported an increase in energy and char yield due to the effect of  $\text{NH}_4\text{H}_2\text{PO}_4$  on rice husk pyrolysis. Uzunov et al. (2012) have carried out fixed bed slow pyrolysis of rice husks for determining the effect of pyrolysis temperature on the properties of solid residues. Carbon black of high specific surface area and pore volume can be synthesized from rice husk by hydrolysis, carbonization and pyrolysis (Wang et al. 2011). Wu et al. (2015a) have suggested that the bio-char from microwave pyrolysis is more uniform with less secondary bio-char which are produced from secondary reactions of volatiles.

Generally, the yield of non-condensable gases increases with increase in the temperature, lower heating rate and longer residence time (Khor et al. 2010). The yield also depends on the conditions, types of biomass and presence of

catalyst (Buzetzi et al. 2012; Xie et al. 2015). Homma et al. (2013) have developed a new pyrolysis technology for wood pyrolysis that has a low manufacturing cost and less maintenance. It was quite feasible in rural areas and the gases obtained could be directly used in gas engine generator. The gases from rice husk pyrolysis can also be used in auto thermal pyrolysis process if the moisture content is controlled (Park et al. 2014). The gases obtained could be further reformed for the production of hydrogen gas (Uddin et al. 2014). Demirbaş (2005) has reported an increase in hydrogen production from agricultural residues via pyrolysis with an increase in temperature. The introduction of steam into the reactor system can drastically increase the hydrogen production (Adebanjo et al. 2007). The yield of methane and hydrogen gases and heating value of the gases can be also increased by torrefaction pretreatment (Chen et al. 2015). The process of mild pyrolysis in the temperature range 200-350°C which leads to removal of water and volatiles through decomposition of hemicellulose in wood, is termed as torrefaction (Kolokolova et al. 2013). Zhang et al. (2015d) have reported the combined water washing-torrefaction pretreatment for effective removal of inorganics. The bio-char was obtained with huge surface area and had the potential to be used as soil amendments.

The most important component obtained during pyrolysis is pyrolysis oil. Oil contains alkanes, alcohols, hydroxybenzenes, alkoxybenzenes, dioxolanes, aldehydes, ketones, carboxylic acids, esters, nitrogen-containing organic compounds (Lu et al. 2012). Due to its potential to be used as fuel, it can replace diesel and gas for on-site power generation and heating in furnaces, boilers, gas turbines etc. (Barth and Kleinert 2008; Zheng and Kong 2010) Literature has reported several methods to increase the quality and yield of pyrolysis oil. Bok et al. (2014) have designed a tilted-slide fast pyrolyzer with spray type condenser for the large-scale production of biocrude-oil from douglas fir in which the bio-oil from first and fourth condensers could be directly applied to conventional combustors. Kunkes et al. (2008) have reported the catalytic pyrolysis of biomass based on the integration of several flow reactors operated in cascade mode,

where the effluent from the one reactor is fed to the next reactor and the first flow reactor contained monofunctional compounds, such as alcohols, ketones, carboxylic acids and heterocycles that could also be used to provide reactive intermediates for fine chemicals and polymers markets. Heo et al. (2010) have reported pyrolysis of rice husk in fluidized bed reactor in which the bio-oil production was most effective when the fluidizing medium was the product gas itself. Thangalazhy-Gopakumar et al. (2011) have reported large reduction in high molecular weight, oxygenated compounds in the pyrolysis oil when the carrier gas was changed from helium to hydrogen during pyrolysis. Williams and Besler (1993) have reported the pyrolysis study of rice husk in thermogravimetric analyzer and static batch reactor wherein water, CO and CO<sub>2</sub> were evolved in lower temperature regime of decomposition and oil, water, hydrogen, hydrocarbon gases and lower concentrations of CO and CO<sub>2</sub> were evolved in higher temperature regime. Le Brech et al. (2015) have reported the pyrolysis in U-shaped fixed bed reactor which allowed external mass transfer control, bed temperature control and char quenching at targeted temperatures. Undri et al. (2014b) have reported microwave assisted pyrolysis of corn derived plastic bags which can avoid the anaerobic digestion of these bags without any energy recovery. Gerçel and Gerçel (2007) have pyrolysed olive cake and found that at optimum conditions, the calorific value of pyrolysis oil is very close to those of petroleum fractions. Santos et al. (2015) have reported that the bio-oil from mangaba seed was promising as fuel after upgradation due to the presence of long chain acids. Demirbas (2009) have pyrolysed olive husk, hazelnut shell, spruce wood, and beech wood samples and reported that the density of bio-oil was 1,170–1,230 kg/m<sup>3</sup>, compared to 800-1000 kg/m<sup>3</sup> of heavy petroleum oil.

Guha et al. (1987) have studied the potential use of pyrolysis oil in germicide manufacture due to the presence of toxic phenolic compounds. Ji-Lu (2007) has conducted pyrolysis of rice husk and reported that the bio-oil can be directly used in boiler or furnace without further upgrading and the cost of pyrolysis can be greatly reduced by



using charcoal combustion for heating and hot flue gas as carrier gas. Torri et al. (2016) have reported an increase in the percentage of aromatic hydrocarbons in bio-oil during catalytic fast pyrolysis of softwood, thus indicating its potential as liquid fuel. Lu et al. (2011) have proposed low temperature fast pyrolysis of biomass impregnated with zinc chloride to obtain furfural from bio-oil while acetic acid was obtained as by-product. The addition of methanol stabilized the bio-oil and enhanced the quality by decreasing viscosity and ageing rates of bio-oil (Lu et al. 2008). Li et al. (2012) have seen an increase in the yield of water soluble organics and heating value with decrease in acetic acid content and ring opening reactions of cellulose during fast pyrolysis of rice husk with mineral bed materials. Qian et al. (2014) have reported the facilitation of dehydration and decarboxylation of higher calorific value bio-oil under elevated pressure in the pyrolysis of rice husk. Banks et al. (2014) have reported that during pyrolysis of *Miscanthus* pretreated with Triton X-100 surfactant, the best quality organic oil was produced with highest concentration of Triton X-100 surfactant. Shen et al. (2015) have reviewed the opportunities of the fast pyrolysis products as value added chemicals and fuels. Damartzis and Zabaniotou (2011) have discussed the emerging challenges and opportunities of the applications of process integration on chemical conversion of biomass to second generation liquid biofuels.

Chen et al. (2011) have reported a decrease in the total bio-oil content, higher water content, higher pH, and lower alkali metal content in the bio-oil when the hot vapor filtration of bio-oil was conducted. It was also reported that the PAH content increased when the temperature increased and around 800°C charcoal liquid was produced (Zhai et al. 2015). Catalysis is one of the assuring approaches for upgrading the bio-oil. The use of catalyst decreased the bio-oil yield, but enhanced the small molecular compound yield and decreased the amount of oxygenated groups in bio-oils (Bridgwater 1996; Zhou et al. 2013). The pyrolysis oil before catalysis was homogeneous, of low viscosity and highly oxygenated with presence of polycyclic aromatic hydrocarbon (PAH) in low

concentration (Williams and Nugranad 2000). Aho et al. (2007) have reported the formation of less organic oil and more water and PAH on the catalytic pyrolysis of pine biomass with zeolites of stronger acidity. Antonakou et al. (2006) have proposed the use of mesoporous catalysts Fe–Al-MCM-41 and Cu–Al-MCM-41 as best metal containing catalyst for phenol production from bio-oil. The phenol concentration can be further increased by upgrading of the bio-oil obtained from hydrothermally pretreated biomass (Stephanidis et al. 2011). Phenol could be further used in adhesive industry (Effendi et al. 2008). Wang et al. (2010) have reported an increased yield of gaseous and char products with use of  $K_2CO_3$  as a stronger catalyst for decomposition of hemicellulose, cellulose and lignin constituents. Various pretreatment techniques and product upgrading via catalysis also facilitate increase in the quality of the bio-oil. Bridgwater and Bridge (1991); French and Czernik (2010), Galadima and Muraza (2015) have studied the catalytic upgrading of the primary fast pyrolysis products for removing oxygen from organic compounds to give aromatics and other hydrocarbon products. The products can be further converted into gasoline and diesel and the condensed liquid can be hydrotreated to a naphtha like product also for up gradation into transport fuels (Kim et al. 2013).

The hydroprocessing increases the intrinsic hydrogen content of the pyrolysis oil, producing polyols and alcohols. The zeolite catalyst then converts these hydrogenated products into light olefins and aromatic hydrocarbons as much as three times higher than that produced with the pure pyrolysis oil (Vispute et al. 2010). Babich et al. (2011) had pretreated *Chlorella* algae with  $Na_2CO_3$  and the decomposition temperature shifted to lower value, yield of gas increased and yield of liquid decreased. Barışçı and Öncel (2014) have reported that bio-char from pyrolysis of combed cotton wastes in a fixed bed reactor with  $Na_2CO_3$  and  $CaCO_3$  as catalyst can be used as additive material or fuel due to its high energy potential. Meesuk et al. (2012) have further reported that the quality of the bio-oil can be further improved to a level suitable for a potential liquid fuel and chemical feedstock by hydrolysis of rice husk using Ni/LY char at

high temperature and the pyrolysis oil contained less acids, higher aromatics and showed higher heating value leading to 40% energy recovery in bio-oil. Zhang et al. (2015a) have studied the microwave assisted catalytic fast pyrolysis of biomass using HZSM-5 catalyst and reported that the relative contents of the aliphatic hydrocarbons, aromatic hydrocarbons and oxygen-containing aromatic compounds first increased and then decreased, whereas the relative content of oxygen-containing aliphatic compounds first decreased and then increased.

## 1.2 Paper wastes

Paper industry generates a significant amount of wastes and the waste composition depends on the type of paper produced and the origin of cellulose fibres. (Méndez et al. 2009). Nearly 11 million tons of paper wastes are generated per year by European pulp and paper industry, of which 70% originated from the production of deinked recycled paper. The paper and pulp production from virgin pulp generates less wastes with less organics than deinked pulp (Monte et al. 2009). Paper mill sludge contain massive heavy metal, pathogen and parasites making it very easy to corrupt and produce odor causing secondary pollution to the environment and threat to human beings and animals (Liu et al. 2010). Therefore one of the most important tasks for environmental protection is the safe disposal of sludge from paper and pulp industry (Yu et al. 2002).

The four main compounds in bio-oil obtained from waste paper pyrolysis are anhydrosugar, carboxyl compounds, carbonyl compounds and aromatic compounds (Li et al. 2005). The gases generated during pyrolysis of newspaper wastes are composed of H<sub>2</sub>, CO, CO<sub>2</sub>, and CH<sub>4</sub> with a trace amount of C<sub>2</sub>H<sub>4</sub> and C<sub>2</sub>H<sub>6</sub> and the production of hydrogen rich gaseous fuel is favored at higher temperature and higher retention time (Bhuiyan et al. 2009). It was also reported that there is an increase in the yield of liquid and gaseous products with an increase in the solid waste pyrolysis temperature (Demirbaş 2002), and char yield increases with an increase in the heating rate (Gupta et al. 1999). The performance of fast pyrolysis for energy transfer from paper waste sludge to liquid and solid products is considerable higher than vacuum

and slow pyrolysis due to higher yield of condensable organic compounds and less water content (Ridout et al. 2016). Fast pyrolysis is quite promising due to low optimal reactor temperatures and high bio-oil yield. The non-condensable gas yield increases due to promotion of exothermic reaction for high heating rates (Ridout et al. 2015). Biswal et al. (2013) have pyrolysed paper cup waste in a stainless steel semibatch reactor and found that the pyrolytic liquid contains around 18 types of compounds having carbon chain length in the range of C<sub>6</sub> – C<sub>20</sub>, and can be used as valuable chemical feedstock. Jiang and Ma (2011) have reported that microwave pyrolysis of paper mill sludge was best performed when 5% NaOH was added as microwave absorber in CO<sub>2</sub> atmosphere. Reckamp et al. (2014) have subjected paper mill sludge to a combination of acid hydrolysis and torrefaction pretreatment and found that the bio-char yield was higher and ideal to be used as soil amendment agent or sorbent material. Mendez et al. (2014) have reported the use of bio-char from deinking paper sludge pyrolysis to treat nickel polluted soil.

Calisto et al. (2014) have reported production of adsorbents obtained in the pyrolysis of paper mill sludge for the removal of highly consumed antidepressant (citalopram) from water. Devi and Saroha (2015) have studied the PAH toxicity and sorption behavior of bio-char obtained in the pyrolysis of paper mill effluent treatment plant and reported that the concentration of PAHs in bio-char were within the permissible limits prescribed by US EPA. Strezov and Evans (2009) have reported that a large fraction of mineral matter (56%) in the charcoal produced by pyrolysis of dry paper sludge and also found that the energy from bio-gas can utilized to recover the heat required for pyrolysis thus reducing the external heat supply requirement. Zhang et al. (2015g) have reported low temperature microwave assisted pyrolysis of paper deinking residue for simultaneously efficient fast recovery and separation of organic and inorganic content in which the organic fraction of bio-oil generated was a potential source of valuable aromatic compounds. Zhang et al. (2015f) have further reported the low temperature microwave assisted fast pyrolysis

of waste office papers (printed or photocopied) and the application of bio-oil as adhesive for aluminum-aluminum bonding.

## 2. Co-pyrolysis of carbonaceous mixed feeds

### 2.1 Biomass with other feeds

The oil obtained from pyrolysis needs upgrading due to considerable amounts of oxygen in them making them unsuitable as a fuel due to low caloric value, corrosion problems, and instability. Generally upgrading is done by addition of a catalyst, solvent and large amount hydrogen, which make the process less cost efficient due to high costs of the additions (Abnisa and Daud 2014; Lee and Kim 2015). Therefore co-pyrolysis of wastes has gained importance due to the certain synergistic effects such as higher quantity and better quality of oil or limited supply of certain feedstock which thus improves the overall pyrolysis process (Oyedun et al. 2014; Sarkar and Chowdhury 2014). Liu et al. (2013) have reported the synergistic effects of the WEEEs and biomass occurring during the co-pyrolysis due to significantly higher yield of bio-oil than individual pyrolysis of components with no formation of polybrominated dibenzo-p-dioxins. Sajdak and Muzyka (2014) have reported a reduction in heat energy requirement during co-pyrolysis of plastics with biomass thus showing synergistic effects. Xue et al. (2015) have observed an increase in the production of furan, acids and water with improved higher heating value of the resulting char due to significant synergetic effects during co-pyrolysis of red oak and high-density polyethylene (HDPE). Wang et al. (2016c) have reported an increase in gas and liquid yields but a decrease in char yield due to the synergetic effect during the co-pyrolysis of sewage sludge and wheat straw which also accelerated the pyrolysis reactions. Zhang et al. (2015c) have reported significant promotion of aromatics due to synergistic effect between corn stalk and food waste thus making catalytic co-pyrolysis an efficient method for production of aromatics and other petrochemicals.

Several studies on the products of biomass co-pyrolysis have been done. Goldfarb and Ceylan (2015) have studied the sustainability of second generation fuels by pyrolysis of highly volatile bituminous Pennsylvanian coal blended at 90,

80, and 50 wt% with one of three biomasses: feed corn stover, brewer's spent grains or cocoa shells. Paradela et al. (2009) have performed slow batch co-pyrolysis using mixtures of plastics, tires and forestry biomass wastes and found that the plastic content in the mixture affects the product yield and composition greatly. Ro et al. (2014) have performed co-pyrolysis of swine manure with agricultural plastic waste and reported the potential of using pyrolysis technology to manage two prominent agricultural waste streams (spent plastic mulch films and swine solids) along with production of value-added biochar that could be used as a power source for local farm operations. Uzun and Yaman (2014) have reported the co-pyrolysis of scrap tire and *Juglans regia* shell as environmental friendly process for production of valuable chemicals and fuels from the wastes.

Alvarez et al. (2015) have studied the co-pyrolysis of the sewage sludge and lignocellulosic biomass in a conical spouted bed reactor and reported minimization of the gas production reactions from bio-oil (mainly promoted by the catalytic activity of the ash in the sludge). Zhang et al. (2014) have carried out co-pyrolysis of pine sawdust and plastics (polyethylene, polypropylene, and polystyrene) in a catalytic fluidized bed reactor in order to improve the yield of hydrocarbons (aromatics and olefins). Zhou et al. (2015a) have conducted co-pyrolysis of three municipal solid waste (MSW) components (rice, poplar wood and PVC) and reported an increase in the generation of CO<sub>2</sub> and CO at slower rate. Zhou et al. (2015c) have co-pyrolysed polyvinyl chloride (PVC) and biomass components (hemi-cellulose, cellulose and lignin) and have reported decrease in HCl and PAH yields and significant increase in tar yield. Onal et al. (2014) have carried out co-pyrolysis of almond shell as biomass and high-density polyethylene and found that the oils produced were having higher carbon (26% higher) and hydrogen content (78% higher), lower oxygen content (%86 less) with a higher heating value (38% higher) than those of biomass oil.

Further upgrading of the product can be done by catalytic co-pyrolysis. Jin and Wang (2015) have reported equal mean temperature of mass loss

of the pyrolysis oil of rice husk and waste tires in 1:1 ratio with SBA-15 catalyst and diesel, thus showing similar evaporation properties of pyrolysis oil and diesel. Pinto et al. (2013) have reported response surface methodology as a method for prediction of liquid yields from the pyrolysis of waste mixtures consisting of 10% of pine, 10% of scrap tyres and 80% recycled plastic as a suitable method for optimizing the experimental conditions that favor the formation of desired gaseous and liquid compounds. Yao et al. (2015) have reported ZSM-5 modification with P and P/Ni for improvement of catalyst's activity and life time for co-pyrolysis of biomass and plastics. Zhang et al. (2015b) have reported catalytic co-pyrolysis of corn stalk and high density polyethylene (HDPE) over HZSM-5 zeolite catalyst for promoting efficient production of aromatic hydrocarbons. Luo and Fu (2015) have reported the use of biomass tar for the production of directly reduced iron by co-pyrolysis of biomass tar and iron ore fines. Zhang et al. (2015e) have carried out co-pyrolysis of sewage sludge and biomass in a vacuum reactor and reported higher gas yield of the blend fuel than both the individual parent fuels thus approving the method feasible for fuel production. Zhang et al. (2011) have studied fraction distribution of heavy metals in co-pyrolysis of sewage sludge and corn straw and reported that the carbon residues obtained were nonhazardous and safe.

## 2.2 Coal and RDF with other feeds

Co-pyrolysis with coal is a good waste management option due to high energy obtained during pyrolysis as well as co-pyrolysis of the coal (Coimbra et al. 2015). The composition and quantity of products during these processes depend greatly on the coal type, pyrolysis temperature and heating method (Ding et al. 2015). The evolution of gases is increased by rising the temperature and longer residence time resulting into secondary cracking of tar and gaseous hydrocarbons (Reichel et al. 2015). During coal pyrolysis, there is a decrease in the differences in the nitrogen distribution in the char precursors to the extent that it cannot influence the formation of nitrogen oxides during combustion of chars significantly (Pels et al. 1995). The formation of  $\text{NH}_3$  can be promoted by the presence of NaOH, KOH and  $\text{Ca}(\text{OH})_2$

which however suppresses HCN formation (Ohtsuka et al. 1997). Similarly, sulfur containing gases are evolved during coal pyrolysis and co-pyrolysis (Calkins 1987; Cleyle et al. 1984). Wang et al. (2016a) have reported  $\text{CO}_2$  atmosphere to be very beneficial for release of  $\text{H}_2\text{S}$ , COS and  $\text{SO}_2$  into gas phase during pyrolysis, thus removing the sulfur from coals. Pyrolysis of refuse derived fuel (RDF) which is generated from municipal solid waste treatment plants is a temperature dependent energy recovery process (Manyà et al. 2015; Tippayawong et al. 2008).

Bicakova and Straka (2016) have co-pyrolysed waste tire/coal mixtures and reported the production of smokeless fuel/carbonaceous sorbent along with a high yield of tar and gases with high amount of hydrogen and methane. Melendi-Espina et al. (2015) have reported synergistic effect between coal and plastic wastes which changed the composition of the volatiles evolved, promoted interactions between the components and had negative effects on coal fluidity. Montiano et al. (2016) have carried out pyrolysis of two types of coals, sawdust and coal tar and reported independent thermal decomposition of the components without any apparent synergism and Alias et al. (2012) also found similar results during co-pyrolysis of the coal and Refuse Derive Fuel (RDF). Lei et al. (2016) have reported pretreatment of lignite coal with ionic liquids at low temperature leading to the increase in yield of oil fractions in the products. Tyler (1980) have reported flash pyrolysis of bituminous coal in a small scale fluidized bed reactor with an increase in the yield of  $\text{CH}_4$  in  $\text{H}_2$  atmosphere. Rizkiana et al. (2016) have reported an improvement in the quality of co-pyrolysis oil of low-rank coal and biomass in presence of Mg-modified ultra-stable Y type zeolite. Whyte et al. (2015) have reported the formation of catalytic bio-oil from pyrolysis of RDF char and oyster shell with similar density, heating value and viscosity as conventional diesel fuel. Tang et al. (2015) have reported an interactive effect during co-pyrolysis of Shenmu coal and cotton stalk leading to an increased tar yield. Vamvuka et al. (2003) pyrolysed olive kernel, forest and cotton residues mixed with lignite coal and reported higher thermochemical reactivity which make them 'solid biofuels'

which can produce faster and higher quantity of volatile compounds in fast kinetics.

### 2.3 Municipal solid wastes

Pyrolysis of municipal solid wastes is an attractive alternative to incineration for energy and resource recovery (Chen et al. 2014). The product yield and composition is affected largely by the feedstock, the pyrolysis temperature, the heating rate and the type of reactor adopted (Han et al. 2015; Nurul Islam et al. 2005). Several studies have been reported for the influence of synergetic interactions during co-pyrolysis of various feeds. Zuo et al. (2014) have conducted co-pyrolysis of sewage sludge and popular sawdust and reported characteristic change in the top phase oil due to the synergetic reactions that took place during co-pyrolysis. Zhou et al. (2014) have co-pyrolysed orange peel, tissue paper and PVC from MSW and reported that the production of alkyls and alkenes was inhibited during pyrolysis at low temperature and residue increased. Zhou et al. (2015b) have reported intense interactions between PVC and rice, poplar wood, tissue paper, wool, terylene, and rubber powder during their co-pyrolysis leading to promotion of low temperature pyrolysis. Fang et al. (2015) have co-pyrolysed paper sludge and municipal solid wastes in different proportions and different heating rates and reported an increase in the initial temperature with increase in paper sludge proportion. Ren et al. (2009) have conducted co-pyrolysis of cotton stalk and municipal solid wastes with high ash content and low calorific value and reported an increase in weight loss as well as  $\text{NH}_3$  emissions with an increase in mass proportion of stalk. Wang et al. (2016b) have reported co-pyrolysis of microalgae and sewage sludge as a promising way to decrease feedstock cost and realize alternative fuel production and to avoid the high ash content and low heat value.

A few negative synergistic effects have also been reported in literature. Kim et al. (2010) have reported negligible interactions between the components of the feed during the co-pyrolysis of different components of municipal solid wastes (polyethylene, cellulose, lignin and sawdust from vinal wood). Wu et al. (1997) have reported insignificant effect of interactions on the rate of pyrolysis of paper mixture from

municipal solid wastes. Chen et al. (2016b) have reported negative synergistic effects during the co-pyrolysis of pork and polypropylene leading to hindered rate of pork pyrolysis and lower weight loss of the blends than the individual feeds. Fang et al. (2016) have studied the effect of MgO (magnesium oxide),  $\text{Al}_2\text{O}_3$  (alumina) and ZnO (zinc oxide) additives and reported reduction of initial temperatures and activation energies. AlOthman et al. (2011) have reported the formation of activated carbon with high adsorption efficiency during co-pyrolysis of mixed solid wastes (biomass, cartons and polystyrene) at low carbonization temperatures. Cao et al. (2014) have developed a novel and improved waste pyrolysis test system with efficient rotary pyrolysis kiln working and high calorific power composite gas generation efficiency.

### CONCLUSION

Pyrolysis can be universally applied to all sorts of carbonaceous wastes with excellent energy and material recovery. The products obtained can not only be used as fuels due to their high calorific value, but also can be a source of many valuable chemicals required in industry. Due to mass and volume reduction to great extent, it can lessen the pressure on land resources caused due to landfilling while the reaction time is very short and hence can be used in small systems with high throughput. Further research is required product upgrading and commercialization of the process. Co-pyrolysis can provide cheap and assuring approach for this purpose. More studies on the interactions of feeds during co-pyrolysis are required. The presence of halides, sulfides and heavy metals in the products can pose a severe challenge to the use of these products. Use of catalyst, microwave assisted heating, various pretreatment processes, efficient reactor design and optimum reaction conditions can improve the quality as well quantity of the desired products.

## REFERENCES

- Abnisa, F. Daud, WMAW. 2014, 'A review on co-pyrolysis of biomass: An optional technique to obtain a high-grade pyrolysis oil', *Energy Convers Manage*, vol.87, pp.71-85.
- Adebanjo, A., Kulkarni, MG., Dalai, AK., Bakhshi, NN., 2007, 'Pyrolysis of waste fryer grease in a fixed-bed reactor', *Energ Fuel*, vol.21, pp.828-835.
- Aguado, J., Serrano, DP., Escola, JM., 2008, 'Fuels from Waste Plastics by Thermal and Catalytic Processes', *A Review Industrial & Engineering Chemistry Research*, vol.47, pp.7982-7992
- Ahmed, I. Gupta, AK. 2009, 'Syngas yield during pyrolysis and steam gasification of paper', *Applied Energy*, vol.86, pp.1813-1821.
- Aho, A., Kumar, N., Eränen, K., Salmi, T., Hupa, M., Murzin, DY., 2007, 'Catalytic pyrolysis of biomass in a fluidized bed reactor: influence of the acidity of H-beta', *zeolite Process Safety and Environmental Protection*, vol. 85, pp.473-480.
- Alias, AB., Rashid, ZA., Abdul Rahman, N., Wan, Ab., Karim Ghani, WA., 2012, 'Thermal behaviour study of senakin coal and Refuse Derived Fuel (RDF) blends during pyrolysis using thermogravimetric analysis', *International Journal of Environment and Waste Management*, vol.10, pp.354-364.
- AlOthman, Z., Habila, M., Ali, R., 2011, 'Preparation of activated carbon using the copyrolysis of agricultural and municipal solid wastes at a low carbonization temperature carbon', *International Conference on Biology, Environment and Chemistry (IPCBE)*, vol.24,
- Alvarez, J., Amutio, M., Lopez, G., Bilbao, J., Olazar, M., 2015, 'Fast co-pyrolysis of sewage sludge and lignocellulosic biomass in a conical spouted bed reactor', *Fuel*, vol.159, pp.810-818.
- Alvarez, J., Lopez, G., Amutio, M., Bilbao, J., Olazar, M., 2014, 'Upgrading the rice husk char obtained by flash pyrolysis for the production of amorphous silica and high quality activated carbon', *Bioresour Technol*, vol.170 pp.132-137.
- Antonakou, E., Lappas, A., Nilsen, MH., Bouzga, A., Stöcker, M., 2006, 'Evaluation of various types of Al-MCM-41 materials as catalysts in biomass pyrolysis for the production of bio-fuels and chemicals', *Fuel*, vol.85, pp.2202-2212.
- Arsova, L., Van Haaren, R., Goldstein, N., Kaufman, SM., Themelis, NJ. 2008, '16th NATIONWIDE SURVEY-THE STATE OF GARBAGE IN AMERICA- Latest national data on municipal solid management--29 percent recycled and composted, 7 percent combusted in waste-to-energy plants and 64 percent landfilled', *BioCycle*. vol.49, no.12. pp.22.
- Ashworth, DC., Elliott, P., Toledano, MB., 2014, 'Waste incineration and adverse birth and neonatal outcomes: a systematic review', *Environ Int*, vol.69, pp.120-132.
- Babich, I., Van der Hulst, M., Lefferts, L., Moulijn, J., O'Connor, P., Seshan, K., 2011, 'Catalytic pyrolysis of microalgae to high-quality liquid bio-fuels', *Biomass Bioenergy*, vol.35, pp.3199-3207.
- Banks, SW., Nowakowski, DJ., Bridgwater, AV., 2014, 'Fast pyrolysis processing of surfactant washed Miscanthus', *Fuel Process Technol*, vol.128, pp.94-103.
- Barişçi, S. Öncel, MS. 2014, 'The Disposal of combed cotton wastes by pyrolysis', *International Journal of Green Energy*, vol.11, pp.255-266.
- Barth, T., Kleinert, M. 2008, 'Motor fuels from biomass pyrolysis', *Chemical engineering & technology*. vol.31, pp.773-781.
- Bernard, C., Guido, P., Colin, J., Le Dû-Delepierre, A. 1996, 'Estimation of the hazard of landfills through toxicity testing of leachates—I. Determination of leachate toxicity with a battery of acute tests', *Chemosphere* vol. 33, no. 11, pp.2303-2320.
- Bhuiyan, M., Ota, M., Murakami, K., Yoshida, H., 2009, 'Pyrolysis kinetics of newspaper and its gasification', *Energy Sources Part A: Recovery, Utilization, and Environmental Effects*, vol.32, pp.108-118.
- Bicakova, O., Straka, P. 2016, 'Co-pyrolysis of waste tire/coal mixtures for smokeless fuel, maltenes and hydrogen-rich gas production', *Energy Convers Manage*. vol.116, pp.203-213.
- Biswal, B., Kumar, S., Singh, R. 2013, 'Production of hydrocarbon liquid by thermal pyrolysis of paper cup waste', *Journal of Waste Management*, 731858.
- Blazsó, M. 1997, 'Recent trends in analytical and applied pyrolysis of polymers', *J Anal Appl Pyrolysis*, vol.39, pp.1-25.
- Boateng, AA., Elkasabi, Y., Mullen, CA., 2016, 'Guayule (parthenium argentatum) pyrolysis biorefining: fuels and chemicals contributed from guayule leaves via tail gas reactive pyrolysis', *Fuel*, vol. 163, pp.240-247.
- Bok, JP., Choi, YS., Choi, SK., Jeong, YW., 2014, 'Fast pyrolysis of Douglas fir by using tilted-slide reactor and characteristics of biocrude-oil fractions', *Renewable Energy*, vol. 65, pp.7-13.
- Bridgwater, A. 1996, 'Production of high grade fuels and chemicals from catalytic pyrolysis of biomass', *Catal Today*. vol. 29, pp.285-295.
- Bridgwater, AV. Bridge, SA. 1991, 'A Review of Biomass Pyrolysis and Pyrolysis Technologies. In: Bridgwater AV, Grassi G (eds) Biomass Pyrolysis Liquids Upgrading and Utilization', *Springer Netherlands, Dordrecht*. pp.11-92.
- Bulushev, DA. Ross, JRH. 2011, 'Catalysis for conversion of biomass to fuels via pyrolysis and gasification', *A review Catal Today*, vol. 171, pp.1-13.
- Butler, E., Devlin, G., McDonnell, K., 2011a, 'Waste Polyolefins to Liquid Fuels via Pyrolysis: Review of Commercial State-of-the-Art and Recent Laboratory

- Research', *Waste and Biomass Valorization*, vol. 2, pp.227-255.
- Butler, E., Devlin, G., Meier, D., McDonnell, K., 2011b, 'A review of recent laboratory research and commercial developments in fast pyrolysis and upgrading', *Renewable and Sustainable Energy Reviews*, vol. 15, pp.4171-4186.
- Buzetzki, E., Rimarčík, J., Cvengrošová, Z., Kleinová, A., Sarközy, I., Cvengroš, J., 2012, 'Liquid Fuels from Biomass Cracking', *Procedia Engineering*. vol.42, pp.1133-1136.
- Calisto, V., Ferreira, CIA., Santos, SM., Gil, MV., Otero, M., Esteves, VI., 2014, 'Production of adsorbents by pyrolysis of paper mill sludge and application on the removal of citalopram from water', *Bioresour Technol*. vol. 166, pp.335-344.
- Calkins, WH. 1987, 'Investigation of organic sulfur-containing structures in coal by flash pyrolysis experiments', *Energ Fuel*, vol. 1, pp.59-64.
- Cameron, RD. Koch, FA. 1980, 'Trace Metals and Anaerobic Digestion of', *Leachate Journal (Water Pollution Control Federation)*. vol. 52, pp.282-292.
- Cao, W., Zha, WW., Ni, WL. 2014, 'A design of pyrolysis test system based on the co-processing of municipal waste with rotary klin', *Appl Mech Mater*. vol. 675-677, pp.693-697.
- Chaiya, C. Reubroycharoen, P. 2013, 'Production of Bio Oil from Para Rubber Seed', *Using Pyrolysis Process Energy Procedia*, vol.34, pp.905-911.
- Chen, D., Yin, L., Wang, H., He, P., 2014, 'Pyrolysis technologies for municipal solid waste A review', *Waste Manage (Oxford)*. vol.34, pp.2466-2486.
- Chen, D., Zheng, Z., Fu, K., Zeng, Z., Wang, J., Lu, M., 2015, 'Torrefaction of biomass stalk and its effect on the yield and quality of pyrolysis products', *Fuel*, vol. 159, pp.27-32.
- Chen, F., Wu, C., Dong, L., Vassallo, A., Williams, PT., Huang, J., 2016a, 'Characteristics and catalytic properties of Ni/CaAlO<sub>x</sub> catalyst for hydrogen-enriched syngas production from pyrolysis-steam reforming of biomass sawdust', *Applied Catalysis B: Environmental*. vol. 183, pp.168-175.
- Chen, L., Wang, SZ., Wu, ZQ., Meng, HY., Zhao, J., Lin, ZH. 2016b, 'Investigation on Thermal and Kinetic Characteristics during Pyrolysis and Co-Pyrolysis of Recovered Fuels Obtained from Municipal Solid Waste in China', *Proceedings of the Asme Power Conference*.
- Chen, T., Liu, R., Scott, NR., 2016c, 'Characterization of energy carriers obtained from the pyrolysis of white ash, switchgrass and corn stover—Biochar, syngas and bio-oil', *Fuel Process Technol*, vol. 142, pp.124-134.
- Chen, T., Wu, C., Liu, R., Fei, W., Liu, S., 2011, 'Effect of hot vapor filtration on the characterization of bio-oil from rice husks with fast pyrolysis in a fluidized-bed reactor', *Bioresour Technol*, vol. 102, pp.6178-6185.
- Chiodo, V., Zafarana, G., Maisano, S., Freni, S., Urbani, F., 2016, 'Pyrolysis of different biomass: Direct comparison among *Posidonia Oceanica*', *Lacustrine Alga and White-Pine Fuel*, vol. 164, pp.220-227.
- Cleyle, PJ., Caley, WF., Stewart, L., whiteway, SG. 1984, 'Decomposition of pyrite and trapping of sulphur in a coal matrix during pyrolysis of coal', *Fuel*, vol. 63, pp.1579-1582.
- Coimbra, RN., Paniagua, S., Escapa, C., Calvo, LF., Otero, M., 2015, 'Thermogravimetric analysis of the co-pyrolysis of a bituminous coal and pulp mill sludge', *J Therm Anal Calorim*. vol. 122, pp.1385-1394.
- Crowley, D., et al. 2003, 'Health and environmental effects of landfilling and incineration of waste-A literature review', *Dublin Institute of Technology*.
- Damartzis, T. Zabaniotou, A. 2011, 'Thermochemical conversion of biomass to second generation biofuels through integrated process design', *A review Renewable and Sustainable Energy Reviews*, vol. 15, pp.366-378.
- Demirbas, A. 2009, 'Fuel properties of pyrolysis oils from biomass', *Energy Sources Part A*, vol. 31, pp.412-419.
- Demirbaş, A. 2002, 'Utilization of urban and pulping wastes to produce synthetic fuel via pyrolysis', *Energy sources*, vol. 24, pp.205-213.
- Demirbaş, A. 2005, 'Hydrogen Production via Pyrolytic Degradation of Agricultural Residues', *Energy Sources*, vol. 27, pp.769-775.
- Demirbas, A. Arin, G. 2002, 'An overview of biomass pyrolysis', *Energy sources*, vol. 24, pp.471-482.
- Demirbas, M. 2010, 'Characterization of bio-oils from spruce wood (*Picea orientalis* L.) via pyrolysis', *Energy Sources, Part A: Recovery, Utilization, and Environmental Effects*. vol. 32, pp.909-916.
- Devi, P., Saroha, AK. 2015, 'Effect of pyrolysis temperature on polycyclic aromatic hydrocarbons toxicity and sorption behaviour of biochars prepared by pyrolysis of paper mill effluent treatment plant sludge', *Bioresour Technol*, vol. 192, pp.312-320.
- Ding, L., Zhou, Z., Dai, Z., Yu, G. 2015, 'Effects of coal drying on the pyrolysis and in-situ gasification characteristics of lignite coals', *Applied Energy*. vol. 155, pp.660-670.
- Effendi, A., Gerhauser, H., Bridgwater, AV. 2008, 'Production of renewable phenolic resins by thermochemical conversion of biomass a review', *Renewable and Sustainable Energy Reviews*, vol. 12, pp.2092-2116.
- El-Fadel, M., Findikakis, AN., Leckie, JO. 1997, 'Environmental Impacts of Solid Waste Landfilling', *Journal of Environmental Management*, vol. 50, pp.1-25.

- Fang, SW., Yu, ZS., Lin, Y., Lin, YS., Fan, YL., Liao, YF., Ma, XQ. 2016, 'Effects of additives on the co-pyrolysis of municipal solid waste and paper sludge by using thermogravimetric analysis', *Bioresour Technol*, vol. 209, pp.265-272.
- Fang, SW., Yu, ZS., Lin, YS., Hu, SC., Liao, YF., Ma, XQ., 2015, 'Thermogravimetric analysis of the co-pyrolysis of paper sludge and municipal solid waste', *Energy Convers Manage*, vol. 101, pp.626-631.
- Fonts, I., Gea, G., Azuara, M., Ábrego, J., Arauzo, J., 2012, 'Sewage sludge pyrolysis for liquid production a review', *Renewable and Sustainable Energy Reviews*, vol. 16, pp.2781-2805.
- French, R., Czernik, S., 2010, 'Catalytic pyrolysis of biomass for biofuels production', *Fuel Process Technol*, vol. 91, pp.25-32.
- Galadima, A., Muraza, O. 2015, 'In situ fast pyrolysis of biomass with zeolite catalysts for bioaromatics/gasoline production a review', *Energy Convers Manage*, vol.105, pp.338-354.
- Gerçel, H. Gerçel, Ö. 2007, 'Bio-oil production from an oilseed by-product: fixed-bed pyrolysis of olive cake', *Energy Sources Part A*, vol. 29, pp.695-704.
- Gil, R., Girón, R., Lozano, M., Ruiz, B., Fuente, E. 2012, 'Pyrolysis of biocollagenic wastes of vegetable tanning. Optimization and kinetic study', *J Anal Appl Pyrolysis*, vol. 98, pp.129-136.
- Goldfarb, JL. Ceylan, S. 2015, 'Second-generation sustainability: Application of the distributed activation energy model to the pyrolysis of locally sourced biomass-coal blends for use in co-firing scenarios', *Fuel*, vol. 160, pp.297-308.
- Guha, R., Das, D., Grover, P., Guha, B. 1987, 'Germicidal activity of tar distillate obtained from pyrolysis of rice husk', *Biological wastes* .vol. 21, pp.93-100.
- Gupta, AK., Muller, P. 1999, 'Pyrolysis of Paper and Cardboard in Inert and Oxidative Environments', *J Propul Power*, vol. 15, pp. 187-194.
- Han, R., Zhao, C., Liu, J., Chen, A., Wang, H., 2015, 'Thermal characterization and syngas production from the pyrolysis of biophysical dried and traditional thermal dried sewage sludge', *Bioresour Technol*, vol. 198, pp.276-282.
- Heo, HS. Et al. 2010, 'Fast pyrolysis of rice husk under different reaction conditions', *Journal of Industrial and Engineering Chemistry*, vol. 16, pp.27-31.
- Homma, H., Homma, H., Idris, M. 2013, 'Wood Pyrolysis in Pre-Vacuum Chamber', *Journal of Sustainable Bioenergy Systems*. vol.3, pp.243.
- Hu, S., Xiang, J., Sun, L., Xu, M., Qiu, J., Fu, P. 2008, 'Characterization of char from rapid pyrolysis of rice husk', *Fuel Process Technol*, vol. 89, pp.1096-1105.
- Isahak, WNRW., Hisham, MWM., Yarmo, MA., Yun Hin,T-y. 2012, 'A review on bio-oil production from biomass by using pyrolysis method Renewable and Sustainable', *Energy Reviews*, vol. 16, pp. 5910-5923.
- Jahirul, M., Rasul, M., Chowdhury, A., Ashwath, N. 2012, 'Biofuels Production through Biomass Pyrolysis A Technological Review', *Energies*, vol. 5, pp.4952.
- Jain, A., Rao, TR., Sambhi, S., Grover, P. 1994, 'Energy and chemicals from rice husk', *Biomass Bioenergy*, vol. 7, pp.285-289.
- Ji-Lu, Z. 2007, 'Bio-oil from fast pyrolysis of rice husk: Yields and related properties and improvement of the pyrolysis system', *J Anal Appl Pyrolysis*, vol. 80, pp.30-35.
- Ji, LJ., Lu, SY., Yang, J., Du, CC., Chen, ZL., Buekens, A., Yan, JH. 2016, 'Municipal solid waste incineration in China and the issue of acidification a review', *Waste Management & Research*, vol. 34, pp.280-297.
- Jiang, J., Ma, X. 2011, 'Experimental research of microwave pyrolysis about paper mill sludge', *Appl Therm Eng*, vol. 31, pp.3897-3903.
- Jin, L., Wang, L. 2015, 'Comparison of the Catalyzed Evaporation of Bio-oils From the Co-pyrolysis of Rice Husk and Waste Tires', *Energ Source Part A*. vol. 37, pp.2655-2661.
- Jones, DA., Lelyveld, TP., Mavrofidis, SD., Kingman, SW., Miles, NJ. 2002, 'Microwave heating applications in environmental engineering—a review', *Resources, Conservation and Recycling*, vol. 34, pp.75-90.
- Khor, K., Lim, K., Alimuddin, ZZ. 2010, 'Laboratory-scale pyrolysis of oil palm trunks', *Energy Sources Part A: Recovery, Utilization, and Environmental Effects*, vol. 32, pp.518-531.
- Kim, M., Buonomo, E., Bonelli, P., Cukierman, A. 2010, 'The thermochemical processing of municipal solid wastes: Thermal events and the kinetics of pyrolysis', *Energy Sources Part A: Recovery, Utilization, and Environmental Effects*. vol. 32, pp.1207-1214.
- Kim, SW. et al. 2013, 'Bio-oil from the pyrolysis of palm and Jatropha wastes in a fluidized bed', *Fuel Process Technol*, vol. 108, pp.118-124.
- Kjeldsen, P., Barlaz, MA., Rooker, AP., Baun, A., Ledin, A., Christensen, TH. 2002, 'Present and long-term composition of MSW landfill leachate a review', *Critical Reviews in Environmental Science and Technology*, vol. 32, pp.297-336.
- Kolokolova, O. Levi, T. Pang, S. Herrington, P. 2013, 'TORREFACTION AND PYROLYSIS OF BIOMASS WASTE IN CONTINUOUS REACTORS', *Proceedings of the 13th International Conference on Environmental Science and Technology, Greece, 5-7 September*
- Krishna, BB., Singh, R., Bhaskar, T. 2015, 'Effect of catalyst contact on the pyrolysis of wheat straw and wheat husk', *Fuel*, vol. 160, pp.64-70.
- Kunkes, EL., Simonetti, DA., West, RM., Serrano-Ruiz, JC., Gärtner, CA., Dumesic, JA., 2008, 'Catalytic conversion of biomass to monofunctional hydrocarbons and targeted liquid-fuel classes', *Science*, vol. 322, pp. 417-421.



- Lam, S.S., Chase, H.A, 2012, 'A review on waste to energy processes using microwave pyrolysis', *Energies*, vol. 5, pp.4209-4232.
- Le Brech, Y., Jia, L., Cissé, S., Mauviel, G., Brosse, N., Dufour, A. 2015, 'Mechanisms of biomass pyrolysis studied by combining a fixed bed reactor with advanced gas analysis', *J Anal Appl Pyrolysis*, vol. 117, pp.334-346.
- Lee, J.W., Hawkins, B., Day, D.M., Reicosky, D.C. 2010, 'Sustainability: the capacity of smokeless biomass pyrolysis for energy production, global carbon capture and sequestration', *Energy & environmental science*, vol. 3, pp.1695-1705.
- Lee, S., Kim, T.Y. 2015, 'Feasibility study of using wood pyrolysis oil-ethanol blended fuel with diesel pilot injection in a diesel engine', *Fuel*, vol. 162, pp.65-73.
- Lee, Y.R., Choi, H.S., Park, H.C., Lee, J.E. 2015, 'A numerical study on biomass fast pyrolysis process: A comparison between full lumped modeling and hybrid modeling combined with CFD', *Computers & Chemical Engineering*, vol. 82, pp.202-215.
- Lei, Z. et al. 2016, 'Pyrolysis of lignite following low temperature ionic liquid pretreatment', *Fuel*, vol.166, pp.124-129.
- Li, H., Han, K., Wang, Q., Lu, C. 2015a, 'Pyrolysis of rice straw with ammonium dihydrogen phosphate: Properties and gaseous potassium release characteristics during combustion of the products', *Bioresour Technol*, vol.197, pp.193-200.
- Li, L., Zhang, H., Zhuang, X. 2005, 'Pyrolysis of waste paper: characterization and composition of pyrolysis oil', *Energy Sources*, vol. 27, pp.867-873.
- Li, R., Zhong, Z., Jin, B., Zheng, A. 2012, 'Application of mineral bed materials during fast pyrolysis of rice husk to improve water-soluble organics production', *Bioresour Technol*, vol. 119, pp.324-330.
- Liu, K., Ma, X.Q., Xiao, H.M. 2010, 'Experimental and kinetic modeling of oxygen-enriched air combustion of paper mill sludge', *Waste Manage Oxford*, vol. 30, pp.1206-1211.
- Liu, W.J., Tian, K., Jiang, H., Zhang, X.S., Yang, G.X. 2013, 'Preparation of liquid chemical feedstocks by co-pyrolysis of electronic waste and biomass without formation of polybrominated dibenzo-p-dioxins', *Bioresour Technol*, vol. 128, pp.1-7.
- Lu, Q., Dong, C-q., Zhang, X-m., Tian, H-y., Yang, Y-p., Zhu, X-f. 2011, 'Selective fast pyrolysis of biomass impregnated with ZnCl<sub>2</sub> to produce furfural: analytical Py-GC/MS study', *J Anal Appl Pyrolysis*, vol. 90, pp.204-212.
- Lu, Q., Yang, X-l., Zhu, X-f. 2008, 'Analysis on chemical and physical properties of bio-oil pyrolyzed from rice husk', *J Anal Appl Pyrolysis*, vol. 82, pp.191-198.
- Lu, Y. et al. 2012, 'Characterization of a bio-oil from pyrolysis of rice husk by detailed compositional analysis and structural investigation of lignin', *Bioresour Technol*, vol. 116, pp.114-119.
- Luo, S.Y., Fu, J. 2015, 'Co-pyrolysis of biomass tar and iron ore fines for the production of direct reduced iron', *J Renew Sustain Ener*, vol. 7, 043131.
- Maiti, S., Dey, S., Purakayastha, S., Ghosh, B. 2006, 'Physical and thermochemical characterization of rice husk char as a potential biomass energy source', *Bioresour Technol*, vol. 97, pp.2065-2070
- Manyà, J.J., García-Ceballos, F., Azuara, M. 2015, 'Pyrolysis and char reactivity of a poor-quality refuse-derived fuel (RDF) from municipal solid waste', *Fuel Process Technol.* vol. 140, pp.276-2070.
- Margallo, M., Taddei MBM., Hernandez-Pellon, A., Aldaco, R. 2015, 'Environmental sustainability assessment of the management of municipal solid waste incineration residues: a review of the current situation', *Clean Technol Envir*, vol. 17, pp.1333-1353.
- Martínez, J.D., Puy N., Murillo R, García T, Navarro, M.V. Mastral, A.M. 2013, 'Waste tyre pyrolysis – A review', *Renewable and Sustainable Energy Reviews*, vol. 23, pp.179-213.
- Marttinen, S.K., Kettunen, R.H., Sormunen, K.M., Soimasuo, R.M., Rintala, J.A. 2002, 'Screening of physical-chemical methods for removal of organic material, nitrogen and toxicity from low strength landfill leachates', *Chemosphere*, vol. 46, pp.851-858.
- Meesuk, S., Cao, J-P., Sato, K., Ogawa, Y., Takarada, T. 2012, 'The effects of temperature on product yields and composition of bio-oils in hydrolysis of rice husk using nickel-loaded brown coal char catalyst', *J Anal Appl Pyrolysis*, vol. 94, pp. 238-245.
- Melendi-Espina, S., Alvarez, R., Diez, M.A., Casal, M.D. 2015, 'Coal and plastic waste co-pyrolysis by thermal analysis-mass spectrometry', *Fuel Process Technol*, vol. 137, pp.351-358.
- Méndez, A., Fidalgo, J.M., Guerrero, F., Gascó, G. 2009, 'Characterization and pyrolysis behaviour of different paper mill waste materials', *J Anal Appl Pyrolysis* vol. 86, pp.66-73.
- Mendez, A., Paz-Ferreiro, J., Araujo, F., Gasco, G. 2014, 'Biochar from pyrolysis of deinking paper sludge and its use in the treatment of a nickel polluted soil. *J Anal Appl Pyrolysis*, vol.107, pp.46-52.
- Mohan, D., Pittman, C.U., Steele, P.H. 2006a, 'Pyrolysis of wood/biomass for bio-oil: a critical review', *Energy & fuels*, vol. 20, pp.848-889.
- Mohan, D., Pittman, C.U., Steele, P.H. 2006b, 'Pyrolysis of Wood/Biomass for Bio-oil: A Critical Review', *Energy Fuel*, vol. 20, pp.848-889.
- Monte, MC., Fuente, E., Blanco, A., Negro, C. 2009, 'Waste management from pulp and paper production in the European Union', *Waste Manage (Oxford)*, vol. 29, pp.293-308.
- Montiano, MG., Diaz-Faes, E., Barriocanal, C. 2016, 'Kinetics of co-pyrolysis of sawdust, coal and tar', *Bioresour Technol*, vol. 205, pp.222-229.

- Nurul Islam, M., Nurul Islam., Rafiqul Alam Beg, M., Rofiqul Islam, M. 2005, 'Pyrolytic oil from fixed bed pyrolysis of municipal solid waste and its characterization, *Renewable Energy*, vol.30, pp.413-420
- Ohtsuka, Y., Zhiheng, W., Furimsky, E. 1997, 'Effect of alkali and alkaline earth metals on nitrogen release during temperature programmed pyrolysis of coal', *Fuel*, vol. 76, pp.1361-1367.
- Omar, H., Rohani, S. 2015, 'Treatment of landfill waste leachate and landfill gas : A review, *Front Chem Sci Eng*, vol. 9, pp.15-32.
- Onal, E., Uzun, BB., Putun, AE. 2014, 'Bio-oil production via co-pyrolysis of almond shell as biomass and high density polyethylene', *Energy Convers Manage*, vol. 78, pp.704-710.
- Oyedun, AO., Gebreegziabher, T., Ng, DK., Hui, CW. 2014, 'Mixed-waste pyrolysis of biomass and plastics waste, A modelling approach to reduce energy usage', *Energy*, vol. 75, pp.704-710/
- Paethanom, A., Yoshikawa, K. 2012, 'Influence of pyrolysis temperature on rice husk char characteristics and its tar adsorption capability', *Energies*, vol. 5, pp.704-710.
- Paradela, F., Pinto, F., Ramos, AM., Gulyurtlu, I., Cabrita, I., 2009, 'Study of the slow batch pyrolysis of mixtures of plastics, tyres and forestry biomass wastes', *J Anal Appl Pyrolysis*, vol. 85, pp.392-398.
- Park, J., Lee, Y., Ryu, C., Park, Y-K. 2014, 'Slow pyrolysis of rice straw: Analysis of products properties, carbon and energy yields', *Bioresour Technol*, vol. 155, pp.63-70.
- Pattiya, A. 2011, 'Bio-oil production via fast pyrolysis of biomass residues from cassava plants in a fluidised-bed reactor', *Bioresour Technol*, vol. 102, pp.1959-1967.
- Pels, JR., Kapteijn, F., Moulijn, JA., Zhu, Q., Thomas, KM. 1995, 'EVOLUTION OF NITROGEN FUNCTIONALITIES IN CARBONACEOUS MATERIALS DURING PYROLYSIS', *Carbon*, vol. 33, pp.1641-1653.
- Phan, AN., Ryu, C., Sharifi, VN., Swithenbank, J. 2008, 'Characterisation of slow pyrolysis products from segregated wastes for energy production, *J Anal Appl Pyrolysis*, vol. 81, pp.65-71.
- Pinto, F., Paradela, F., Gulyurtlu, I., Ramos, AM. 2013, 'Prediction of liquid yields from the pyrolysis of waste mixtures using response surface methodology', *Fuel Process Technol*, vol. 116, pp.271-283.
- Qian, Y., Zhang, J., Wang, J. 2014, 'Pressurized pyrolysis of rice husk in an inert gas sweeping fixed-bed reactor with a focus on bio-oil deoxygenation', *Bioresour Technol*, vol. 174, pp.95-102.
- Reckamp, J.M., Garrido, R.A., Satrio, J.A. 2014, 'Selective pyrolysis of paper mill sludge by using pretreatment processes to enhance the quality of bio-oil and biochar products', *Biomass Bioenergy*, vol. 71, pp.235-244.
- Reichel, D., Siegl, S., Neubert, C., Krzack, S. 2015, 'Determination of pyrolysis behavior of brown coal in a pressurized drop tube reactor', *Fuel*, vol. 158, pp.983-998.
- Ren. Q. et al. 2009, 'TG-FTIR study on co-pyrolysis of municipal solid waste with biomass' *Bioresour Technol*, vol. 100, pp.4054-4057.
- Ridout, A.J., Carrier, M., Collard, F.X., Gorgens, J. 2016, 'Energy conversion assessment of vacuum, slow and fast pyrolysis processes for low and high ash paper waste sludge', *Energy Convers Manage*, vol. 111, pp.103-114.
- Ridout, A.J., Carrier, M., Gorgens, J. 2015, 'Fast pyrolysis of low and high ash paper waste sludge: Influence of reactor temperature and pellet size', *J Anal Appl Pyrolysis*, vol.111, pp.64-75.
- Rizkiana, J., Guan, G., Widayatno, W.B., Yang, J., Hao, X., Matsuoka, K., Abudula, A. 2016, 'Mg-modified ultra-stable Y type zeolite for the rapid catalytic co-pyrolysis of low-rank coal and biomass', *Rsc Adv*, vol. 6, pp.2096-2105.
- Ro KS, Hunt PG, Jackson MA, Compton DL, Yates SR, Cantrell K, Chang S 2014 Co-pyrolysis of swine manure with agricultural plastic waste: Laboratory-scale study *Waste Manage Oxford* 34:1520-1528
- Roy, M.M., Dutta, A., Corscadden, K., Havard, P., Dickie, L. 2011, 'Review of biosolids management options and co-incineration of a biosolid-derived fuel', *Waste Manage Oxford*, vol. 31, pp.2228-2235
- Rushton, L. 2003. 'Health hazards and waste management', *British medical bulletin*, vol. 68, pp.183-197.
- Sannita, E., Aliakbarian, B., Casazza, A.A., Perego, P., Busca, G. 2012, 'Medium-temperature conversion of biomass and wastes into liquid products, a review', *Renewable and Sustainable Energy Reviews*, vol. 16, pp.6455-6475.
- Santos, R.M., Santos, A.O., Sussuchi, E.M., Nascimento, J.S., Lima, Á.S., Freitas, L.S. 2015, 'Pyrolysis of mangaba seed: Production and characterization of bio-oil', *Bioresour Technol*, vol. 196, pp.43-48.
- Sarkar, A., Chowdhury, R. 2014, 'Co-Pyrolysis of Paper Waste and Mustard Press Cake in a Semi-Batch Pyrolyser-Optimization and Bio-Oil Characterization', *International Journal of Green Energy*, vol. 13, no.4, pp.373-382.
- Serrano-Ruiz, J.C., Dumesic, J.A. 2011, 'Catalytic routes for the conversion of biomass into liquid hydrocarbon transportation fuels', *Energy & Environmental Science*, vol. 4, pp.83-99.
- Shen, D., Jin, W., Hu, J., Xiao, R., Luo, K. 2015, 'An overview on fast pyrolysis of the main constituents in lignocellulosic biomass to valued-added chemicals: Structures, pathways and interactions', *Renewable and Sustainable Energy Reviews*, vol. 51, pp.761-774.

- Smets, K., Adriaensens, P., Reggers, G., Schreurs, S., Carleer, R., Yperman, J. 2011, 'Flash pyrolysis of rapeseed cake: influence of temperature on the yield and the characteristics of the pyrolysis liquid', *J Anal Appl Pyrolysis*, vol. 90, pp.118-125.
- Stephanidis S, Nitsos C, Kalogiannis K, Iliopoulou E, Lappas A, Triantafyllidis K 2011 Catalytic upgrading of lignocellulosic biomass pyrolysis vapours: Effect of hydrothermal pre-treatment of biomass *Catal Today* 167:37-45
- Strezov, V., Evans, T.J. 2009, 'Thermal processing of paper sludge and characterisation of its pyrolysis products', *Waste Manage Oxford*, vol. 29, pp.1644-1648.
- Tang, C.Y., Zhang, D.X., Lu, X.L. 2015, 'Improving the Yield and Quality of Tar during Co-pyrolysis of Coal and Cotton Stalk', *Bioresources*, vol.10, pp.7667-7680.
- Thangalazhy-Gopakumar, S., Adhikari, S., Gupta, R.B., Tu, M., Taylor, S. 2011, 'Production of hydrocarbon fuels from biomass using catalytic pyrolysis under helium and hydrogen environments', *Bioresour Technol*, vol. 102, pp.6742-6749.
- Tippayawong, N., Kinorn. J., Thavornun, S, 2008,' Yields and gaseous composition from slow pyrolysis of refuse-derived fuels', *Energy Sources, Part A*, vol. 30, pp.1572-1580.
- Torri, IDV et al. 2016, 'Bio-oil production of softwood and hardwood forest industry residues through fast and intermediate pyrolysis and its chromatographic characterization', *Bioresour Technol*, vol. 200, pp.680-690.
- Tyler, R.J. 1980, 'Flash pyrolysis of coals. Devolatilization of bituminous coals in a small fluidized-bed reactor', *Fuel*, vol.59, pp.218-226.
- Uddin, M.N., Daud, W.W., Abbas, H.F. 2014, 'Effects of pyrolysis parameters on hydrogen formations from biomass: a review', *Rsc Adv*, vol.4, pp.10467-10490.
- Undri, A., Rosi, L., Frediani, M., Frediani, P. 2014b, 'Microwave assisted pyrolysis of corn derived plastic bags', *J Anal Appl Pyrolysis*, vol. 108, pp.86-97.
- Uzun, B.B., Yaman, E. 2014, 'Thermogravimetric characteristics and kinetics of scrap tyre and Juglans regia shell co-pyrolysis', *Waste Management & Research*, vol. 32, pp.961-970.
- Uzunov, I., Uzunova, S., Angelova, D., Gigova, A. 2012, 'Effects of the pyrolysis process on the oil sorption capacity of rice husk', *J Anal Appl Pyrolysis*, vol. 98, pp.166-176.
- Vamvuka, D., Kakaras, E., Kastanaki, E., Grammelis, P. 2003, 'Pyrolysis characteristics and kinetics of biomass residuals mixtures with lignite', *Fuel*, vol. 82, pp.1949-1960.
- van Velzen, D., Langenkamp, H., Herb, G. 2002, 'Review: Mercury in waste incineration', *Waste Management & Research*, vol. 20, pp.556-568.
- Vispute, T.P., Zhang, H., Sanna, A., Xiao, R., Huber, G.W. 2010, 'Renewable chemical commodity feedstocks from integrated catalytic processing of pyrolysis oils', *Science*, vol. 330, pp.1222-1227.
- Vrijheid, M. 2000, 'Health effects of residence near hazardous waste landfill sites: a review of epidemiologic literature', *Environ Health Perspect*, vol. 108, pp.101-112.
- Wang, L. et al. 2011, 'Preparation of carbon black from rice husk by hydrolysis, carbonization and pyrolysis', *Bioresour Technol*, vol. 102, pp.8220-8224.
- Wang, X., Guo, H., Liu, F., Hu, R., Wang, M. 2016a,' Effects of CO 2 on sulfur removal and its release behavior during coal pyrolysis', *Fuel*, vol. 165, pp.484-489.
- Wang, X., Zhao, B.W., Yang, X.Y. 2016b, 'Co-pyrolysis of microalgae and sewage sludge: Biocrude assessment and char yield prediction', *Energy Convers Manage*, vol. 117, pp.326-334.
- Wang, X.B., Deng, S.H., Tan, H.Z., Adeosun, A., Vujanovic, M., Yang, F.X., Duic, N, 2016c, 'Synergetic effect of sewage sludge and biomass co-pyrolysis: A combined study in thermogravimetric analyzer and a fixed bed reactor', *Energy Convers Manage*, vol. 118, pp.399-405.
- Wang, Z., Wang, F., Cao, J., Wang, J. 2010, 'Pyrolysis of pine wood in a slowly heating fixed-bed reactor: potassium carbonate versus calcium hydroxide as a catalyst', *Fuel Process Technol*, vol. 91, pp.942-950.
- White, J.E., Catallo, W.J., Legendre, B.L. 2011, 'Biomass pyrolysis kinetics: A comparative critical review with relevant agricultural residue case studies', *J Anal Appl Pyrolysis*, vol. 91, pp.1-33.
- Whyte, H.E., Loubar, K., Awad, S., Tazerout, M. 2015, 'Pyrolytic oil production by catalytic pyrolysis of refuse-derived fuels: Investigation of low cost catalysts', *Fuel Process Technol*, vol. 140, pp.32-38.
- Williams, P.T. 1990, 'A Review of Pollution from Waste Incineration', *J Inst Water Env Man*, vol. 4, pp.26-34.
- Williams, P.T., Besler, S. 1993, 'The pyrolysis of rice husks in a thermogravimetric analyser and static batch reactor', *Fuel*, vol. 72, pp.151-159.
- Williams, P.T., Nugranad, N. 2000, 'Comparison of products from the pyrolysis and catalytic pyrolysis of rice husks', *Energy*, vol. 25, pp.493-513.
- Wiszniowski, J., Robert, D., Surmacz-Gorska, J., Miksch, K., Weber, J.V. 2006, 'Landfill leachate treatment methods: A review', *Environmental Chemistry Letters*, vol. 4, pp.51-61.
- Worasuwannarak, N., Sonobe, T., Tanthapanichakoon, W. 2007, 'Pyrolysis behaviors of rice straw, rice husk, and corncob by TG-MS technique', *J Anal Appl Pyrolysis*, vol. 78, pp.265-271.
- Wu, C, et al. 2015a, 'CO 2 gasification of bio-char derived from conventional and microwave pyrolysis', *Applied Energy*, vol. 157, pp.533-539.

- Wu, C.H., Chang, C.Y., Lin, J.P. 1997, 'Pyrolysis kinetics of paper mixtures in municipal solid waste', *J Chem Technol Biotechnol*, vol. 68, pp.65-74.
- Wu, W., Mei, Y., Zhang, L., Liu, R., Cai, J. 2015b, 'Kinetics and reaction chemistry of pyrolysis and combustion of tobacco waste', *Fuel*, vol. 156, pp.71-80.
- Xie, Q. et al. 2015, 'Fast microwave-assisted catalytic co-pyrolysis of microalgae and scum for bio-oil production', *Fuel*, vol. 160, pp.577-582
- Xue, Y., Zhou, S., Brown, R.C., Kelkar, A., Bai, X. 2015, 'Fast pyrolysis of biomass and waste plastic in a fluidized bed reactor', *Fuel*, vol. 156, pp.40-46.
- Yang, H., Yan, R., Liang, D.T., Chen, H., Zheng, C. 2006, 'Pyrolysis of palm oil wastes for biofuel production', *As J Energy Env*, vol. 7, pp.315-323.
- Yang, X., Sun, L., Xiang, J., Hu, S., Su, S. 2013, 'Pyrolysis and dehalogenation of plastics from waste electrical and electronic equipment WEEE: A review', *Waste Manage Oxford*, vol. 33, pp.462-473.
- Yao, W.K. et al. 2015, 'Thermally stable phosphorus and nickel modified ZSM-5 zeolites for catalytic co-pyrolysis of biomass and plastics', *Rsc Adv*, vol. 5, pp.30485-30494.
- Yu F, Steele P, Ruan R 2010 Microwave pyrolysis of corn cob and characteristics of the pyrolytic chars Energy Sources, Part A: Recovery, Utilization, and Environmental Effects 32:475-484
- Yu, Y.H., Kim, S.D., Lee, J.M., Lee, K.H. 2002, 'Kinetic studies of dehydration, pyrolysis and combustion of paper sludge', *Energy*, vol. 27, pp.457-469.
- Zhai, M., Wang, X., Zhang, Y., Dong, P., Qi, G. 2015, 'Characteristics of rice husk tar pyrolysis by external flue gas', *Int J Hydrogen Energy*, vol. 40, pp.10780-10787.
- Zhang, B., Zhong, Z., Chen, P., Ruan, R. 2015a, 'Microwave-assisted catalytic fast pyrolysis of biomass for bio-oil production using chemical vapor deposition modified HZSM-5 catalyst', *Bioresour Technol*, vol. 197, pp.79-84.
- Zhang, B., Zhong, ZP., Ding, K., Song, Z.W. 2015b, 'Production of aromatic hydrocarbons from catalytic co-pyrolysis of biomass and high density polyethylene: Analytical Py-GC/MS study' *Fuel*, vol. 139, pp.622-628.
- Zhang, B., Zhong, ZP., Min, M., Ding, K., Xie, Q.L., Ruan, R. 2015c, 'Catalytic fast co-pyrolysis of biomass and food waste to produce aromatics: Analytical Py-GC/MS study', *Bioresour Technol*, vol. 189, pp.30-35.
- Zhang, H.Y., Nie, J.L., Xiao, R., Jin, B.S., Dong, C.Q., Xiao, G.M. 2014, 'Catalytic Co-pyrolysis of Biomass and Different Plastics Polyethylene, Polypropylene, and Polystyrene To Improve Hydrocarbon Yield in a Fluidized-Bed Reactor', *Energ Fuel*, vol. 28, pp.1940-1947.
- Zhang, QR, Zhang, SQ, Pan, TT 2011, 'Fraction Distribution Changes of Heavy Metals in Co-pyrolysis of Sewage Sludge and Corn Straw', *Adv Mater Res-Switz*, vol. 236-238, pp.187-191.
- Zhang, S., Dong, Q., Zhang, L., Xiong, Y., Liu, X., Zhu, S, 2015d, 'Effects of water washing and torrefaction pretreatments on rice husk pyrolysis by microwave heating', *Bioresour Technol* vol. 193, pp.442-448.
- Zhang, W.J., Yuan, C.Y., Xu, J., Yang, X. 2015e, 'Beneficial synergetic effect on gas production during co-pyrolysis of sewage sludge and biomass in a vacuum reactor', *Bioresour Technol*, vol. 183, pp.255-258.
- Zhang, Z. et al. 2015f, 'Low-temperature microwave-assisted pyrolysis of waste office paper and the application of bio-oil as an AI adhesive', *Green Chemistry*, vol.17, pp.260-270.
- Zhang, Z.R., Macquarrie, D.J., Aguiar, PM, Clark, JH, Matharu, AS. 2015g, 'Simultaneous Recovery of Organic and Inorganic Content of Paper Deinking Residue through Low-Temperature Microwave-Assisted Pyrolysis', *Environmental Science & Technology*, vol. 49, pp.2398-2404.
- Zheng, J-L., Kong, Y-P. 2010 'Spray combustion properties of fast pyrolysis bio-oil produced from rice husk', *Energy Convers Manage*, vol. 51, pp.182-18

# Green Synthesis of Magnetite Nanoparticles using Banana Leaves

Ravindra D. Kale\*, Sangeeta Barwar, Prerana Kane, Latika Bhatt

## ABSTRACT

In this study a simple, environment friendly and cost-effective method has been developed to synthesize metallic nanoparticles (NPs) from plant leaves. The study proposes that magnetite NPs can be synthesized using banana leaves as reducing agent. The effect of temperature and concentration of reducing agent on absorbance of solution was studied; optimization of the parameters was done using response surface methodology (RSM) as per central composite design (CCD). The results of X-ray diffraction (XRD) and Fourier Transform Infrared spectrometer (FTIR) indicated formation of iron oxide crystalline NPs in which polyols such as flavones, terpenoids and polysaccharides acted as reducing and capping agent. The characterization of synthesized magnetite NPs was also done through transmission electron microscopy (TEM), nanoparticle size analyzer and UV-Visible spectroscopy.

## KEYWORDS

Nano Particle, Green Synthesis, Banana Leaves, Metal, Magnetite

## INTRODUCTION

The advances in nano science and technology have made humans believe that it can ameliorate their current living standard (Priest 2006).

-----  
Department of Fibers and Textile Processing  
Technology  
Institute of Chemical Technology  
Nathalal Parekh Marg, Matunga (E)  
Mumbai 400019  
Maharashtra, India

\*Corresponding author; email:  
ravikale73pub@gmail.com

The specific characteristics of nanoparticles such as shape, size, and distribution can be utilized in various fields of applications, which make it a topic of interest for researchers globally (Zargar et al. 2011). The synthesis of Fe<sub>3</sub>O<sub>4</sub> nanoparticles (MFeNPs) has been carried out because of its unique properties, such as being super paramagnetic (Mahdavian & Mirrahimi 2010), biocompatible, biodegradable, and non-toxic to human beings (Wei et al. 2006; Zhao et al. 2009; Zhang et al. 2013). These properties of MFeNPs make them applicable in various areas, such as catalysis (Gwande and Varma 2013; Sharad et al. 2014), magnetic storage media (Terris & Thomson 2005), biosensors (Kavitha et al. 2013), magnetic resonance imaging (MRI) (Haw et al. 2010; Qiao & Gao 2009), and targeted drug delivery (Salem et al. 2015; Li et al. 2012; Wani et al. 2014).

MFeNPs can be fabricated through various methods such as sol-gel method (Lemine et al. 2012), solid state synthesis (Paiva et al. 2015), and flame spray synthesis (Kumfer et al. 2010). The chemical and physical methods of synthesis involve complicated procedures and are very time consuming while green synthesis method is much easier and safer to use. The green synthesis of NPs is a new scheme and researchers are still studying its outcomes. Few successful studies in synthesizing MFeNPs by using plant extract have been done before. For instance, fruit extract of *Artemisia annua* (Basavegowda et al. 2014), leaf extract of *Perillafrutescens* (Basavegowda et al. 2014), *Tridaxprocumbens* (Senthil & Ramesh 2012) and *caricaya papaya* (Latha et al. 2014), peel extract of plantain (Venkateswarlu et al. 2013), and also seed extract of grape proanthocyanidin (Narayanan et al. 2012). However, only few studies have been done

using marine plants for the synthesis of MFeNPs.

In the present work, Response Surface Methodology (RSM) is applied to see the effect of temperature and reducing agent concentration on the synthesis of MFeNPs using banana leaves as reducing agent thereby providing a green route of NPs synthesis. Synthesized NPs were then characterized using different techniques.

## RESULTS AND DISCUSSION

### Optimization

The optimization of magnetite nanoparticles was performed by 13 experiments as per Table 1 and the values of each response was measured as solution absorbance at maximum wavelength of MFeNPs.

The quadratic model was checked, using the Design- Expert 7.0, trial version for ANOVA and the results are shown in Table 2. P-values were used as a tool to check the significance of each coefficient which also indicates the interaction strength of each parameter. In the present study, the F-value (28.44276) and P-values ( $p = 0.0009$ ) indicated statistical significance of the obtained model. The degree of significance shows that the quadratic effects of temperature and concentration of reducing agent are significant; which means they can act as limiting factors and little variation in their value will alter the production rate. (Hamed et al. 2014) Value of adjusted  $R^2 = 0.9196$  suggested that total variation of 91.96% of absorbance is attributed to the independent variables and only 8.04% cannot be explained by the model.

A second-order polynomial model (equation 1) was proposed to calculate the optimum levels of dependent and independent variables and to determine the maximum MFeNP synthesis corresponding to the optimum levels of temperature and concentration of reducing agent. By applying the multiple regression analysis on experimental data, the second-order polynomial equation that defines predicted response (Absorbance) in terms of the independent variables (A, B) was obtained.

$$\text{Absorbance} = -0.19907 + 0.011524A - 0.074627B + .00105160AB - 0.0000624497A^2 + 0.00427503B^2 \dots\dots\dots(1)$$

With the increase in temperature and concentration of reducing agent, absorbance of synthesized NPs increases (Fig. 1) which indicates increase in concentration of MFeNPs. According to the RSM, the results predicted by the model showed that the maximum absorbance can be achieved when the temperature and concentration of reducing agent are set at 70.47°C and 2.5 g/100mL respectively. The maximum predicted value of absorbance obtained was 0.328339. Under suggested conditions, the mean value of the absorbance was found to be 0.3278, which is in agreement with the predicted value.

### Characterization

#### UV-Visible spectral Analysis

Fig. 2 shows the UV-visible absorption spectrum of MFeNPs synthesized using banana leaves. The absorption peak at 360 nm indicates the presence of MFeNPs. (Chaki et al. 2015).

The appearance of green to grayish black colour of colloidal solution indicates the formation of MFeNPs with the increasing time (Fig. 3). (Latha et al. 2014) The colour changes arise due to the excitation of the surface plasma resonance (SPR) phenomenon typically of MFeNPs (Shankar et al. 2004). The optical absorption spectrum of MFeNPs depends on the particle size, shape, state of aggregation and the surrounding dielectric medium. (Petla et al. 2012)

#### Particle size analysis

Dynamic Light Scattering technique, TEM and XRD technique were used for particles size analysis of MFeNPs and shown in Figs. 4a-c and Table 3. From the light scattering technique, mean particle size of the nano particle was 31 nm. (Fig. 4a). The TEM images of MFeNPs synthesized by banana leaves showed spherical morphology in (Fig. 4b) and the size ranged from 45 to 120 nm with an average diameter of 72 nm. (Fig. 4c) shows four peaks for the XRD pattern of MFeNPs at 35.7561°,

43.8031°, 54.6528° and 64.2351° with (311), (400), (422) and (440) Miller indices respectively. (JCPDS card no. 00-003-0863) (Yen et al. 2016) DOI 10.1186/s11671-016-1498-2. The synthesized particles had 19.22% of crystallinity which was calculated from the (400) peak. Thus, the MFENPs had more amorphous structure. The reason being the fast-chemical reaction during synthesis which

resulted in no clear reflection peak due to other crystalline phase, which might be present as impurity. Thus, the nano particles essentially consists of a binary mixture of the two spinel magnetic iron oxides, meaning magnetite-Fe<sub>3</sub>O<sub>4</sub> and maghemite -  $\gamma$ -Fe<sub>2</sub>O<sub>3</sub>. {Ref: Journal of Magnetism and Magnetic Materials 324 (2012) 1753–1757}}

Run	Temperature	Concentration of reducing agent (gm/100 ml)	Absorbance at 360nm	
	(° C)		Experimental	Predicted
1	50	7.5	0.3001	0.296131
2	75	7.5	0.5507	0.586254
3	50	5	0.2361	0.217654
4	75	5	0.5204	0.442052
5	50	2.5	0.1702	0.192615
6	100	2.5	0.4371	0.431898
7	100	7.5	0.8299	0.798315
8	75	5	0.4647	0.442052
9	100	5	0.5516	0.588387
10	75	5	0.4443	0.442052
11	75	2.5	0.3685	0.351287
12	75	5	0.3885	0.442052
13	75	5	0.4107	0.442052

**Table 1:** CCD experimental run of trials for synthesis of MFENPs

Source	Sum of Squares	df	Mean Square	F Value	p-value (Prob> F)
Model	0.310919	5	0.062184	28.44276	0.0002
Pure error	0.01044	4	0.00261		
R <sup>2</sup>	0.9531				
Adj. R <sup>2</sup>	91.96%				

**Table 2** Analysis of Variance (ANOVA) for optimization of synthesis of MFENPs

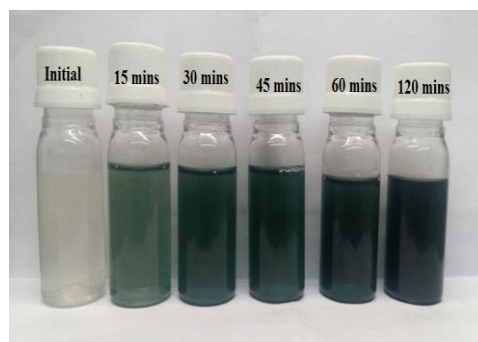
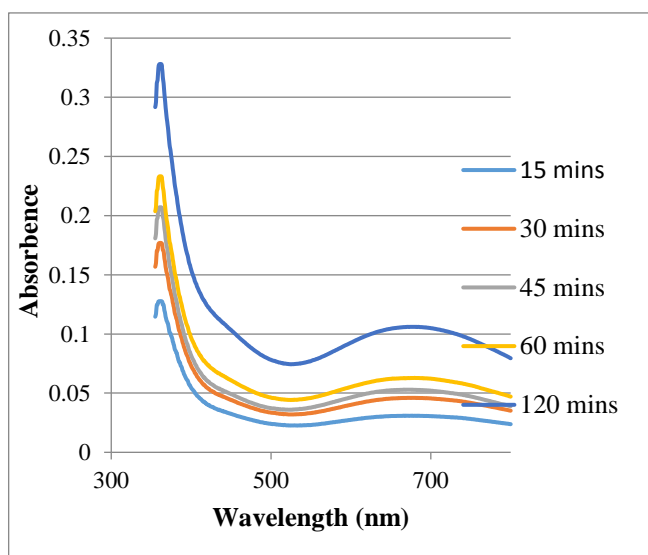
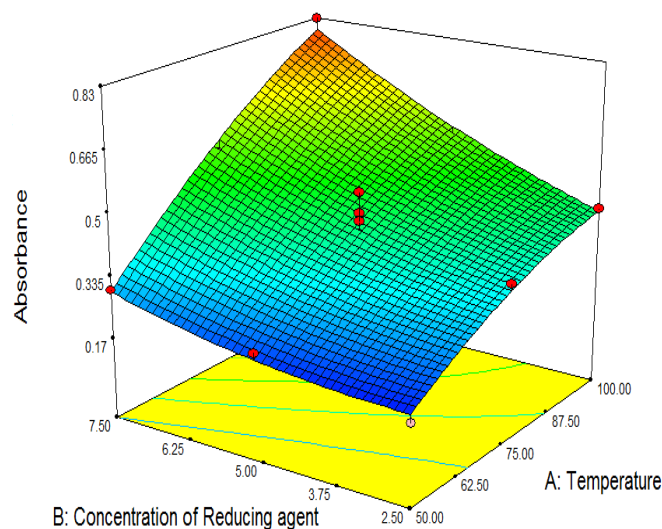


**Fig. 1** Response surface plot of Absorbance vs Temperature and concentration of reducing agent **Fig. 2** UV-Vis absorption spectrum of MFeNPs solutions at different time intervals.

**Fig. 3** Images of MFeNPs solutions at different time intervals.

The average particle size was calculated by Debye-Scherrer's formula,

$$D = \frac{0.94\lambda}{\beta \cos\theta}$$

Where  $\lambda$  is X-ray wavelength (0.15406 nm),  $\beta$  is full width at half maximum (FWHM) of the diffraction peak in radians,  $\theta$  is Bragg's diffraction angle respectively. The particle size obtained was 61.94 nm. (Prabhu et al. 2015)

The calculated particle size by the XRD, TEM and Dynamic Light Scattering technique are listed in Table 3. The differences in the particle size for these techniques may be due to the aggregation during the sample preparation. (Liu & Hurt 2010)

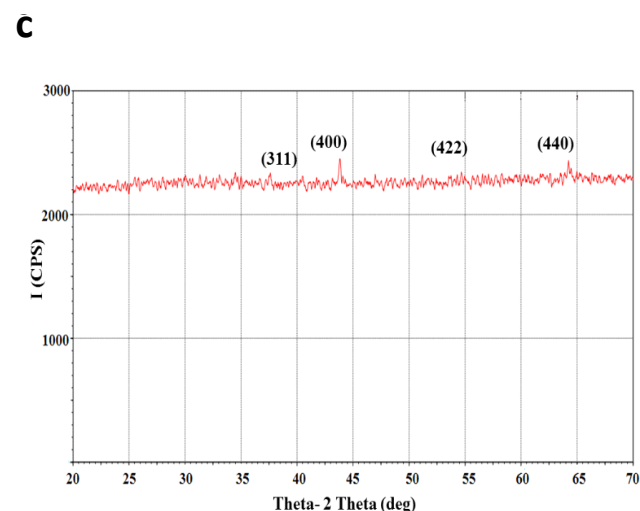
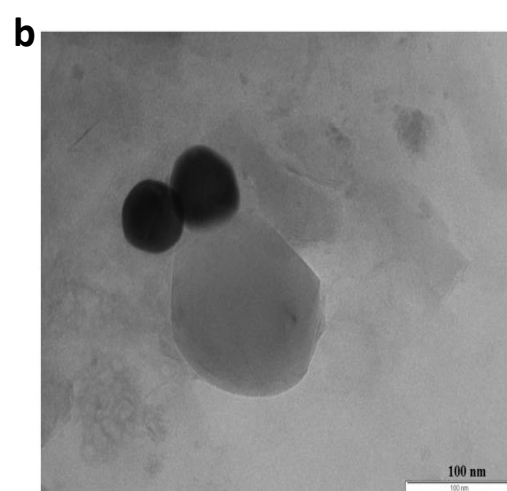
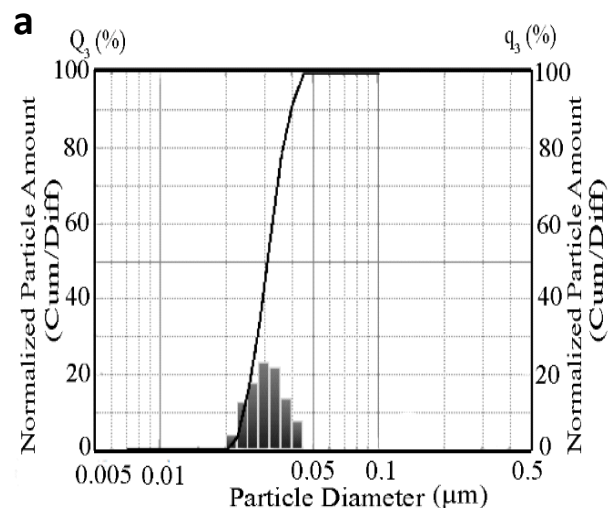
#### Energy Dispersive X-Ray analysis

Fig. 5 shows the Energy-Dispersive Absorption Spectroscopy of derived MFeNPs, which confirmed the presence of elemental iron by the signals in the range of 6 to 6.5 keV. (Muhammad et al. 2016)



Fourier transforms infrared spectroscopy

FTIR measurements were carried out to identify the possible bio-molecules responsible for the reduction of ferrous sulphate and capping of the reduced MFeNPs (Fig. 6). The banana leaves and the synthesized MFeNPs were subjected to FTIR that showed various bands, the O-H stretching around  $3400\text{cm}^{-1}$  shows the presence of hydroxyl groups from the polyols such as flavones, terpenoids and polysaccharides present in the leaf extract. The bands at  $1645\text{cm}^{-1}$  and  $1041\text{cm}^{-1}$  denotes the presence of organic material in the sample majorly contributed by banana leaves. The rational decrease in intensity of O-H stretching might be due to interaction of nanoparticles. These bands confirmed the presence of compounds like flavonoids and terpenoids and hence may be held responsible for efficient capping and stabilization of obtained magnetite nanoparticles. (Ting et al. 2014; Balamurugan et al. 2014)



**Fig. 4 a.** Particle size of MfeNPs. **b.** TEM image of MfeNPs **c.** XRD pattern of MfeNPs

**Crystallite size (nm)**

Debey-Scherrer formula	Dynamic Light Scattering technique	TEM
61.94	31	72

**Table 3** Particle size of MFeNPs calculated by different methods

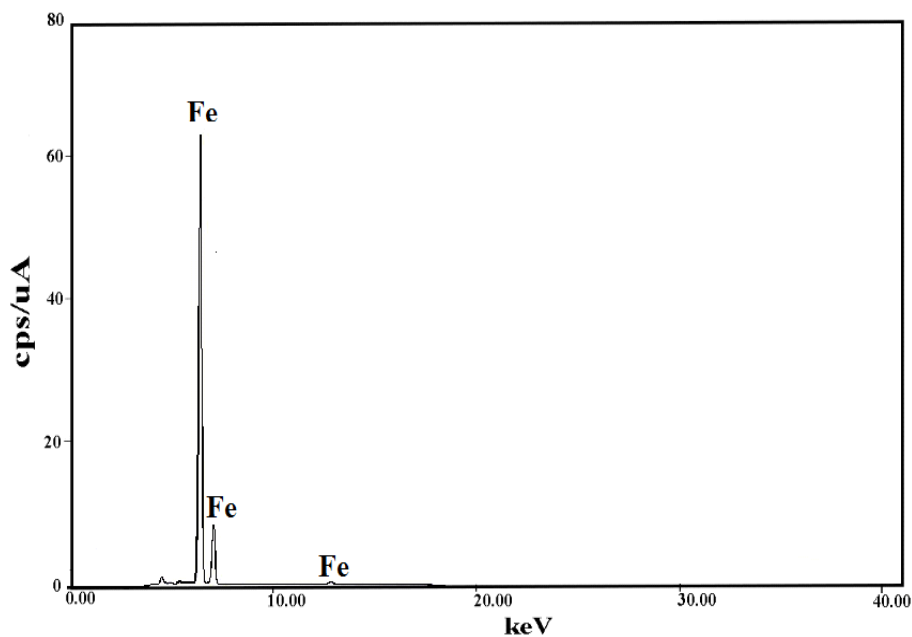


Fig. 5 EDX pattern of synthesized MFeNPs

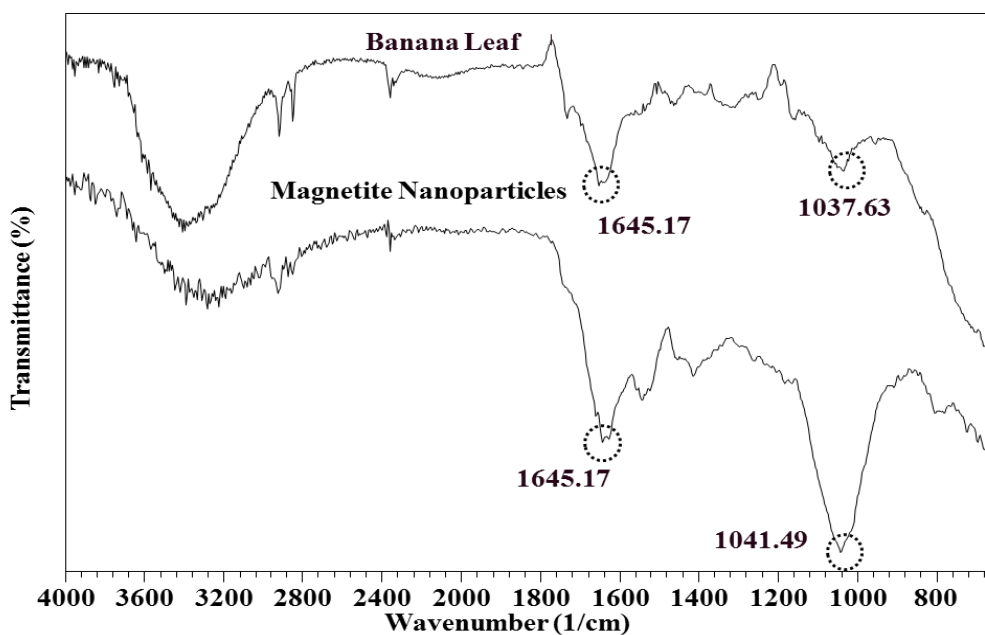


Fig. 6 FTIR spectrum of banana leaf and magnetite nanoparticles

## MATERIAL AND METHODS

### Materials

Ferrous sulphate heptahydrate  $\text{FeSO}_4 \cdot 7\text{H}_2\text{O}$  (Mol. Wt. 278.01) and acetic acid of analytical grade were obtained.

### Synthesis of MFeNPs

Banana leaves collected from the institute campus were washed with distilled water and cut into small pieces. 100 ml of 0.1 M aqueous

solutions of ferrous sulfate was prepared in a conical flask using distilled water and then pH 3 was adjusted with the help of acetic acid. In this salt solution, banana leaves were added while stirring continuously on a shaker bath machine (RossariLabtech, Mumbai, India) at 70 rpm for two hours. Experiments were carried out according to the Design of Expert 7 to study the effect of two parameters: temperature and concentration of reducing agent on

absorbance of MFeNPs. Reduction of ferrous sulphate into MFeNPs was observed through change in colour of solution from light yellow to greyish black, confirming the formation of NPs (Latha et al. 2014). After complete reduction of the ferrous sulphate, the solution was filtered through nylon mesh. The residual solution which contained NPs was centrifuged for 15 min at 12,000 rpm later washed with distilled water and then dried in oven at 80 °C.

### Experimental Design

When the design economy and precise prediction variance are desired the use of second-order designs such as central composite design (CCD) plays vital role. In the present study, central composite design was used to study the effect of independent variables, *i.e.* temperature and concentration of reducing agent on the response (absorbance of MFeNPs).

### Characterization

UV-Visible spectrophotometer (UV-1800 ENG 240 V, Shimadzu, Japan) was used for the analysis of synthesized MFeNPs periodically as a function of time in the wavelengths ranging from 200-800 nm with a resolution of 1 nm. The particle size analysis was done using nano particle size analyser (SALD 7500 nano, Shimadzu, Japan). Surface morphology was studied with transmission electron microscopy (Phillips TEM-200 Supertwin STEM, accelerating voltage-200kV, resolution-0.23 nm). Crystallographic study of NPs was carried out using X-ray diffractometer (Shimadzu XRD-6100, Japan) with CuK  $\alpha$  radiation from 40kV/30mA using the  $2\theta$  range of 20–70°. Chemical functional group identification on MFeNPs was determined using FTIR (FTIR 8400S Shimadzu, Japan) in the spectral range of 750-4000  $\text{cm}^{-1}$  and elemental analysis was done in the Na-U channel using EDAX (EDX-720, Shimadzu, Japan).

### CONCLUSION

MFeNPs were successfully synthesized using banana leaves as a reducing agent. The protein present in banana leaves was responsible for reduction of ferrous sulphate into MFeNPs which is also present on the surface of

nanoparticle and provide stability. The formation of nanoparticles was accompanied with change colour of the solution from light yellow to grayish black giving absorbance peak at 360 nm in UV-visible spectroscopy. For maximum absorbance (0.328339) the optimized conditions were 70.47°C temperature and 2.5 gm/100mL concentration of reducing agent as per CCD. The MFeNPs formed were of predominantly spherical in shape and crystalline in nature with crystallinity of 19.2212%. The average particle size of magnetite nanoparticles was 31 nm, 61.94nm and 72nm observed with Particle size analyser, XRD and TEM respectively.

### ACKNOWLEDGEMENT

The authors would like to thank the TEQIP-II and DST-FIST for financial support and testing facilities.

### REFERENCES

- Balamurugan, M.G., Mohanraj, S., Kodhaiyolii, S., Pugalenthi, V. 2014, 'Ocimum sanctum leaf extract mediated green synthesis of iron oxide nanoparticles: spectroscopic and microscopic studies', *J. of Chemical and Pharmaceutical Sci*, vol. 4, pp. 201-204.
- Basavegowda, N., Magar, K.B.S., Mishra, K., Lee, Y.R. 2014, 'Green fabrication of ferromagnetic Fe<sub>3</sub>O<sub>4</sub> nanoparticles and their novel catalytic applications for the synthesis of biologically interesting benzoxazinone and benzthioxazinone derivatives', *New J. Chem*, vol. 38, pp. 5415-5420.
- Basavegowda, N., Mishra, K., Lee, Y. R. 2014, 'Sonochemically synthesized ferromagnetic Fe<sub>3</sub>O<sub>4</sub> nanoparticles as a recyclable catalyst for the preparation of pyrrolo [3, 4-c] quinoline-1,3-dione derivatives', *RSC Adv*, vol. 4, pp. 61660-61666.
- Chaki, S.H., Tasmira, J.M., Chaudhary, M.D., Tailor, J.P., Deshpande, M.P. 2015, 'Magnetite Fe<sub>3</sub>O<sub>4</sub> nanoparticles synthesis by wet chemical reduction and their characterization', *Adv. Nat. Sci: Nanosci and Nanotechnology*, vol. 6, pp. 1-6.
- Gawande, M.B.B.P.S. and Varma, R.S. 2013, 'Nano-magnetite (Fe<sub>3</sub>O<sub>4</sub>) as a support for recyclable catalysts in the development of sustainable methodologies', *Chem. Soc. Rev*, vol. 42, pp. 3371-3393.
- Hamed, B., Soheila, H., Pouneh, E., Milad, M.A., Ahad, A., Farzaneh, N. 2014, 'Microbial mediated preparation, characterization and optimization of gold nanoparticles', *Brazilian Journal of Microbiology*, vol. 45, pp. 1493-1501.

- Haw, C.Y., Mohamed, F., Chia, C.H., Radiman, S., Zakaria, S., Huang, N.M., Lim, H.N. 2010, 'Hydrothermal synthesis of magnetite nanoparticles as MRI contrast agents', *Ceram Int*, vol. 36, pp. 1417-1422.
- Hu, F.Q., Wei, L., Zhou, Z., Ran, Y.L., Li, Z., Gao, M.Y. 2006, 'Preparation of biocompatible magnetite nanocrystals for in vivo magnetic resonance detection of cancer', *Adv. Mater*, vol. 18, pp. 2553-2556.
- Kavitha, A.I., Prabhu, H.G., Babu, S.A. Suja, S.K. 2013, 'Magnetite nanoparticles-chitosan composite containing carbon paste electrode for glucose biosensor application', *J.Nanosci. Nanotech*, vol.13, pp. 98-104.
- Kumfer, B.M., Shinoda, K., Jeyadevan, B., Kennedy, I.M. 2010, 'Gas-phase flame synthesis and properties of magnetic iron oxide nanoparticles with reduced oxidation state', *J. Aerosol Sci*, vol. 41, pp. 257-265.
- Latha, N. and Gowri, M., 2014, 'and characterization of Fe<sub>3</sub>O<sub>4</sub> nanoparticles using Caricaya papaya leaves extract', *Int. J. Sci. Res*, vol. 3, pp. 1551-1556.
- Lemine, O.M., Omri, K., Zhang, B., Mir, E.L., Sajieddine, M., Alyamani, A., Bououdina, M. 2012, 'Sol-gel synthesis of 8 nm magnetite (Fe<sub>3</sub>O<sub>4</sub>) nanoparticles and their magnetic properties', *Superlattice Microst*, vol. 52, pp. 793-799.
- Li, X.L., Li, H., Liu, G.Q., Deng, Z.W., Wu, S.L., Li, P.H., Xu, Z.S., Xu, H.B., Chu, P.K., 2012, 'Magnetite-loaded fluorine-containing polymeric micelles for magnetic resonance imaging and drug delivery', *Biomaterials*, vol. 33, pp. 3013-3025.
- Liu, J., and Hurt, R.H., 2010, 'Ion release kinetics and particle persistence in aqueous nanosilver colloids', *Environ. Sci. Technol.* 44(2010), pp. 169-2175'
- Mahadavian, A.R. and Mirrahimi, M.A.S. 2010, 'Efficient separation of heavy metal cations by anchoring polyacrylic acid on superparamagnetic magnetite nanoparticles through surface modification', *Chem. Eng. J*, vol. 159, pp. 264-271.
- Muhammad, A.Z., Sonita, A., Deana, W., Mia, L. 2016, 'LedyastutiPreparation of Fe<sub>3</sub>O<sub>4</sub>-chitosan hybrid nano-particles used for humic Acid adsorption', *Environmental Nanotechnology*, vol. 6, pp. 64-75.
- Narayanan, S., Sathy, B.N., Mony, U., Koyakutty, M., Nair, S.V., Menon, D. 2012, 'Biocompatible magnetite/gold nanohybrid contrast agents via green chemistry for MRI and CT bioimaging', *ACS Appl. Mater Interfaces*, vol. 4, pp. 251-260.
- Paiva, D.L., Andrade, A.L., Pereira, M.C., Fabris, J.D., Domingues, R.Z., Alvarenga, M.E. 2015, 'ME Novel protocol for the solid-state synthesis of magnetite for medical practices', *Hyperfine Interact*, vol. 232, pp. 19-27.
- Petla, K., Vivekanandhan, S., Misra, M., Mohanty, A.K., Satyanarayana, N. 2012, 'Soybean (Glycine Max) Leaf Extract Based Green Synthesis of Palladium Nanoparticles', *J. Biomat. Nanobiotechnol*, vol. 3, pp. 14-19.
- Prabhu, Y.T., VenkateswaraRao, K., SessaSai, V., Tambur, P. 2015, 'A facile biosynthesis of copper nanoparticles: A micro-structural and antibacterial activity Investigation', *J. of Saudi Chemical Society*, vol.21, pp. 180-185.
- Priest, S. 2006, 'The North American opinion climate for nanotechnology and its products: opportunities and challenges', *J Nanopart*, vol. 8, pp. 563-568.
- Qiao, R.R., Yang, C.H., Gao, M.Y. 2009, 'Superparamagnetic iron oxide nanoparticles: from preparations to in vivo MRI applications', *J. Mater. Chem*, vol. 19, pp. 6274-6293.
- Salem, M., Xia, Y., Allan, A., Rohani, S., Gillies, E.R. 2015, 'Curcumin-loaded, folic acid-functionalized magnetite particles for targeted drug delivery', *RSC Adv*, vol. 5, pp. 37521-37366.
- Shankar, S.S., Rai, A., Ankamwar, B., Singh, A., Ahmad, A., Sastry, M. 2004, 'Biological synthesis of triangular gold nanoprisms', *Nat. Mater*, vol. 3 pp. 482-487.
- Sharad, N.S., Swapnil, R.B., Ganesh, R.M., Samadhan, S.K., Dinesh, K.M., Shashikant, B.B., Anuj, K.R., Nenad, B., Orlando, M.N.D.T., Radek, Z., Rajender, S.V., Manoj, B.G. 2014, 'Iron oxide-supported copper oxide nanoparticles (nanocat-Fe-CuO): magnetically recyclable catalysts for the synthesis of pyrazole derivatives, 4-methoxyaniline, and ullmann-type condensation reactions', *ACS Sustainable Chem. Eng*, vol. 2, pp. 69-75.
- Senthil, M. and Ramesh, C. 2012, 'Synthesis of Fe<sub>3</sub>O<sub>4</sub> nanoparticles using Tridaxprocumbens leaf extract and its antibacterial activity on pseudomonas aeruginosa', *J. Nanomater Biostruct*, vol. 7, pp. 1655-1659.
- Ting, W., Jiajiang, L., Zuliang, C., Mallavarapu, M., Ravendra, N., 2014, 'Green synthesized iron nanoparticles by green tea and eucalyptus leaves extracts used for removal of nitrate in aqueous solution, Journal of Cleaner Production', *J. of Cleaner Production*, vol. 7, no. 83, pp.413-419.
- Terris, B.D. and Thomson, T. 2005, 'Nanofabricated and self-assembled magnetic structures as data storage media', *J Phys D Appl. Phys*, vol. 38, pp. 1-9.
- Venkateswarlu, S., Rao, Y.S., Balaji, T., Prathima, B., Jyothi, N.V.V. 2013, 'Biogenic synthesis of Fe<sub>3</sub>O<sub>4</sub> magnetic nanoparticles using plantain peel extract', *Mater Lett*, vol. 100, pp. 241-248.
- Wani, K.D., Kadu, B.S., Mansara, P., Gupta, P., Deore, A.V., Chikate, R.C., Poddar, P., Dhole, S.D., Kaul-Ghanekar, R. 2014, 'Synthesis,

characterization and in vitro study of biocompatiblecinnamaldehyde functionalized magnetite nanoparticles (CPGF Nps) for hyperthermia and drug delivery applications in breast cancer', *Plos One*, vol. 9, pp. 1-13.

Yen, P.Y., Kamyar, S., Mikio, M., Noriyunki, K., NurulBahiyah, B.A.K., ShazaBtMohamad, E., Kar, L.X. 2016, 'Green Synthesis of Magnetite (Fe<sub>3</sub>O<sub>4</sub>) Nanoparticles Using Seaweed (Kappaphycusalvarezii) Extract', *Nanoscale Research Letters*, vol. 11, pp. 276-284.

Zargar, M., Hamid, A.A., Bakar, F.A., Shamsudin, M.N., Shameli, K., Jahanshiri, F., Farahani, F. 2011, 'Green synthesis and antibacterial effect of silver nanoparticles using Vitexnegundo L. Molecules', *Molecules*, vol. 16, pp. 6667-6676.

Zhang, L., Dong, W.F., Sun, H.B. 2013, 'Multifunctional superparamagnetic iron oxide nanoparticles: design, synthesis and biomedical photonic applications', *Nanoscale*, vol. 5, pp. 7664-7684.

Zhao, H., Saatchi, K., Hafeli, U.O. 2009, 'Preparation of biodegradable magnetic microspheres with poly (lactic acid)-coated magnetite', *J. Magn. Mater*, vol. 321, pp. 1356-1363.

# Rapid method for determination of dehydro abietic acid in gum rosin and disproportionated rosin by proton nuclear magnetic resonance spectroscopy

Ravindra Kumar\*, K. Chattopadhyay, Bantu Bhasker, Sujit Mondal, J. Christopher and G.S. Kapur

## ABSTRACT

In present work a simple, direct and rapid method developed based on proton nuclear magnetic resonance spectroscopy for the quantitative determination of dehydroabietic acid in gum rosin and disproportionated rosins and validated. This method can also be applied to the determination of other acids of gum rosins like abietic acid, pimaric acid isopimaric acid, palustric acid, neo abietic acid, levopimaric acid, tetrahydro abietic acid, dihydro abietic acid. Dehydroabietic acid has been estimated using aromatic proton while vinyl proton was used for estimation of other acids in gum rosins. Analysis of rosin acid methyl ester derivative in disproportionated rosins was also carried out by gas chromatography-mass spectroscopy to identify peak of dehydro abietic acid along with abietic acid based on their mass fragmentation pattern and quantified using gas chromatography with flame ionization detector. Good correlation was observed between the results of gas chromatography with flame ionization detector with newly developed nuclear magnetic resonance method.

## KEYWORDS

Dehydro abietic acid, disproportionated rosin, nuclear magnetic resonance spectroscopy, gas chromatography-mass spectroscopy.

-----  
Indian Oil Corporation Limited, Research & Development Centre, Sector-13, Faridabad 121007, Haryana, India

\*Corresponding author; email: kumarr88@indianoil.in

## INTRODUCTION

Rosin acid is a raw material used in adhesives industry either as such or derivatives. Three sources of rosin are used for resin manufacture viz., gum rosin, wood rosin and tall oil rosin, all generated from the pine tree. Rosin acid unlike hydrocarbon resins, is not a polymer. It is a blend of distinct molecules. Rosin acid is a mixture of eight closely related rosin acids characterized by three fused six-carbon rings, double bonds that vary in number and location, and a single carboxylic acid group. The ratio of these isomers in rosin depends on the collection method and the species of the tree from which the rosin was harvested.

Gum rosin was once the only commercial source of rosin. It is the oleoresin (pine gum) of the living pine tree. The harvesting of the oleoresin is simple, involving only periodic wounding of the tree and collecting the sap into cups. Gum rosin contains abietic acid (AA) (Fig. 1a), dehydro abietic acid (DAA) (Fig. 1b), pimaric acid, isopimaric acid, palustric acid, neo abietic acid, levopimaric acid, tetrahydro abietic acid and dihydro abietic acid. Major component of gum rosin is AA, which has a conjugated diene and is easily oxidizable. The stability of gum rosin increases by disproportionation reaction to produce disproportionated rosin (DPR) that is resistance to oxidation. Dehydro abietic acid (DAA) is the main component of DPR rosin, an important rosin derivative used industrially in paper sizing, coating compositions, synthetic resins and especially an emulsifying agent in the manufacturing of styrene butadiene rubber. There are several commercial grades of DPR rosins available in the market containing 30 to

65% DAA. Variation in disproportion processes causes considerable variation in DAA content as result of incomplete disproportion of the conjugated diene acids such as abietic, neoabietic and palustic acids. This reduces the overall stability to oxidation and the usefulness of the end product, hence need for a method of DAA quantitation.

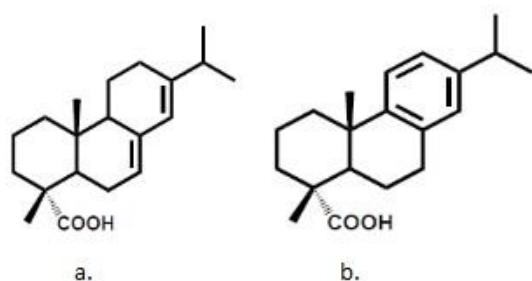


**Fig. 1** Structure of a. Abietic Acid and b. Dehydro Abietic Acid

The need to find a simple, rapid, accurate and reproducible method for quantitative analyses of DAA in gum rosins and DPR for the usefulness of gum rosins. There is no method available for direct estimation of Dehydro Abietic Acid and different isomers of Abietic acid in gum rosin and DPR. Separation of the methyl esters of resin acids has been carried out by gas chromatography (Huddy JA, 1959; Nestler and Zinkel, 1963) and estimation of diterpene and fatty acids (Joye et al., 1974; Nestler and Zinkel, 1967; Zingle and Engler, 1977; Holmbom et al., 1974; Foster and Zinkel 1982) by gas-liquid chromatography and capillary gas chromatography-mass spectrometry. Total abietic type acids can be determined by acid isomerization and determination of the abietic acids by the gas liquid chromatography of the methyl esters (Hans and Zinkel, 1991; Hanson and Kulkarni 1972; Mayr et al., 1982). In particular situations, other techniques may be more suitable than gas chromatography, first due to hydrogen bonding; unmodified fatty acids and rosin acids cannot be volatilized at atmospheric pressure without undergoing decomposition. So, it is necessary to convert the free acids to the more volatile and more stable methyl esters, prior to chromatographic separation. Secondly, the presence of fatty acid esters in the sample would result in

transesterification during the derivatization step that may affect the results.

In the present work, a new analytical method based on proton nuclear magnetic resonance ( $^1\text{H}$  NMR) spectroscopy has been developed for the direct estimation of dehydroabietic acid in gum rosin and disproportionated rosins. This method can also be applied for the determination of other acids of gum rosins like Abietic acid (AA), pimaric acid, isopimaric acid, palustric acid, neo abietic acid, levopimaric acid, tetrahydro abietic acid, dihydro abietic acid. DAA has been estimated using aromatic proton and other acids have been estimated using unsaturated proton by quantitative NMR (qnmr). Gas chromatography-mass spectrometry (GC-MS) analysis of methyl ester derivative of rosin acid and its DPR was carried out for detection of Dehydro Abietic acid (DAA) based on their mass fragmentation pattern (EI, 70 eV) and NIST library matching. However, their content in samples was estimated by gas chromatography with flame ionization detector (GC-FID). The outcome of NMR analysis was validated with GC results to check the appropriateness of the developed method, and good correlation was found.

## RESULTS AND DISCUSSION

All gum rosins and DPR NMR spectra were recorded in acetone- $d_6$  instead of Chloroform- $d$  due to auto-oxidation of gum rosins in Chloroform- $d$ . This auto oxidation of gum rosins in chloroform starts after 30 minutes and the residual peak of chloroform at 7.26 ppm overlap with DAA peaks in  $^1\text{H}$  NMR spectrum of gum rosin and DPR; hence acetone- $d_6$  is the best solvent for estimation of DAA.

The chemical shifts of the protons were more difficult to assign because of extensive overlap caused mainly by proton-proton coupling interactions. The assignments of  $^1\text{H}$  NMR spectrum of gum rosin and DPR have been assigned as per Landucci et al., 1991, which is given in Table 1.  $^1\text{H}$  NMR spectra of different origin gum rosins are given in Fig. 2 with their olefinic and aromatic regions and  $^1\text{H}$  NMR spectrum of DPR is given in Fig.3.

The vinyl protons of abietic acid (2) appeared at 5.76 ppm (1H, s) and at 5.35 ppm (1H, broad), levopimaric acid (3) appeared at 5.56 ppm (1H, s) and at 5.16 ppm (1H, broad), and only one vinyl proton in palustric acid (4) appeared at 5.38 ppm (1H, s). The protons of neoabietic acid (5) appeared at 6.21 ppm (1H, s) and Pimaric acid (6) at 4.95-4.84 (2H, m) and 5.84-5.71 (1H, m). For quantitative determination of the component acids present in the rosin acid, the respective areas of the

vinyl proton signals were used throughout this work. Dehydroabietic acid which appeared at 7.34-6.87 ppm (3H) (1) and neoabietic acid (5) were able to be determined without being disturbed by the presence of other rosin acids. Abietic acid (2), levopimaric acid (3), palustric acid (4) and pimeric acid (6) were interfered by other rosin acid peaks which are also estimated using their characteristic peak integrations which is given in Table 1. Stacked 1H NMR spectra of reactant (Gum rosin) and treated rosin (DPR) has been given in Fig. 4.

S. No	Rosin Acids	Chemical Shift used for quantification (ppm)	No of Protons
1	Dehydroabietic acid	7.34-6.87 (I <sub>DA</sub> )	3H
2	Abietic acid	5.76 (I <sub>A</sub> )	1H
3	Levopimaric acid	5.16 (I <sub>L</sub> )	1H
4	Palustric acid	5.38 (I <sub>P</sub> )	1H
5	Neoabietic acid	6.21 (I <sub>N</sub> )	1H
6	Pimeric acid	4.95-4.84 (I <sub>PM</sub> ) 5.84-5.71 (I <sub>pm</sub> )	2H

**Table 1** Characteristic peaks of different type rosin acids

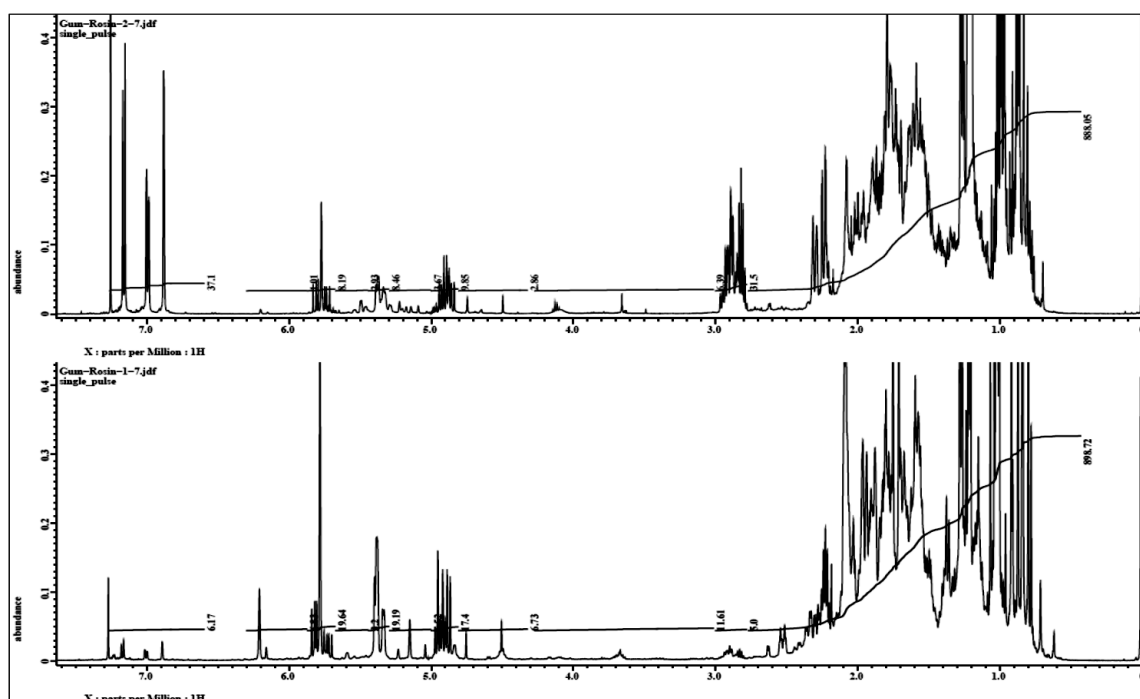


**Fig. 2** <sup>1</sup>H NMR spectra of different origin Gum rosins



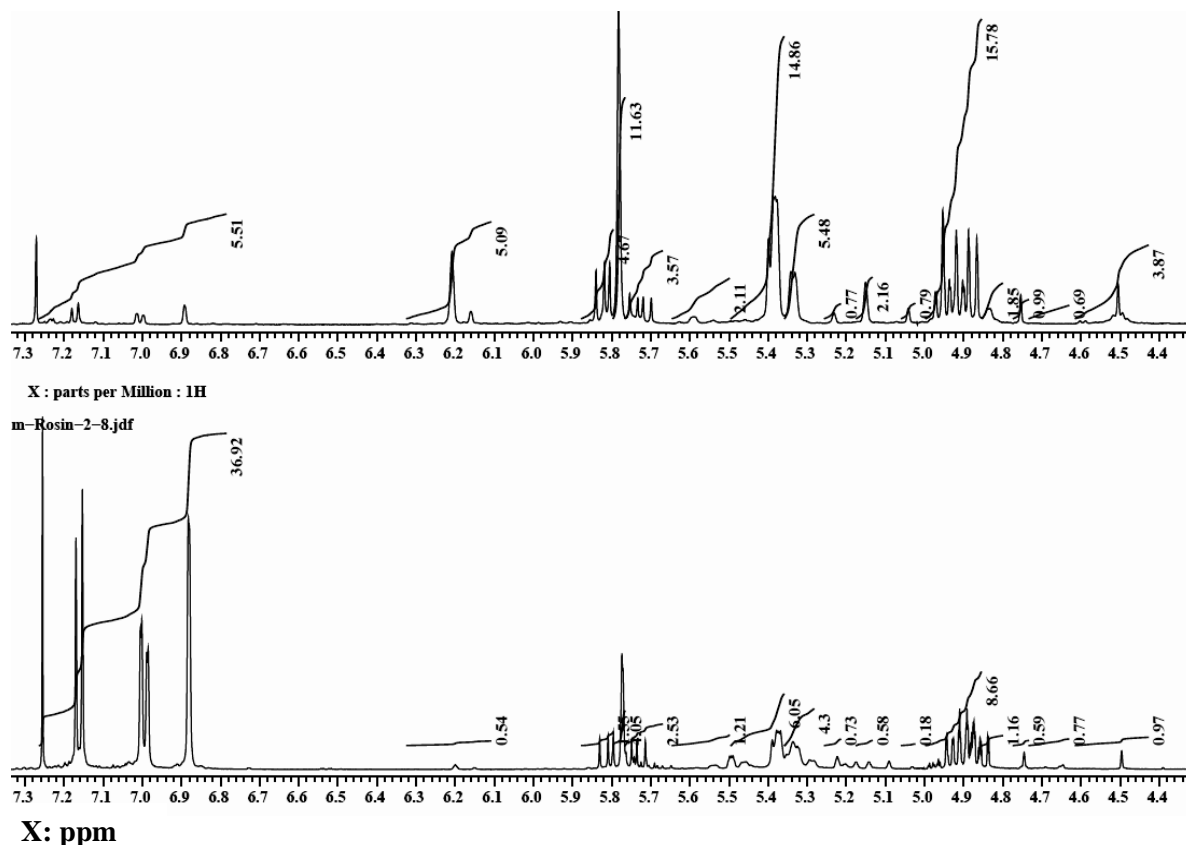


**Fig. 3** Olefinic and aromatic regions of disproportionate rosin <sup>1</sup>H NMR spectra

DAA has been estimated using aromatic proton and other acids have been estimated using vinyl proton. Three aromatic protons integration of DAA has been used for quantitative estimation of DAA. The amount (%) of DAA ( $W_{DA}$ ) has been estimated by quantitative <sup>1</sup>H NMR experimentation while compared with known amount of HMDSO ( $W_{HMDSO}$ ). The following equations have been used for the estimation.

$$W_{DA} = \frac{(W_{HMDSO} * M_{DA} * N_{HMDSO} * I_{DA})}{(M_{HMDSO} * N_{DA} * I_{HMDSO})}$$

$$= \frac{0.11085 * (W_{HMDSO} * M_{DA} * I_{DA})}{(N_{DA} * I_{HMDSO})} \text{----- (1)}$$

Where,  $W_{DA}$  = Weight of component to be estimated,  $W_{HMDSO}$  = Weight of HMDSO taken,  $M_{DA}$  = Molecular weight of component,  $I_{DA}$  = Integral value of the relevant chemical shift region of the component,  $N_{DA}$  = Number of protons in the chemical shift region with

integral  $I_{DA}$ ,  $I_{HMDSO}$  = Integration value for HMDSO at 0.07,  $N_{HMDSO}$  = 18 and  $M_{HMDSO}$  = 162.38.

An analogous equation has been used to estimate other acids and given as follows:

$$W_x = \frac{(W_{HMDSO} * M_x * N_{HMDSO} * I_x)}{(M_{HMDSO} * N_x * I_{HMDSO})}$$

$$= \frac{0.11085 * (W_{HMDSO} * M_x * I_x)}{(N_x * I_{HMDSO})} \text{----- (2)}$$

Where,  $W_x$  = Weight of acid to be estimated,  $W_{HMDSO}$  = Weight of HMDSO taken,  $M_x$  = Molecular weight of acid,  $I_x$  = Integral value of the relevant chemical shift region of the acid as given in Table 1,  $N_x$  = Number of protons in the chemical shift region with integral  $I_x$  as given in Table 1,  $I_{HMDSO}$  = Integration value for HMDSO at 0.07,  $N_{HMDSO}$  = 18 and  $M_{HMDSO}$  = 162.38.

Characteristics peak of abietic acid at 5.76 ppm overlapped with pimeric acid one proton (I<sub>pm</sub>), so I<sub>A</sub> has been estimated as per eq. 3.

$$I_A = I_{pm} - I_{PM}/2 \text{ ----- (3)}$$

DAA estimated in DPR of different origin gum rosins by <sup>1</sup>H NMR is, given in Table II. Analysis of rosin acid methyl ester derivative in DPR was carried out in GC-MS to identify peak of Dehydro Abeitic acid (DAA) along with Abeitic acid (AA) based on their mass fragmentation pattern (EI, 70 eV). The peak eluting at 22.185 minutes was compared to Dehydroabeitic acid (DAA) and unambiguously confirmed by NIST library matching. Dehydroabeitic and Abeitic acid were quantified in DPR treated rosin acids using GC-FID (Fig. 5) and results were compared with newly developed NMR method (Table 2). A good correlation was observed between NMR and GC results for DAA in DPR. Other rosin acids have also been estimated in different origins DPR by 1H NMR spectroscopy, which is given in Table 3.

After the synthesis of DPR from gum rosins, it has been observed that, 75-80% of abietic acid,

neoabeitic acid and palusteric acid were converted in DAA while 40-45% of pimeric acid and isopimeric acids were converted in DAA. It is important to mention here that isomerization of levopimaric acid and neoabeitic acid into abietic acid followed by auto-oxidation to DAA was observed in Chloroform-d after a certain time (6 hours). Several investigations have been made for the transformations of individual component resin acids during rosin disproportionation (Fleck and Palkin 1937; Fleck and Palkin1938; Mostafalu et al., 2017)

### CONCLUSION

A simple, direct and rapid <sup>1</sup>H NMR method for the quantitative determination of dehydroabietic acid in gum rosin and disproportionated rosins was developed and validated. This NMR method has also applied for the determination of other acids of gum rosins like Abietic acid (AA), pimaric acid isopimaric acid, palustric acid, neo abietic acid, levopimaric acid, tetrahydro abietic acid and dihydro abietic acid.

Sample	DAA (Wt%)	
	NMR	GC
GR-1	59.6	58.9
GR-2	52.1	52.2
GR-3	53.5	53.5
GR-4	54.7	54.3
GR-5	60.7	61.2

**Table 2** Dehydroabeitic acid in DPR by 1H NMR and GC method

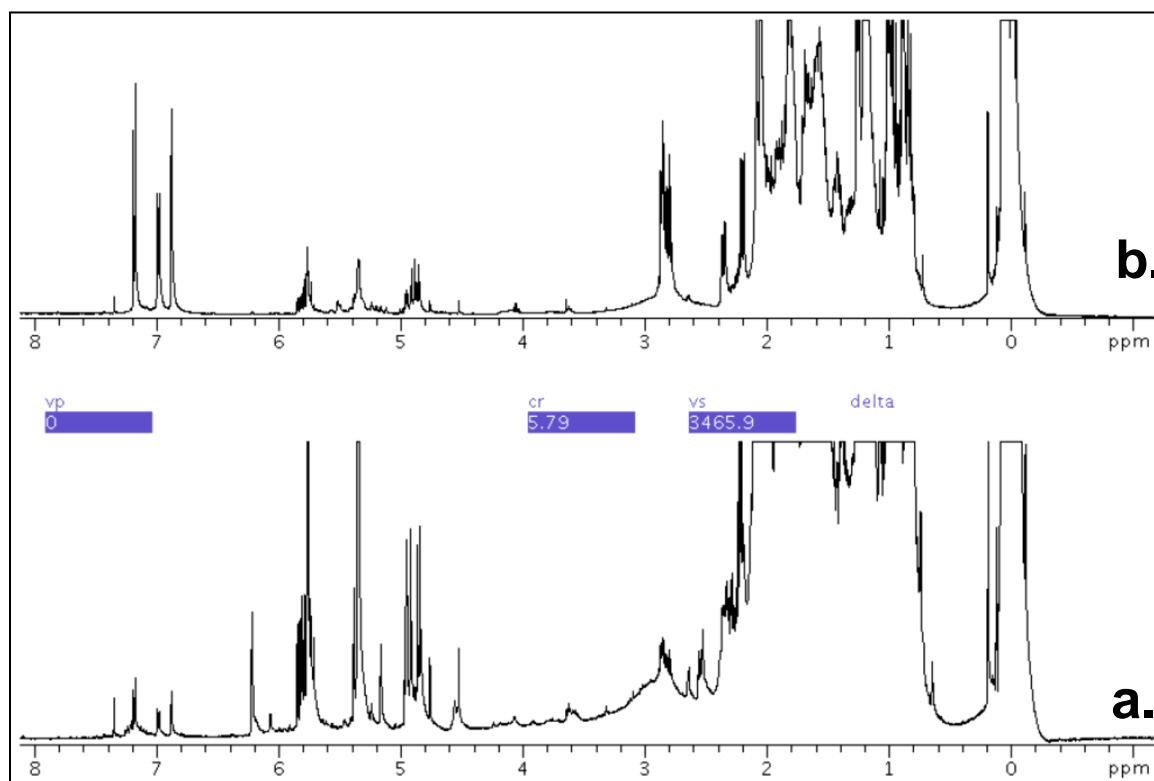


Fig.4: Stacked <sup>1</sup>H NMR spectra of **a.** reactant (Gum rosin) and **b.** treated rosin (DPR)

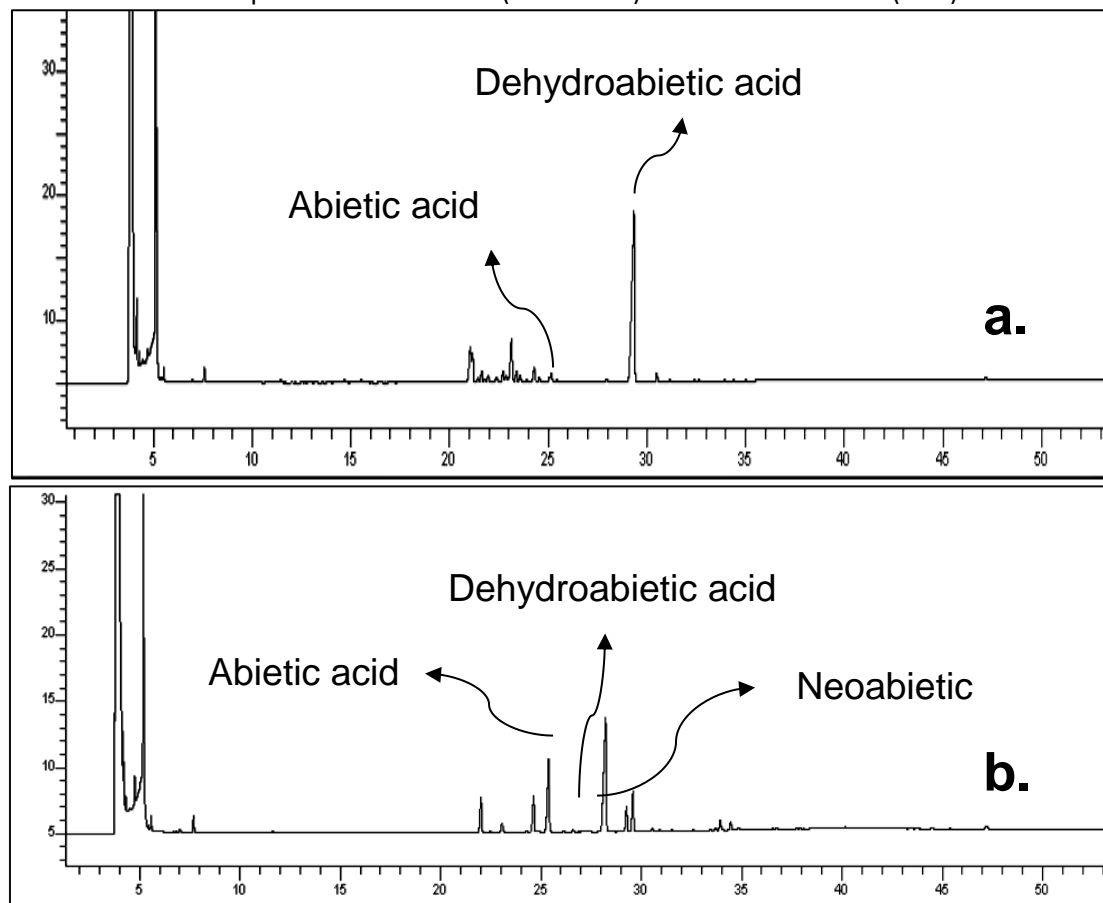


Fig. 5 GC-FID chromatogram of methyl ester derivative of gum rosin acid (**b.**) and its DPR (**a.**)

Sample	DAA (Wt%)	
	NMR	GC
GR-1	59.6	58.9
GR-2	52.1	52.2
GR-3	53.5	53.5
GR-4	54.7	54.3
GR-5	60.7	61.2

**Table 2** Dehydroabietic acid in DPR by <sup>1</sup>H NMR and GC method

## MATERIAL AND METHODS

### Sample

Gum resins from China and India origin and their DPR have been used for this study.

### Synthesis of DPR

Disproportionate reaction of gum rosin was carried out by using Palladium charcoal catalyst. In Disproportionation experiment, 100g of gum rosin was heated under nitrogen (hot plate) in a 250 ml of glass bottle equipped with magnetic stirrer and thermometer. The 5% Pd on charcoal catalyst (290 mg) was added when temperature reached to 230°C and then the reaction temperature was slowly increased to 270°C. The mixture was heated at 270°C for 6 hours. The reaction mixture was cooled to RT and then the solid was dissolved in dichloromethane and filtered. The final product, DPR was obtained after removal of the solvent.

### Sample Preparation

The sample of gum rosin and DPR (40 to 60 mg) were weighed into a NMR tube with its cap fitted at the top and allowed it to reach equilibrium. The standard reference compound (5 to 15 mg) was then added and recorded the amount up to 5 digits for both the cases. The sample was then diluted with CDCl<sub>3</sub> (~0.7 mL) and recorded the spectra.

A highly sensitive balance (Sartorius BP 211D, Gottingen, Germany) was used to weigh the sample and standard (upto 5-decimal). The methyl peak of HMDSO was used as a

frequency reference and set to 0.07 ppm downfield from TMS.

### Selection of a Suitable Reference Compound for Quantitative NMR Spectroscopy

For quantitative <sup>1</sup>H NMR spectroscopy, hexamethyldisiloxane (HMDSO) has been selected as an excellent internal reference standard which meets all the desirable characteristics. Purity of HMDSO used has also been thoroughly checked. It has been found that increasing the relaxation delay from 5s to 20s does significantly influences the integral value and so most of the samples were recorded with 20s relaxation delay.

### NMR Method

All proton NMR spectra were recorded on a Jeol ECA-500 NMR spectrometer operating at the proton frequency of 500 MHz, spectral width 7512 Hz (-2.5-12.5 ppm), 90° pulse = 10.7 μs, relaxation delay = 20s, digital resolution 0.49 Hz/point. 32 repetitions were averaged with 32K data point and 6.38 minutes experimental time. All the NMR spectra were integrated after baseline correction, and a mean of minimum three integration values has been taken for each calculation.

### GC and GC-MS

The conversion of acids present in the gum rosin samples to methyl ester was carried out by N,N-Dimethylformamide Dimethyl Acetal (DMF-DMA) reagent as per the ASTM D 5975 method. 0.5 gm rosin acid was taken in an appropriate anhydrous vial and dissolved in approximately 0.5 mL of toluene. Then

approximately 1 mL of DMF-DMA was added to the mixture and maintained at 50°C for 120 minutes. Finally, the resultants were used for GC analysis

The qualitative analysis was carried out on using Bruker GC-MS (Scion SQ, 436-GC) with the help of a polar column; (RTX-2330; 60m x 0.32 mm ID x 0.2 µm) procured from M/s Restek to identify the compound. However, quantification of DPR was achieved using PerkinElmer Clarus 500 GC instrument equipped with FID and split/split less injector. The following analytical conditions were used during analysis in GC-FID and GC-MS respectively.

#### Parameters of GC-FID

Split ratio: 10:1

Oven programme: 150 °C (5 minutes hold) - 3°C/ minute -250°C (15 minutes hold)

Injector and Detector temperature: 300 and 320 °C respectively

Carrier (Helium) gas Flow: 1.5 ml/min

Sample injection volume: 0.2 µl.

#### Parameters of GC-MS

Operating Mode: Scan mode with 10:0 split

Carrier Flow: 1 ml/min column flow for GC-MS

Oven programme: 150 °C (5 minutes hold) - 3°C/ minute -250°C (15 minutes hold) 250°C (10 minutes hold)

Injector temperature: 300 °C

MS Source and transfer line: 230 and 250 °C respectively

Ionization: EI (70 eV)

Scan Range: m/z 40 - 500

Injection Volume: 0.4 µl.

#### **REFERENCES**

Fleck, E.E. and Palkin, S. 1937, 'atalytic isomerization of the acids of pine oleoresin and rosin', *J. Am. Chem. Soc.*, vol. 59, pp. 1593-1595.

Fleck, E.E. and Palkin, S. 1938, 'On the nature of pyroabietic acids', *J. Am. Chem. Soc.*, vol. 60, pp. 921-925.

Foster, D.O. and Zinkel, D.F. 1982, 'Qualitative and quantitative analysis of diterpene resin acids by glass capillary gas—liquid chromatography', *J. Chromatogr.*, vol. 248, no. 1, pp. 89-98.

Han, J.S. and Zinkel, D.F. 1991, 'Gas chromatography of resin acids with a BDS fused-

silica capillary column', *Naval Stores Rev.*, vol. 101, pp. 13-16.

Hanson, J.C. and Kulkani, M.V. 1972, 'Open-tube-column gas chromatography of rosin fluxes', *Anal. Chem.*, vol. 44. no. 9, pp. 1586-1589.

Holmbom, B., Avela, E., Pekkala, S. 1974, 'Capillary gas chromatography-mass spectrometry of resin acids in tall oil rosin', *J. Am. Oil Chem. Soc.*, vol. 51, no. 397.

Huddy, J.A. 1959, 'Resin Acids. Gas chromatography of their methyl esters', *Anal. Chem.*, vol. 31, no. 11, pp. 1754-1756.

Joye, Jr. N.M., Rouveax, A.T. and Lawrence, R.V. 1974, 'Improved procedure for the analysis (GLC) of resin acids', *J. Am. Oil Chem. Soc.*, vol. 51, no. 5, pp. 195-197.

Landucci, L.L. and Zinkel, D.F. 1991, 'the 1H and 13C NMR spectra of the Abietadienoic resin acids', *Holzforchung*, vol. 45, no. 5, pp. 341-346.

Mayr, M., Lorbeer, E., Kratzl, K. 1982, 'chromatographic separation of diterpene acids on glass capillary columns of different polarity', *J. Am. Oil. Chem.*, vol. 59, no. 1, pp. 52-57.

Mostafalu, R. et al. 2017, 'The use of palladium nanoparticles supported on active carbon for synthesis of disproportionated rosin (DPR)', *J Nanostruct Chem.*, vol. 7, pp. 61-66.

Nestle, F.H.M. and Zinkel, D.F. 1963, 'Separation of the methyl esters of resin acids by gas liquid chromatography', *Anal. Chem.*, vol. 35, no. 11, pp. 1747-1749.

Nestler, F.H.M. and Zinkler, D.F. 1967, 'Quantitative gas-liquid chromatography of fatty and resin acid methyl esters', *Anal. Chem.*, vol.39, pp. 1118-1124.

Zingle, D.F. and Engler, C.C. 1977, 'Gas-liquid chromatography of resin acid esters', *J. Chromatogr.*, vol. 136, no. 2, pp. 1118-1124.

# Parabolic trough solar collectors

TVR Sekhar, Gopal Nandan, Ravi Prakash\*

## ABSTRACT

Solar collector in the shape of a parabolic mirror reflects the incident solar energy on the longitudinal axis of the solar collector. This line is called the focal axis of the parabolic collector. Unlike in flat plate collectors which have absorbent coatings and where the solar radiation is absorbed and distributed uniformly in the flat plate area, parabolic collectors concentrate the radiation in the focal axis of the collector. This major difference in the geometrical feature of the parabolic collectors helps in a large way. This feature enables the parabolic collectors to achieve high outlet temperatures of the working fluids, sometimes 120°C or as high as 140°C. This feature allows the parabolic concentrators to be integrated with solar thermal systems. The present work intends to review contemporary research work undertaken on parabolic trough type solar collectors. The present study has classified various investigations on the basis of collection of the data like direct experimentation as well as numeration methods and by using simulation methods on collectors and it is inferred that there is a potential for experimenting with nano-fluids in parabolic trough solar collectors and validating the obtained data with simulation results.

## KEYWORDS

Parabolic Trough, Simulation, Solar Collector, optical efficiency, thermal efficiency

## INTRODUCTION

Harnessing solar energy has been a constant endeavor of mankind since the development of mankind. However, with the development of the concept of photovoltaic cells, commercial development of solar energy for electrical power production and community energy distribution has commenced. But today the scenario requires a greater contribution from the renewable energy sector than ever before and more so from the solar energy sources.

---

Amity University, Sector-125, Noida 201313, Uttar Pradesh, India

\*Corresponding author; email: rprakash@amity.edu

This demand comes with a condition of cleaner solar energy than yesterday. We know that poly crystalline cells used in solar PV have inherent problems. Battery banks are required for such PV panels wherein the converted electrical energy is stored. The polycrystalline cells are manufactured using a refined form of silica which is obtained by mining huge deposits of natural riverside sands. Again, this is a source of air and river pollution. Considering these drawbacks of PV technology solar thermal concentrating technology offers energy conversion at a much-reduced footprint of pollution, after the completion of their useful life periods. It is imminent that a rapid transition to solar thermal based technologies on a large scale integrated energy conversion system takes place replacing the presently practiced small and medium scaled application of solar PV technology.

## Basic Features of Parabolic Solar Collectors

The parabolic solar collector consists of the main three components, the parabolic solar reflector, a mounting stand and the receiver engine or the absorber pipe. The parabolic reflector could be a dish type construction or a trough type construction. In case of a parabolic dish the entire incident solar radiation is concentrated at a focal point and it is collected by a receiver device called the engine. This highly concentrated energy is converted into thermal energy by this engine for further storage in thermal devices. In the case of a parabolic trough, the insolation is reflected from the reflector surface and concentrated in a linear axis of the parabolic receiver. The heat absorbing tube containing the working fluid is mounted in this axis and picks up the heat from the heated tube and thus converts into thermal energy of the working fluid. The same is either stored in thermal storage tanks or used to heat other fluid in heat exchangers.

## Parabolic Solar Collectors

Parabolic solar collectors are classified as Parabolic Dish type or Parabolic Trough type collectors. Classification is based on the geometry of the receiver i.e. dish or trough.

The parabolic trough collectors are further classified as tracking and non-tracking type collectors depending on the applications and the desired outlet temperature parameters of the output fluid. The non-tracking types are fixed type collectors. The tracking collectors are again classified into single-axis tracking and two-axis tracking.

### Parabolic Dish Solar Collectors

A Sterling engine based parabolic type collector is seen in Fig.1. The focused rays are concentrated at a small area. The receiver shown in Fig. 1 is usually made of a sheet of high thermal conductivity metal, (copper or aluminum) with integrated tubes. A highly absorbent material is coated to improve the absorptivity and reduce the reflectivity.

### Parabolic Trough Solar Collectors

The two types of parabolic collectors are Simple Parabolic collector and compound parabolic collector. The simple parabolic collector consists of a single parabolic reflective surface. The compound parabolic concentrator consists of two parabolic reflective surfaces and the superimposed focal axis of both the parabolic surfaces receives radiation of much higher intensity when compared with a simple parabolic collector.



**Fig.1** Parabolic Dish Type solar collector

### Objective of the overview

In the present work, overview of parabolic solar collectors has been segmented into three parts. First part focuses on the experimental studies, second part highlights the numerical studies and third part focuses on the simulation studies available in literature. Application

of simulation study provides detail insights into the performance and geometrical aspects of the parabolic trough solar collector. The future scope of work seeks to benefit researchers employing experimental methods for the testing of the parabolic trough solar collectors for validating their results with the numerical and simulation techniques and widening the applications of parabolic trough collectors for newer applications.

## **1. EXPERIMENTAL STUDIES ON PARABOLIC SOLAR**

Bellos et al. conducted experimental investigation on a trough collector comprising of a 70 mm diameter receiver tube with water as the working fluid. For this set up, at different mass flow rates, thermal performance is calculated. Optimum thermal performance was recorded at a flow of 2 kg/s in this study. Wang et al. attempted to enhance the optical efficiency of a parabolic trough collector. In order to achieve a high efficiency, heat exchanger with synthetic oil and water as the fluids were used in the absorber section of the collector. Higher order optical efficiencies of around 77% were recorded in the experimental study. Kordmahaleh et al. integrated thermal storage tanks to capture extra solar heat for use at night times. By this integration, total operating time of the plant increased from 1726 hrs to 2785 hrs. Kasaeian et al. experimented with a steel mirrored reflector surface collector of 1.5m<sup>2</sup>. They used painted tube surface of absorber and compared their optical and thermal efficiency according to ASHRAE standard 93 (2010). The thermal efficiency increased in vacuumed absorber tube in compare to exposed absorber tube. Khullar et al. used nanofluid in receiver and found that thermal efficiencies increased 4 % from conventional collector.

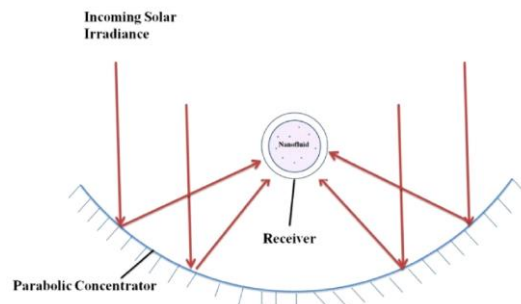


**Fig. 2** Nanofluid as cooling fluid in Parabolic Solar Collector (Khullar et al. 2012)

Sokhansefat et al. made valuable experimental contributions by understanding the direct dependency of convective heat transfer coefficient on the volume concentrations of the alumina nano-particles when used as a working fluid in a parabolic trough collector. Heat flux distributions are shown in Fig.3 and Fig.4. It is clearly evident that flux concentration zone is in the bottom of the absorber tube and the temperature distribution follows a like pattern.

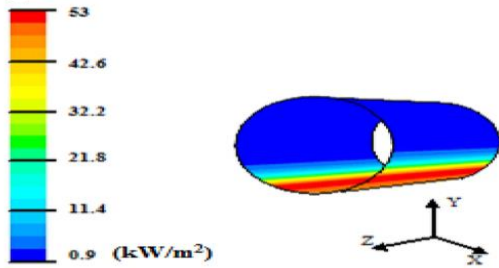


**Fig. 3** Heat flux distributions on the outer surface of the absorber tube (Sokhansefat et al. 2014)

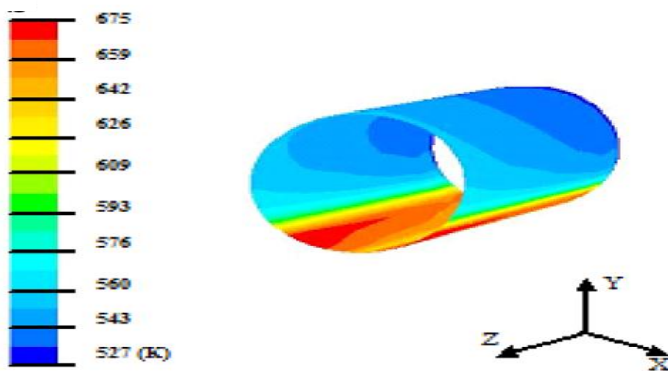


**Fig. 4** Temperature distributions on the outer surface of the absorber tube (Sokhansefat et al. 2014)

Eames et al. introduced baffles into the parabolic collector cavity and studied the improvements in thermal and optical efficiency. Valenzuela et al. conducted sensitivity analysis on a parabolic trough collector in industrial scale and studied the effect of temperature, pressure and direct normal irradiance on the pressure losses at higher ranges of operation. Tayade et al. used Aluminum sheet in the shape of a parabolic cylinder to reflect and concentrate sun radiations towards an absorber tube. Fernandez et al. employed Titanium oxide nanoparticles to study the

catalytic behavior of the sunlight on the organic contamination agents in the aquatic environment. They proved that it is an economical option.

Kalogirou et al. conducted investigations on parabolic (PTC), compound-parabolic (CPC) and Fresnel prism (FPC) collectors and it was deduced from the analysis that the parabolic trough collector based desalinating plant was the economical option best suited as per Fig.5.

Abu-Hamdeh et al. experimentally demonstrated an olive waste and methanol based adsorbent refrigeration system which runs on solar heating source such as a parabolic trough solar collector. The coefficient of performance that was obtained was around 0.75 for the device studied. Several researchers have conducted experiment in the African country of Algeria to estimate the harnessing potential of solar radiation with the help of parabolic trough collectors (Ouagued et al.). Different heat transfer fluids were tested in different climatic regions of Algeria with the help of tracking type collectors. Calisea et al. used a triangular shaped receiver test section as shown in Fig.6. Exergetic analysis for the set up as well as sensitivity analysis for the experimental set up was carried out.

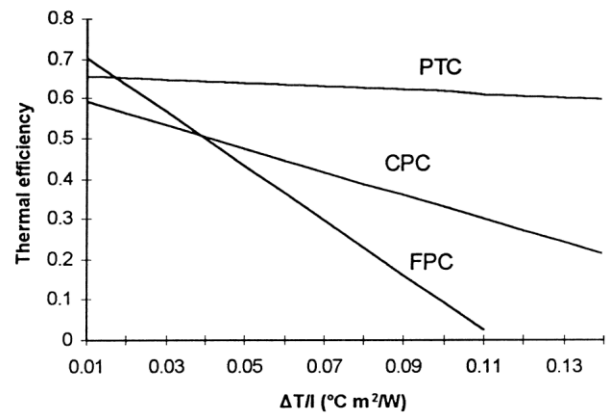


**Fig. 5** Comparison of the efficiencies of Parabolic, CPC & Fresnel Prism Collectors (FPC) (Ouagued et al. 2013)



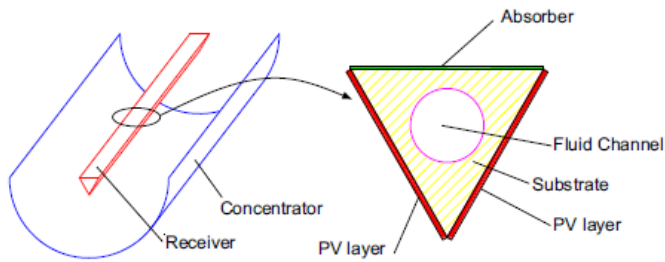


**Fig. 6** A triangular absorber tube placed in a parabolic collector (Calisea et al. 2012)

Nalwanga et al. performed an interesting experiment of disinfecting bacterial infested samples by placing them in a transparent absorber tube in the focal axis of a parabolic trough collector as seen in Fig.7. The study was conducted across the regions of the sub-Saharan desert regions of Africa.



**Fig.7** A compound parabolic collector with borosilicate glass absorber tube (Nalwanga et al. 2014)

Pecha et al. conducted experiments to determine the instantaneous efficiency of the collector as per ASHRAE guidelines. Optical efficiency was also determined. Chaudhary et al. studied a solar cooker with a thermal storage device like the phase change material. The study compared the efficiencies of the solar cooker coated with black paint and glazed surfaces in relation to conventional solar cookers with thermal storage arrangements. The experimental studies are tabulated as below.

**2. NUMERICAL STUDIES ON PARABOLIC SOLAR COLLECTORS**

Various researchers reported numerical studies. Hachicha et al. conducted numerical study on a Parabolic trough collector based on FVM (Finite Volume method) to predict the performance of the collector. The study

determined the solar flux distribution around the absorber tube with relatively high accuracies. Ghasemi et al. numerically investigated on the performance of the CuO water nano-fluid and reported the effect of volume fractions, absorber tube dimensions. It was deduced that Volume fraction of nano-particles plays a significant role in the improvement of the thermal efficiency of the collector. Figs 8 and 9 show the numerical investigation results of the study.

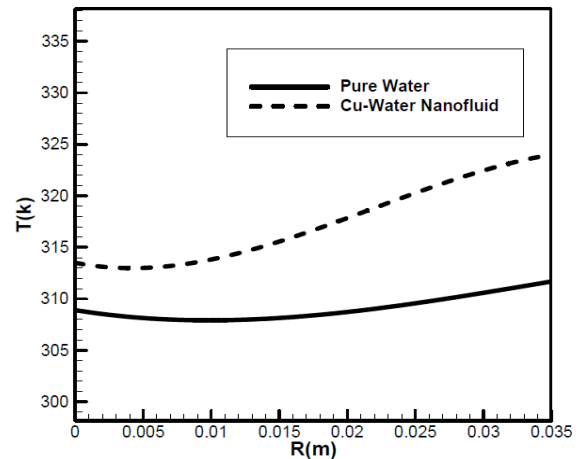


**Fig. 8** Two Dimensional temperature fields for water and Copper water nanofluid (Ghasemi et al. 2014)

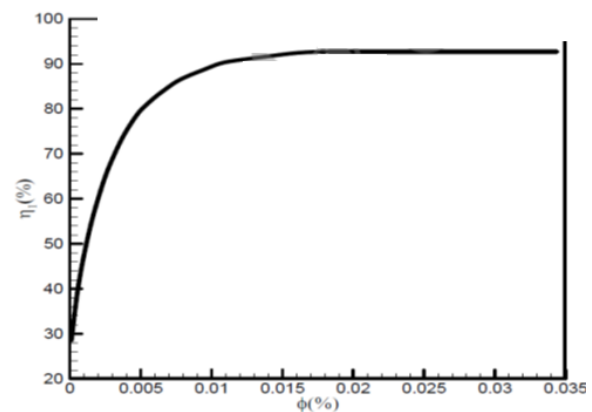


**Fig.9** Thermal efficiency vs Volume fractions of copper oxide nanofluid (Ghasemi et al. 2014)

Khullar et al. compared the heat absorbing capacities of different nano-fluids by subjecting them to a direct absorption based linear parabolic trough collector. Different aspects like absorber tube radius are studied in relation to the solar irradiance absorbing capacity of the

subjected nano-fluids. The results of the numerical investigations are shown in Fig.10. Montes et al. numerically investigated on an integrated Solar Combined Cycle (ISCC) power plant. This plant consists of a direct steam generating parabolic trough collector (PTC) with a combined cycle gas turbine-based power

plant. This hybrid model utilizes direct solar radiation which is available in the desert like climate. It improved thermal cycle efficiency of the power plant. Fig. 11 shows the direct normal incidence versus efficiency plot for the integrated cycle.

Investigators reference	Fluid used in collector	Efficiency Study Conducted & Reasons
Bellos et al.	Water	At Lower flow rates lower thermal efficiencies of collector were obtained.
Wang et al.	Water/synthetic oil	Using heat exchanger in absorber section led to high optical efficiency of collector.
Kordmahaleh et al.	Water	Integration with thermal storage tanks increased total operating time of plant by 61%.
Kasaeiana et al.	water	thermal efficiency is higher in vacuumed absorber
Khullar et al.	Aluminum oxide nano-fluid with Therminol VP	5-10% increase in collector efficiency
Sokhansefat et al	Water/alumina nanofluid	Heat flux concentration zones were developed at bottom of receiver tube.
Eames et al.	Water	thermal and optical efficiency improved due to baffles in collector
Valenzeula et al	water	Sensitivity analysis of collector was conducted using parameters like temperature, pressure and solar insolation on collector efficiency.
Tayade et al.	Water	Low cost parabolic trough
Fernandez et al.	Titanium-oxide nanoparticles	Higher efficiency is achieved using nanoparticles
SoterisKalogirou et al.	Saline water	Efficiency of collector using PTC increased desalinated water output
Abu-Hamdeh et al.	Olive waste as adsorbent and methanol as adsorbate	Collector efficiency improved refrigeration performance.
Ouagueda et al.	Syltherm 800, Therminol D12, Santotherm LT, Marlotherm X	Higher outlet temperature increased efficiency of collector.
Jie Zhu et al.	water	Installation area reduction led to higher efficiency per unit area of the collector.
Calisea et al.	water	Exergetic efficiency is calculated for comparison with circular shaped collector.
Nalawanga et al.	Bacteria Infested water	Efficiency of disinfection of bacteria using concentrated solar radiation was improved
Pecha et al.	water	Instantaneous efficiency of collector using ASHRAE guidelines was determined in the study.
Chaudhary et al.	Acetanilide	Increase of efficiency by 32.3%

**Table 1** Results of Experimental Studies on Parabolic Solar Collectors

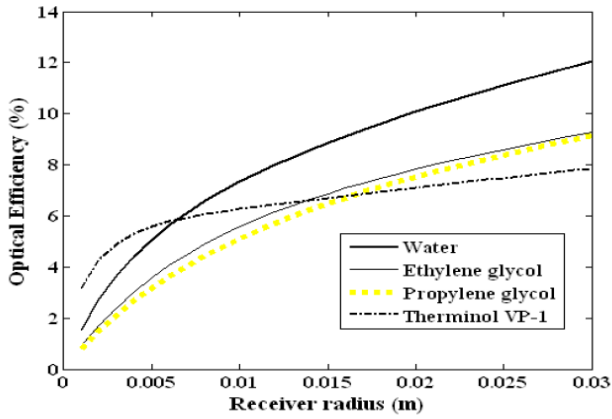


**Fig. 10** Optical efficiency vs Receiver tube radius for different working fluids (Khullar et al. 2011)

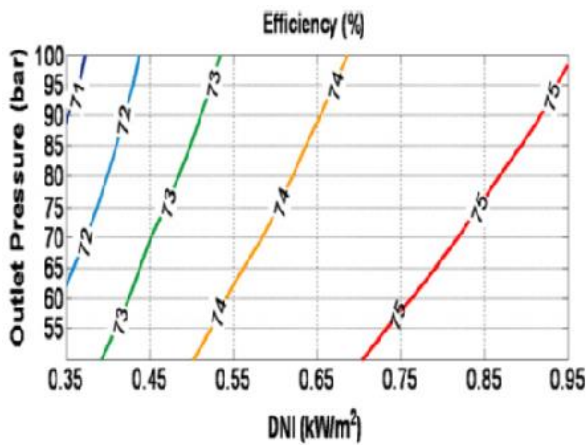


**Fig. 11** Solar efficiency per collector loop as a function of the DNI vs and outlet solar field pressure (Montes et al. 2011)

The heat losses occurred at the receiver tube of the PTC is estimated. The arrangement of the absorber tube as shown in Fig.12 is investigated by Mohammed et al. The variations in the temperatures of the absorber tube are calculated in this study.

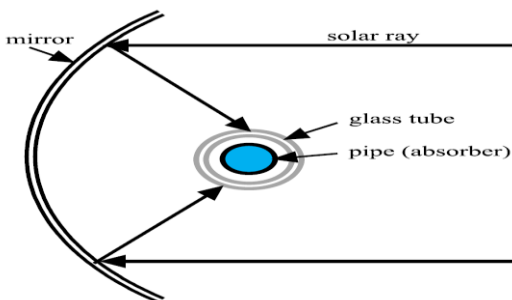


**Fig. 12** Partially vacuumed absorber tube in a parabolic collector (Mohamadi et al. 2013)

A homogenizing reflector (HR) is introduced to improve the flux distribution homogeneity in a PTC. It was observed by Wang et al. that circumferential distribution of the temperature of the receiver was homogenous after the introduction of the HR. Hachicha et al. developed a code based on Finite volume method to analyze the different segments of the receiver of PTC. By placing baffles into the receiver cavity of the solar PTC, Singh et al. observed that the performance of the solar collectors improved. Reddy et al. numerically studied the solar parabolic trough collector and the aspects of the collector and their impact on the collector performance are thoroughly analyzed. The angle of the collector its distance of space between collectors, the irradiance levels at the locations are considered for the analysis and the optimum sizing of the collector obtained. Al-Ansary et al. numerically investigated the performance of a half-insulated receiver as against a conventional air-filled receiver. The arrangement of the study is shown as in Fig. 13. The results are very promising as they suggest that when compared to air filled annulus there is a reduction of 25% in heat losses when half annulus insulation is used. Cheng et al. used Finite Volume Method and Monte Carlo Ray-Trace method for numerical model development. Based on it, temperature distribution of the receiver is plotted which is shown in Fig 14. The property of high temperature fluids affects heat loss conditions of the receiver.

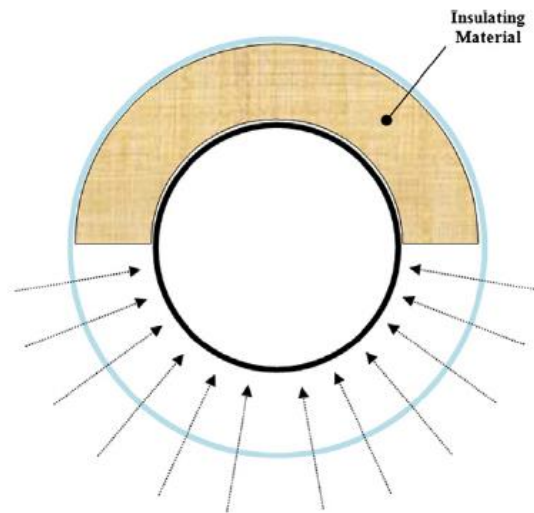


**Fig. 13** Schematic of the proposed receiver having top half insulating material (Ansary et al. 2012)

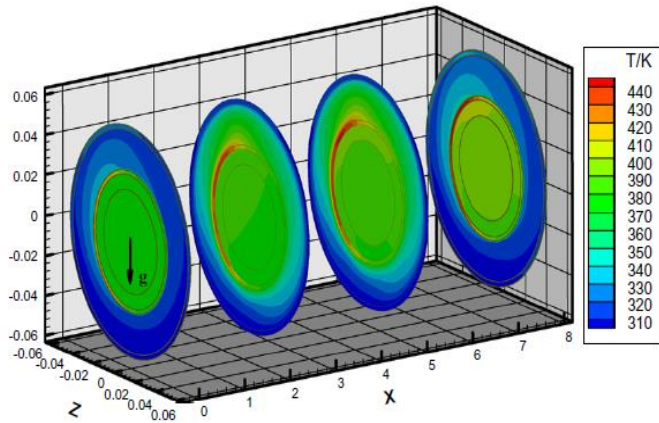


**Fig. 14** Visible computational results of temperature distributions in the receiver (Cheng et al. 2012)

Penga et al. deployed the integrated solar parabolic trough collector with the fossil fired thermal power plant. The rotatable type two axes collector concentrates the solar irradiance and helps in the generation of elevated temperature of the preheated condensate thereby improving the hybrid power plants overall efficiency by about 4%. The seasonal patterns are seen in Fig. 15.

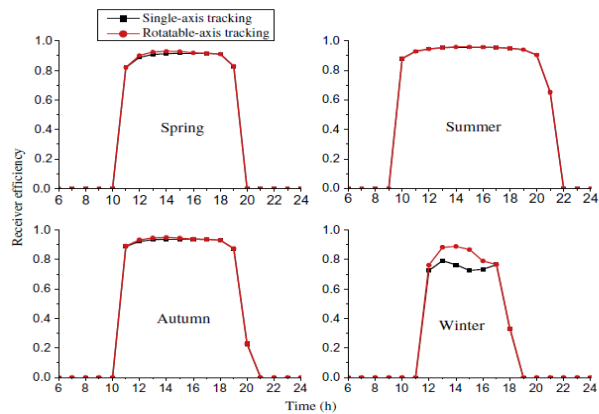


**Fig. 15** Improvements in collector efficiency under different seasonal (Penga et al. 2013)

Coccia et al. developed and tested mathematical model and validated the results on a prototype model. The model envisages calculation of thermal efficiency and optical efficiency of the parabolic trough collector. The details of Numerical studies as reported by various investigators are presented in Table 2.

### 3. SIMULATION STUDIES ON PARABOLIC SOLAR COLLECTORS

Ibarra et al. conducted simulation on a parabolic trough collector-based power plant. The model is compared with performance of a solar plant in a desert condition. Actual values of power output obtained in the field were compared with model values for the same solar insolation rates and ambient temperatures. An acceptable error of 10% due to over estimation of solar field production was recorded.

Murtaza et al. used ANSYS software for simulating outlet temperature of absorber tube under varying flow conditions. At a flow rates of 0.4 LPM to 1.2LPM, the outlet temperature obtained were in the range of 93°C to 103°C. Using ANSYS the tube displacement of 0.2mm, Von Mises stress within the strength limits of the material were obtained and small values of thermal strain were inferred using ANSYS software. Riffelmann et al. conducted simulation studies to measure the solar flux in the focal axis of the parabolic collector. They used a Parabolic Trough Flux Scanner (PARASCAN) instrument to quantify the solar flux in the concentrated region. A camera target method (CTM) is used to track the paths of the reflected rays and detect any errors in the reflective surface. Kalogirou et al. employed a transient simulation system TRNSYS with a PTC water heating system and the tracking in the E-W and N-S has been conducted and compared. Benefit analysis is performed for the use of this scheme. Odeh et al. studied with the help of a synthetic oil heat transfer fluid to simulate the losses of the collector.

Risi et al. investigated on an innovative solar Transparent Parabolic Trough Collector (TPTC) with gas based nano-fluid as the working fluid. Due to gaseous medium and an increase in the heat exchange surface, the feature helps in additional solar radiation absorption when compared to nanoparticles dispersed in the base liquid. Odeh et al. employed a transient condition for simulation model wherein the size of the thermal storage tank in relation to the receiver collector area is deduced. For transient response to temperature changes it is found that the storage tank should be at least 14.5 liters capacity per 1 square meter of the collector area. Gonzalez et al. used methanol and combination of an activated carbon in an absorption chiller device and coupled to PTC. The chiller performance is checked at varying conditions.

Investigators reference	Heat Transfer Fluid used in the collector	Findings
Hachicha et al.	water	Numerical study predicted solar flux along receiver tube to high accuracies (error band<10%)
Ghasemi et al.	Copper oxide-water nano-fluid	Thermal efficiency of the collector improved
Khullar et al.	Aluminum nano-particles, Ethylene glycol, Propylene glycol, therminol VP-1	Optical efficiency compared for four nano-fluids
Montes et al.	water	High pressure steam is obtained and marginally improves the gas turbine efficiency.
Mohamad et al.	water	effect of the collector length on the heat losses from the absorber is analyzed
Kun et al.	water	Homogenizing reflector reduced the variability of circumferential temperature
Hachicha et al.	water	Different segments of receiver studied
Singh et al.	water	baffles into the receiver cavity improved the performance
Reddy et al.	water	Detailed numerical analysis of aspects of trough collector are made.
Al-Ansary et al.	Air-filled annulus	Reduction of heat loss by 25% when half annulus insulation is used.
Cheng et al.	Syltherm 800, therminol, VP nitrate salt, Hitec XL	Properties of heat transfer fluid affects the heat losses
Penga et al.	water	Improved the hybrid power plants overall efficiency by about 4%.
Coccia et al.	water	Mathematical model predicted thermal & optical efficiency of the prototype.

**Table 2** Results of Numerical Studies on Parabolic Solar Collectors

He et al. investigated by simulation on a heat tube by employing Monte Carlo Ray Tracing technique. It is implied that the geometric concentration ratios are playing a role in the heat flux distribution. Mazloumi et al. simulated on a lithium bromide absorption cycle in which a PTC is used along with an insulated storage tank. By simulation it is calculated that a collector area of 57.6m<sup>2</sup> was required for supplying the cooling loads during the summer months. Huang et al. simulated on a PTC receiver fitted with a vacuum receiver tube.

Hedayatizadeh et al. simulated on a combined model consisting of a thermal model with a compound parabolic collector CPC and an electrical model consisting of a photovoltaic panel. Computational simulations are carried out for various conditions of climate. The results of simulation are in good agreement with their experimental measurements as can be seen in Fig. 16.

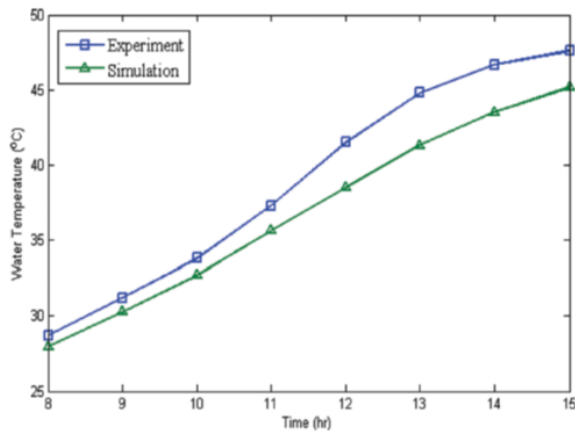


**Fig. 16** Hourly variation of water temperature experimental vs Theoretical (Mazloumi et al. 2008)

The details of simulation studies have been reported in the Table 3.

### CONCLUSION

The presented overview sought to publish an account of rich findings in the study of Parabolic Trough Solar collectors. The method of experimentation conducted by several researchers for studying the various parameters linked to parabolic troughs collector has been analyzed exhaustively. Researchers have employed numerical methods and studied the efficiencies of the parabolic collectors under different conditions. As a parallel process, the researchers also focused on subjecting the collector to simulation studies progressively improving the aspects of the collector surface for better absorptivity and emissivity. The research findings point to the evidence that good agreements of results across all the three types of studies are obtained. Use of nano-fluids in liquid as well as gaseous phases in reflective and transparent collectors holds promise for further research in the field of improvements of parabolic solar trough type receivers.

Investigators reference	Findings
Ibarra et al.	Simulation model predicted actual power output from a desert-based power plant close to 90% accuracy.
Murtaza et al.	ANSYS simulation model predicted outlet temperature of absorber tube at varying flow rates.
Riffelmann et al.	A camera target method (CTM) is used
Kalogirou et al.	Transient simulation system TRNSYS is used
S.D. Odeh et al.	Synthetic oil used to simulate the losses of the collector
A de Risi et al.	Transparent Parabolic Trough Collector (TPTC) used
Odeh et al..	Employed a transient condition for simulation model
Gonzalez et al.	Simulation of performance was conducted on an integrated chiller coupled to PTC.
Ya-Ling He et al.	MCRT technique suggested heat flux distribution to be dependent on geometric concentration ratio of PTC.
Mazloumi et al.	Simulation of a thermal storage integrated PTC was employed for calculating the collector area requirement.
Huang et al.	Evacuated vacuum tube integrated PTC was simulated to note heat loss distribution in PTC.
Hedayatizadeh et al.	Solar thermal-SPV hybrid model was simulated at varying conditions of solar radiation for comparison with experimental results.

**Table 3:** Results of Simulation Studies on Parabolic Solar Collectors

## ACKNOWLEDGEMENT

The work reported in this review paper was partially presented at the International Conference on Manufacturing Excellence, held at Amity University, Uttar Pradesh, India.

## ABBREVIATIONS USED

ASHRAE: American Society of Heating Refrigeration and Air-conditioning Engineers  
CCGT: Combined Cycle Gas Turbine  
CFD: Computational Fluid Dynamics  
COP: Coefficient of Performance  
CPC: Compound Parabolic Concentrator  
CTM: Camera Target Method  
DSG: Direct Steam Generation  
FPC: Fresnel Prism Collectors  
FVM: Finite Volume Method  
GC: Geometric concentration ratio  
HCE: Heat Collector Element  
HR: Homogenizing Reflector  
HTF: Heat Transfer Fluid  
ISCC: Integrated Solar Combined Cycle  
MCRT: Monte Carlo Ray-Trace  
NCPS: Nanofluid based Parabolic solar collector  
PARASCAN: Parabolic Trough Scanner  
PCM: Phase Change Material  
PTC: Parabolic Trough Collector  
PTSC: Parabolic Trough Solar Collector  
SEGS: Steam based electric generation system  
SODIS: Solar water Disinfectant  
SPLFR: Semi Parabolic Linear Fresnel Reactor  
TPTC: Transparent Parabolic Trough Collector  
TRNSYS: Transient System Simulation Tool

## REFERENCES

Abu-Hamdeh, H.N., Alnefaie, A.K., Almitani, H.K. 2013, 'Design and performance characteristics of solar adsorption refrigeration system using parabolic trough collector: Experimental and statistical optimization technique', *Energy Conversion and Management*, vol. 74, pp. 162 – 170.  
Al-Ansary, H. and Zeitoun, O. 2011, 'Numerical study of conduction and convection heat losses from a half-insulated air-filled annulus of the receiver of a parabolic trough collector', *Solar Energy*, vol. 85, pp. 3036 – 3045.  
Bellos, E., Tzivanidis, C., Antonopoulos, A.K. 2017, 'A detailed working fluid investigation for solar parabolic trough collectors' *Applied Thermal Engineering*, DOI: 10.16/j.applthermaleng.2016.11.201.  
Calisea, F., Palomboa, A., Vanolib, L. 2012, 'Finite-volume

model of a parabolic trough photovoltaic/thermal collector: Energetic and exergetic analyses', *Energy*, vol. 46, pp. 283 – 294.

Chaudhary, A., Kumar, A., Yadav, A. 2013, 'Experimental investigation of a solar cooker based on parabolic dish collector with phase change thermal storage unit in Indian climatic conditions', *Journal of Renewable and Sustainable Energy*, vol. 5, 023107

Cheng, Z.D., He, Y.L., Cui, F.Q., Xu, R.J., Tao, Y.B. 2012, 'Numerical simulation of a parabolic trough solar collector with non-uniform solar flux conditions by coupling FVM and MCRT method', *Solar Energy*, vol. 86, pp. 1770 – 1784.

Coccia, G., 2012, 'Mathematical modelling of a prototype of a parabolic trough solar collector', *Journal of Renewable and sustainable energy*, vol. 4, pp. 023110.

Eames, C. and Norton, B. 1995, 'Thermal and Optical consequences of the introduction of baffles into compound parabolic concentrating solar energy collector cavities', *Solar Energy*, vol. 55, no. 2, pp. 139 – 150.

Fernandez, P., Blanco, J., Sichel, C., Malato, S. 2005, 'Water disinfection by solar photocatalysis using compound parabolic collectors', *Catalysis Today*, vol. 101, pp. 345 – 352.

Ghasemi, S.E., Mehdizadeh, G.H.R., Ahangar. 2014, 'Numerical analysis of performance of solar parabolic trough collector with Cu-Water nanofluid', *International Journal of Nano dimension*, vol. 5, no. 3, pp. 233 – 240.

Gonzalez, I.M., Rodriguez, R.L., Lucio, H.J. 2009, 'Evaluation of thermal parameters and simulation of a solar-powered, solid-sorption chiller with a CPC collector', *Renewable Energy*, vol. 34, no. 3, pp. 570 – 577.

Hachicha, A.A., Rodriguez, I., Capdevila, R., Oliva, A., 2013, 'Heat transfer analysis and numerical simulation of a parabolic trough solar collector', *Applied Energy*, vol. 111, pp. 581 – 592.

Hachicha, A.A. 2016, 'Numerical simulation of a Parabolic Trough Solar Collector for Hot Water and Steam Generation', *AIP Conference Proceedings*, vol. 1734, 070013.

He, Y.L., Xiao, J., Cheng, Z.D., Tao, Y.B. 2011, 'AMCRT and FVM coupled simulation method for energy conversion process in parabolic trough solar collector', *Renewable Energy*, vol. 36, no. 3, pp. 976 – 985.

Hedayatzadeh, M., Ajabshirchi, Y., Sarhaddi, F., Safavinejad, A., Farahat, S., Chaji, H. 2013, 'Thermal and Electrical Assessment of an integrated solar photo voltaic thermal water collector equipped with a compound parabolic collector', *International Journal of Green Energy*, vol. 10, pp. 494 – 522.

Huang, W., Hub, P., Chen, Z. 2012, 'Performance simulation of a parabolic trough solar collector', *Solar Energy*, vol. 86, pp. 746 – 755.

Kasaeian, A.B.S. and Kowsary, F. 2014, 'Heat transfer enhancement in parabolic trough collector tube using Al<sub>2</sub>O<sub>3</sub>/synthetic oil nano fluid', *Renewable and Sustainable Energy Reviews*, vol. 33, pp. 636 – 644.

Kasaeian, A., Davirana, S., Azarian, D.R., Rashidi, A. 2015,

- 'Performance evaluation using nanofluid and capability study of a solar parabolic trough collector', *Energy conversion and management*, vol. 89, pp. 368 – 375.
- Kalogirou, A.S. 2002, 'Parabolic trough collectors for industrial process heat in Cyprus', *Energy*, vol. 27, pp. 813 – 830.
- Khullar, V., and Tyagi, H. 2011, 'Enhancing Optical Efficiency of a Linear Parabolic Solar Collector through Nanofluids', *AIP conference proceedings*, vol. 1391, no. 353.
- Khullar, V., Tyagi, H., Phelan, E.P, Otanicar, P.T, Singh, H., Taylor, A.R. 2012, 'Solar energy harvesting by using nanofluids based concentrating solar collector', *Conference on Micro/Nanoscale Heat and Mass Transfer. ASME*, pp. 259-267.
- Kordmahaleh, AA., Naghashzadegan, M., Javaherdeh, K., Khoshgoftar, M. 2017, 'Design of a 25MWe Solar Thermal Power Plant in Iran with Using Parabolic Trough Collectors and a Two-Tank Molten Salt Storage System', *International Journal of Photoenergy. Hindawi*, no. 11, Article ID 4210184.
- Mazloumi, M., Naghashzadegan, M., Javaherdeh, K. 2008, 'Simulation of solar lithium bromide water absorption cooling system with parabolic trough collector', *Energy Conversion and Management*, vol. 49, no. 10, pp. 2820 – 2832.
- Mohamadi, A., Orfi, J., ansary, Al, H. 2013, 'Heat losses from parabolic trough solar collectors', *Journal of Energy Research*, vol. 38, no. 1, pp. 20 – 28
- Montes, MJ., Rovir, A., Munoz, M., Martinez-Val, JM., 2011, 'Performance analysis of an Integrated Solar Combined Cycle using Direct Steam Generation in parabolic trough collectors', *Applied Energy*, vol. 88, no. 9, pp. 3228 – 3238.
- Murtuza, A.S., Byregowda, H.V., Ali, M.M.H., Imran, M. 2017, 'Experimental and simulation studies of parabolic trough collector design for obtaining solar energy', *Resource-Efficient Technologies*, vol. 3, pp. 414 – 421.
- Nalwanga, R., Quilty, B., Muyanja, C., Fernandez-Iban, P. 2014, 'Evaluation of solar disinfection of Eschereschia coli bacterium under Sub-Saharan field conditions using a 25L borosilicate glass batch reactor fitted with a compound parabolic collector', *Solar Energy volume*, vol. 100, pp. 195 – 202.
- Odeh, S.D., Morrison, G.L., Behnia, M. 1998, 'Modelling of Parabolic Trough Direct Steam Generation Solar Collectors', *Solar Energy*, vol. 62, no. 6, pp. 395 – 406.
- Odeh, D.S. and Morrison, G.L. 2006, 'Optimization of parabolic trough solar collector system', *International Journal of Energy Research*, vol. 30, no. 4, pp. 256 – 271.
- Ouagued, M., Khellaf, A., Loukar, L. 2013, 'Estimation of the temperature, Heat gain and Heat loss by solar parabolic trough collector under Algerian climate using different thermal oils', *Energy Conversion and Management*, vol. 75, pp. 191 – 201.
- Pecha, A., and Soberanis, MA Escalante. 2012, 'Efficiency curves analysis of a parabolic trough solar collector in the Yucatan Peninsula', *Journal of Renewable and Sustainable Energy 4*, 021203.
- Penga, S., Honga, H., Jina, H., Zhang, Z. 2013, 'A New rotatable-axis tracking solar parabolic-trough collector for solar-hybrid coal-red power plants', *Solar Energy*, vol. 98, pp. 1770 – 1784.
- Riffelmann, K.J. 2006, 'Performance enhancement of parabolic trough collectors by solar flux measurement in the focal region', *Solar Energy*, vol. 80, no. 10, pp. 1303 – 1313.
- Reddy, K.S. and Kumar, R.K. 2012, 'Solar collector field design and viability analysis of stand-alone parabolic trough power plants for Indian conditions', *Energy for Sustainable Development*, vol. 16, pp. 456 – 470.
- Risi, d.A., Milanese, M., Laforgia, D. 2013, 'Modelling and optimization of transparent parabolic trough collector based on gas-phase nanofluids', *Renewable Energy*, vol. 58, pp. 134 – 139.
- Singh, H. and Eames, PC. 2011, 'A Review of natural convective heat transfer correlations in rectangular cross-section cavities and their potential applications to compound parabolic concentrating (CPC) solar collector cavities', *Applied Thermal Engineering*, vol. 31, pp. 2186 – 2196.
- Tayade, G., Mayur., Thombre, E. R., Dutt, S. 2014, 'Performance Evaluation of Solar Parabolic Trough', *International Journal of Nano Dimension*, vol. 5, no. 3, pp. 233 – 240.
- Valenzuela, L., Hernandez-Lobon, D., Zarzaa, E. 2012, 'Sensitivity analysis of saturated steam production in parabolic trough collectors', *Energy Procedia*, vol. 30, pp. 765 – 774.
- Wang, K., He, Y., Cheng, Z. 2014, 'A design method and numerical study for a new type parabolic trough collector with uniform solar flux distribution', *Science China Technological Sciences*, vol. 57, pp. 531 – 540.
- Wang, R., Qu, W., Sun, J., Hong, Hu. 2017, 'An on-site test method for optical efficiency of large-size parabolic trough collectors', *Energy Procedia*, vol. 105, pp. 486 – 491.



# Scientific European®

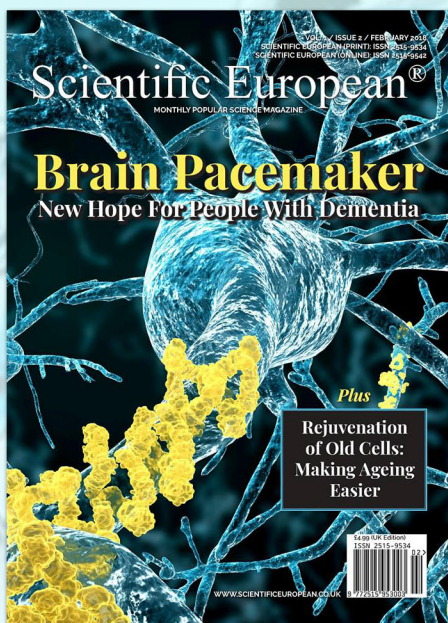
A MONTHLY POPULAR SCIENCE MAGAZINE

ISSN 2515-9534 (Print)

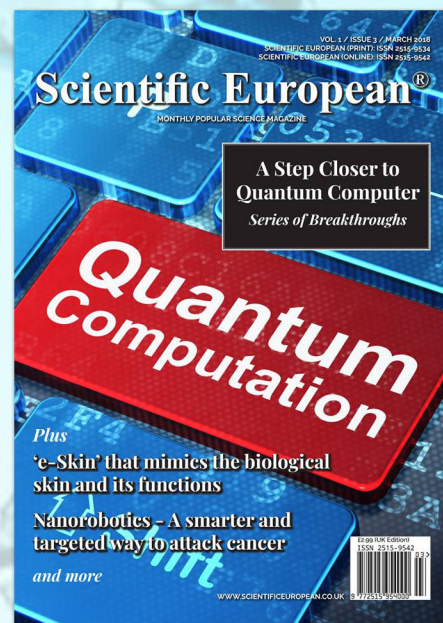
ISSN 2515-9542 (Online)



January 2018



February 2018



March 2018

Scientific European® (SCIEU®) aims to bring current happenings in science to a wider audience to make them aware of advances in the scientific fields.

The articles will present interesting and relevant ideas from diverse areas of science that have already been published in the peer-reviewed scientific literature in the recent past.

We are happy and proud to embark on the eternal journey to bring scientific advances to the living rooms of the people across the world!

Visit us at:

[www.scientificeuropean.co.uk](http://www.scientificeuropean.co.uk)

[www.scieu.com](http://www.scieu.com)

For general enquiries write to [info@scieu.com](mailto:info@scieu.com)

For editorial enquires write to [editors@scieu.com](mailto:editors@scieu.com)

**Publisher's statement:** Scientific European® is both online and print science magazine published by UK Education Consultancy Services Ltd, (Company Number 10459935 Registered in England); city: Tadworth, Surrey; Country of publication: United Kingdom, ISSN 2515-9534 (Print) ISSN 2515-9542 (Online)

# European Journal of Social Sciences (EJSS)<sup>®</sup>

Monthly Academic Journal of Social Sciences



[www.europeanjournalofsocialsciences.co.uk](http://www.europeanjournalofsocialsciences.co.uk) / [info@ejss.co.uk](mailto:info@ejss.co.uk)

## European Journal of Medicine and Dentistry (EJMD)<sup>®</sup>

Academic Journal of Medicine and Dentistry



Visit the website:  
[www.ejmd.co.uk](http://www.ejmd.co.uk)

Email:  
[info@ejmd.co.uk](mailto:info@ejmd.co.uk)

## European Journal of Law and Management (EJLM)<sup>®</sup>

Academic Journal of Law and Management



Visit the website:  
[www.ejlm.co.uk](http://www.ejlm.co.uk)

Email:  
[info@ejlm.co.uk](mailto:info@ejlm.co.uk)